

Republic of Iraq  
Ministry of Higher Education  
and Scientific Research  
University of Babylon  
College of Science/ Department of Physics



*Statistical Distribution of the Energy Spectrum of  
(<sup>137</sup>Cs , <sup>60</sup>Co, <sup>22</sup>Na) Nuclei by Using NaI(Tl) Detector*

*A Thesis*

*Submitted to the Council of the College of Science, University of  
Babylon in Partial Fulfillment of the Requirements for the  
Degree of Doctorate of Philosophy in Physics*

*By*

**Inaam Hani Kadhim Hadi**

B.Sc. in Physics /2005  
M.Sc. in Physics / 2012

Supervised by

**Prof. Dr. Khalid Hussain Hatif Al-Attayah**

**2021 A.D**

**1443 A.H**

بِسْمِ اللَّهِ  
الرَّحْمَنِ الرَّحِيمِ  
\*يَرْفَعُ اللَّهُ الَّذِينَ  
آمَنُوا مِنْكُمْ  
وَالَّذِينَ أُوتُوا  
الْعِلْمَ دَرَجَاتٍ وَاللَّهُ  
بِمَا تَعْمَلُونَ خَبِيرٌ\*

صَدَقَ اللهُ الْعَلِيُّ

الْعَظِيمِ

{ سُورَةُ الْمَجَادِلَةِ }

(الآيَةُ - 11)

*Dedication*

*To my great parents who gave their love and encouragement and sacrificed their time to teach me the value of hard work and study.*

*To those who inspired me, encouraged me, stood by me step by step, and gave me strength, patience, love and tenderness to my dearest friend (Balsam).*

**Inaam**

### ***Acknowledgments***

**Praise be to Allah, the merciful, the beneficent.**

The first and deepest gratitude goes to Allah for his uncountable blessings, lord of the whole creation and peace is upon his messenger Mohammad for giving me strength to accomplish this thesis.

I would like to express my great thanks to my supervisor and spiritual father, **Prof. Dr. Khalid Hussain Hatif** for his supervision, guidance and valuable opinions.

My great thanks are expressed to the head of the department of physics the dean of the college of science and staff of the Physics department at University of Babylon to help me during the study period and to all my postgraduate colleagues and all friends Specially **Ameera Hassan Salim** and **Salar Hussain Ibrahim**.

Finally, I would like to thank each person who was hopes me, whether directly or indirectly .

With my regards to all

**Inaam**

## *Contents*

Subjects	Pages
Summary	I

List of Figures	III
List of Tables	VI
List of Symbols and Abbreviations	IX

No.	Subjects	Pages
<b>Chapter One " General Introduction"</b>		
1.1	Introduction	1
1.2	Literature Review	2
1.3	Aims of The Work	13
<b>Chapter Two "Theoretical Part"</b>		
2.1	Introduction	14
2.2	Statistical Computing in Programming Language R	14
2.2.1	Statistical Features of R	15
2.2.2	Programming Features of R	16
2.2.3	Programming in R	16
2.2.4	Advantages of R	17
2.2.5	Applications of R	17
2.3	Statistical Applications	19
2.3.1	Mean and Standard Deviation	20
2.4	Random Variables	21
2.5	Probability Distributions in the R Statistical Program	23
2.5.1	Binomial Distribution	23
2.5.2	Poisson Distribution	25
2.5.3	The Uniform Distribution	27
2.5.4	The Exponential Distribution	27
2.5.5	The Normal Distribution	28
2.6	Normality Tests and Homogeneity of Variances Tests	31
2.6.1	Kolmogorov-Smirnov Test and Shapiro-Wilk Test	31
2.6.2	Q-Q Plot	32

2.6.3	Bartlett's Test	32
2.6.4	T-Test Independent Samples	33
2.6.5	Wilcoxon Test	33
2.7	Correlation and Regression	33
2.8	Simple Linear Regression	34
2.9	Multiple Linear Regression	35
<b>Chapter Three "Experimental Part"</b>		
3.1	Introduction	37
3.2	Gamma Spectroscopy System	37
3.2.1	The NaI(Tl) Detector	38
3.2.2	Preamplifier	38
3.2.3	Main Amplifier	38
3.2.4	High Voltage Power Supply	39
3.2.5	Multichannel Analyzer	39
3.2.6	Computer	39
3.3	Radioactive Sources	39
3.4	Gamma-Ray Spectra	40
3.4.1	Total Area of Spectrum (T.A.)	41
3.4.2	Net Total Area (N.T.A.)	41
3.4.3	Cross Total Area (C.T.A.)	41
3.4.4	Photopeak Area (P.P.A.)	41
3.4.5	Photopeak Net Area (P.N.A.)	41
3.4.6	Photopeak Cross Area (P.C.A.)	41
3.4.7	Energy Resolution	42
3.5	UCS-30 Universal Computer Spectrometer	43
<b>Chapter Four " Results and Discussion"</b>		
4.1	Spectrum for Total area and Photopeak	45
4.2	Spectrum for Energy resolution and P/V ratio	55

4.3	Normality Test	65
4.4	Correlation and Regression	
4.5	Statistical Distributions	99
<b>Chapter Five "Conclusions and Recommendations"</b>		
5.1	Conclusions	120
5.2	Future Work	121
<b>References</b>		121-129
<b>Appendices</b>		130



## Summary

There are some phenomena in nuclear physics do not have a clear and direct explanation, such as the phenomenon of radioactive decay and nuclear fission so, they are based on statistics and probability. Therefore, in this study, the laws of statistics and statistical programming were used, represented by the R programming language to study the decay and interaction of gamma rays in cesium, cobalt and sodium sources by collecting 200 spectra for each source and studying the spectral regions of radioactive sources in terms of the total area of the spectrum, the photopeak area, energy resolution and peak/valley ratio before and after the subtract the background radiation.

The R programming language is a widely used open source system for statistical analysis and statistical programming was used in calculating the statistical applications represented by the mean, median, variance and standard deviation, as it was noted that these values applications before the subtract background radiation are greater than it is after the subtract background radiation for all the studied samples for the radioactive sources used.

It was also found in the  $^{137}\text{Cs}$  source samples that the median value was greater than the mean which means that the data is asymmetric, in contrast to the samples for  $^{60}\text{Co}$  and  $^{22}\text{Na}$  sources where the mean was greater than the median for  $^{60}\text{Co}$  and  $^{22}\text{Na}$  respectively.

The normality tests and homogeneity of variances tests were calculated by the R programming language was found that all the samples studied were homogeneous. For Pearson's coefficient it was found that there is a direct relation between the number of samples and the total area whether before or after the subtract

the background radiation. Also, by the linear regression test was found that linear relation between the total area and the number of samples.

Statistical distributions such as the binomial distribution, Poisson distribution, exponential distribution, uniform distribution and normal distribution were also calculated on the studied samples it had been found that these distributions dose not succeed to give a clear explanation for the behavior of radioactive decay, which requires reconsidering the prevailing concept about the random nature of decay, which means that more studies and research should be done in this field. So that the use of different distributions and methods to try to get a better explanation for this phenomenon.

## *List of Figures*

<b>Figure (2-1)</b>	R Graphical user interface	15
<b>Figure (2-2)</b>	The interface of R-Studio	18
<b>Figure (2-3)</b>	Central 95% of the standard normal distribution	30
<b>Figure (3-1)</b>	Explanation of the electronic system used	37
<b>Figure (3-2)</b>	Gamma spectrum	40
<b>Figure (3-3)</b>	Net and Cross Photopeak	42
<b>Figure (3-4)</b>	Gamma spectrometer system, UCS-30	43
<b>Figure (3-5)</b>	Demonstrates a sample of a gamma-ray spectrum in the USC-30 program window	44
<b>Figure (4-1)</b>	The general behavior of total area before and after subtraction background for $^{137}\text{Cs}$ source a-Net. b- Cross	47
<b>Figure (4-2)</b>	The general behavior of photopeak before and after subtraction B.G. for $^{137}\text{Cs}$ source a-Net. b- Cross	48
<b>Figure (4-3)</b>	The general behavior of total area before and after subtraction B.G. for $^{60}\text{Co}$ source a-Net. b- Cross	50
<b>Figure (4-4)</b>	The general behavior of photopeak before and after subtraction B.G. for $^{60}\text{Co}$ source a-Net. b- Cross	51
<b>Figure (4-5)</b>	The general behavior of total area before and after subtraction B.G. for $^{22}\text{Na}$ source a-Net. b- Cross	53
<b>Figure (4-6)</b>	The general behavior of photopeak before and after subtraction B.G. for $^{22}\text{Na}$ source a-Net. b- Cross	55
<b>Figure (4-7)</b>	The general behavior for energy resolution before and after subtraction B.G. for $^{137}\text{Cs}$ source. for E.R.	57
<b>Figure (4-8)</b>	The general behavior for energy resolution before and after subtraction B.G. for $^{60}\text{Co}$ source	59
<b>Figure (4-9)</b>	The general behavior for energy resolution before and after subtraction B.G. for $^{22}\text{Na}$ source	61
<b>Figure (4-10)</b>	The general behavior for P/V ratio before and after subtraction B.G. for $^{137}\text{Cs}$ source	62
<b>Figure (4-11)</b>	The general behavior for P/V ratio before and after subtraction B.G. for $^{60}\text{Co}$ source	63

<b>Figure (4-12)</b>	The general behavior for P/V ratio before and after subtraction B.G. for $^{22}\text{Na}$ source	64
<b>Figure (4-13)</b>	Comparative of sampling mean by T-Test for total area of $^{137}\text{Cs}$ source. 1- N.T.A. 2- C.T.A.	68
<b>Figure (4-14)</b>	Comparative of sampling mean by T-Test for photopeak area of $^{137}\text{Cs}$ source. 1. P.N.A. 2. P.C.A.	69
<b>Figure (4-15)</b>	Comparative of sampling mean by T-Test for total area of $^{60}\text{Co}$ source. 1- N.T.A. 2- C.T.A.	70
<b>Figure (4-16)</b>	Comparative of sampling mean by T-Test for photopeak area of $^{60}\text{Co}$ source. a & b P.N.A. 1 (before and after). c & d P.N.A. 2 (before and after subtraction B.G.).	71
<b>Figure (4-17)</b>	Comparative of sampling mean by t-test for total area of $^{22}\text{Na}$ source. a- N.T.A. b- C.T.A.	72
<b>Figure (4-18)</b>	Comparative of sampling mean by t-test for photopeak area of $^{22}\text{Na}$ source. a & b P.N.A.1 (before and after). c & d P.N.A.2 (before and after subtraction B.G.).	73
<b>Figure (4-19)</b>	Comparative of sampling mean by T-Test for energy resolution of $^{137}\text{Cs}$ source. a- before b- after subtraction B.G.	76
<b>Figure (4-20)</b>	Comparative of sampling mean by T-Test for energy resolution of $^{60}\text{Co}$ source. a & b E.R. 1 c & d E.R.2.	77
<b>Figure (4-21)</b>	Comparative of sampling mean by T-Test for energy resolution of $^{22}\text{Na}$ source. a & b E.R. 1 c & d E.R. 2.	77
<b>Figure (4-22)</b>	Comparative of sampling mean by T-Test for P/V ratio of $^{137}\text{Cs}$ source. a- before b- after subtraction B.G.	78
<b>Figure (4-23)</b>	Comparative of sampling mean by T-Test for P/V ratio of $^{60}\text{Co}$ source. a- & b p/v ratio 1 c- & d p/v ratio 2.	79
<b>Figure (4-24)</b>	Comparative of sampling mean by T-Test for P/V ratio of $^{22}\text{Na}$ source. a & b p/v ratio1 (before and after subtraction B.G.). c & d p/v ratio2 (before and after subtraction B.G.).	80
<b>Figure (4-25)</b>	Q-Q-Norm to spread of data for samples for $^{137}\text{Cs}$ source. a- T.A. b- P.P.A. c -R.E. e- p/v ratio.	81
<b>Figure (4-26)</b>	Q-Q-Norm to spread of data for samples for $^{60}\text{Co}$ source. a- T.A. b- P.N.A. c- P.C.A. d -R.E. e- P/V ratio	83

<b>Figure (4-27)</b>	Q-Q-Norm to spread of data for samples for $^{22}\text{Na}$ source. a- T.A. b- P.N.A. c- P.C.A. d -R.E. e- P/V ratio	84
<b>Figure (4-28)</b>	Multiple Linear Regression for $^{137}\text{Cs}$ Source of all samples (1,2,3 and 4)	94
<b>Figure (4-29)</b>	Multiple Linear Regression for $^{60}\text{Co}$ Source of all samples (1,2,3,4 and 5)	99
<b>Figure (4-30)</b>	Multiple Linear Regression for $^{22}\text{Na}$ Source of all samples (1,2,3,4 and 5)	105
<b>Figure (4-31)</b>	Poisson distribution for radioactive sources	107
<b>Figure (4-32)</b>	Exponential distribution for total area of $^{137}\text{Cs}$ source A- before subtraction B.G. B-after background	108
<b>Figure (4-33)</b>	Exponential distribution for total area of $^{60}\text{Co}$ source A- before subtraction B.G. B-after subtraction B.G.	109
<b>Figure (4-34)</b>	Exponential distribution for total area of $^{22}\text{Na}$ source A- before subtraction B.G. B-after subtraction B.G.	109
<b>Figure (4-35)</b>	Uniform distribution for $^{137}\text{Cs}$ source A -before subtraction B.G. B-after subtraction B.G.	111
<b>Figure (4-36)</b>	Uniform distribution for $^{60}\text{Co}$ source A -before subtraction B.G. B-after subtraction B.G.	112
<b>Figure (4-37)</b>	Uniform distribution for $^{22}\text{Na}$ source A -before subtraction B.G. B-after subtraction B.G.	113
<b>Figure (4-38)</b>	Normal distribution for $^{137}\text{Cs}$ source a-Total area b- Photopeak area c-Energy resolution d- P/V ratio	115
<b>Figure (4-39)</b>	Normal distribution for $^{60}\text{Co}$ source a-Total area b- Photopeak area c-Energy resolution d-P/v ratio	116
<b>Figure (4-40)</b>	Normal distribution for $^{22}\text{Na}$ source a-Total area b- Photopeak area c-Energy resolution d- P/V ratio	117

## *List of Tables*

<b>Table (3-1)</b>	Radioactive Sources Used in This Study	40
<b>Table (4-1)</b>	Summary Spectrum $^{137}\text{Cs}$ for Total Area and Photopeak.	45
<b>Table (4-2)</b>	Summary Spectrum $^{60}\text{Co}$ for Total Area and Photopeak.	49
<b>Table (4-3)</b>	Summary Spectrum $^{22}\text{Na}$ for Total Area and Photopeak.	52
<b>Table (4-4)</b>	Summary Spectrum $^{137}\text{Cs}$ for Energy Resolution and P/V Ratio.	56
<b>Table (4-5)</b>	Summary Spectrum $^{60}\text{Co}$ for Energy Resolution and P/V Ratio.	58
<b>Table (4-6)</b>	Summary Spectrum $^{22}\text{Na}$ for Energy Resolution and P/V Ratio.	60
<b>Table (4-7)</b>	Normality for Total Area and Photopeak Area of Three Sources.	65
<b>Table (4-8)</b>	Normality for E.R and p/v Ratio for Three Sources.	74
<b>Table (4-9)</b>	Pearson Correlation for $^{137}\text{Cs}$ Source.	85
<b>Table (4-10)</b>	Pearson Correlation for $^{60}\text{Co}$ Source.	86
<b>Table (4-11)</b>	Pearson Correlation for $^{22}\text{Na}$ Source.	88
<b>Table (4-12)</b>	Linear Regression Test for $^{137}\text{Cs}$ Source.	90
<b>Table (4-13)</b>	Multiple Linear Regression for $^{137}\text{Cs}$ Source.	91
<b>Table (4-14)</b>	Linear Regression Test for $^{60}\text{Co}$ Source.	95
<b>Table (4-15)</b>	Multiple Linear Regression for $^{60}\text{Co}$ Source.	96
<b>Table (4-16)</b>	Linear Regression Test for $^{22}\text{Na}$ Source.	100
<b>Table (4-17)</b>	Multiple Linear Regression $^{22}\text{Na}$ .	102

## *List of Symbols and Abbreviations*

Symbols	Meaning
Preamp	Primary amplifier
Amp	Main amplifier
H.V.	High voltages
MCA	Multi-Channel Analyzer
T.A.	Total Area of Spectrum
N.T.A.	Net Total Area
C.T.A.	Cross Total Area
P.P.A.	Photopeak Area
P.N.A.	Photopeak Net Area
P.C.A.	Photopeak Cross Area
B.G.	background
P.N.A.bef.	Total net area before subtraction background
P.N.A.aft.	Total net area after subtraction background
P.C.A.bef.	Total cross area before subtraction background
P.C.A.aft.	Total cross area after subtraction background
E.R.bef.	Energy resolution before subtraction background
E.R.aft.	Energy resolution after subtraction background
P/V.bef.	Peak/valley ratio before subtraction background
P/V.aft.	Peak/valley (p/v) ratio after subtraction background
RGui	R Graphical User Interface
UCS-30	Universal Computer Spectrometer
GPL	General Public License
CRAN	Comprehensive R Archive Network
X	Random variable
x	Value samples
d	Probability density function
p	Cumulative distribution function
q	The quantile function
r	Random variable Probability
mu	Expectation value (mean parameter $\mu$ )

<b>Symbols</b>	<b>Meaning</b>
sigma	Standard deviation (parameter $\sigma$ ).
ks. test	Kolmogorov-Smirnov Test
IQR	the quartile range which is the distance between the third quartile (3rd Qu) an account of the first (1st Qu)
$\mu$	The mean for population
var	The variance to sample
$\sigma$	The variance to population
x.bar	Standard mean
sd	Standard deviation
o-up	Max outliers
o-down	Min outliers
$\lambda$	Rate of the distribution
a	The minimum value at uniform distribution
b	The maximum value at uniform distribution



# **Chapter one**

## **General Introduction**

# Chapter One

## General introduction

### 1.1 Introduction

There are some phenomena in nuclear physics that do not have a direct explanation and are not subject to clear laws, so they are based on probability and statistics theory [1]. These phenomena include radioactive decay [2], decay of compound nuclei [3], nuclear fission products [4], and nuclear reactions [3]. There are many studies on this topic from a statistical point of view [5].

The emission of photons from a radioactive source is a random process, that is, the number of emitted radiation is subject to a certain degree of statistical fluctuation and this makes it difficult to obtain an accurate measurement of the radioactivity as the random distribution reduces the ability to see and discover objects with low contrast [4] so a continuous change is made in source activity from one moment to the next due to the random nature of radioactive decay and there are also fluctuations in the rate of decay due to the half life of the radionuclides [2]. Meaning, when repeating the same measurement several times, we will notice that the number of recorded charges of the spectrum varies for each of them, and this is a natural difference because over time an error occurs in measuring the activity and it is statistically called an error in counting [1], as the observed values are distributed around the sample mean and this is the best estimate true value. Moreover, theoretical statistical distributions can assist in determining the extent to which the sample mean deviates from the true value [5].

A scintillation detector was used to explore the statistics of independent random events in physical measurements of gamma rays. And obtaining our experimental results, then using statistical and software distributions on experimental data as an attempt to understand and explain the random nature and monitor these nuclear phenomena that are subject to any law and then discuss this result.

In this study R is used which is a programming language and analytics tool widely used by software programmers, statisticians, data scientists and data miners. It is one of the most popular analytics tools used in data analytics and business analytics. It has many applications in fields such as healthcare, academics, consulting, finance, media and many more. Its wide application in statistics, data visualization and machine learning has increased the demand for trained professionals certified in R [6].

## **1.2 Literature Review**

There are several substantial developments in both the hardware and software which used at nuclear spectrometry over the recently. In order to minimize statistical noise and routine data processing, substantial changes have been made in the computer processing power of full spectrum measurement methods new ways to refine and present the data have also been created and these developments have significantly improved the amount of useful information that can be derived from the gamma spectrum. Here, we are going to present some studies in this field:

In 1966, (Wainio and Knoll) [7] used a Monte Carlo program to calculate the properties of fully depleted silicon and germanium radiation detectors' responses to gamma rays, the computations are expected to be applicable in circumstances where

secondary electron energies do not exceed 2 MeV, and Bremsstrahlung energy loss by secondary electrons is also calculated.

In 1974, (Lima and Atalla) [8] proposed a program in the language "INSTRUMENT BASIC" to analyze gamma ray spectra that were collected using Ge(Li) detectors with a program in a "basic" language to analyze gamma spectra. where the software determines the location of the peaks, evaluates the corresponding power values, the net-peak areas and the standard deviations of the spectrum regions.

While (Gavron) in 1980 [9], used the statistical model calculations for experiments of nuclear reactions and nuclear fusion and made a comparison between the practical experiments of heavy ions with the predictions of calculations of statistical models and found that in some interactions there are non-statistical effects based on large differences between the calculations and the experimental results.

(Aarnio, *et al.*) in 1995 [10], developed the SAMPO system to identify radionuclides and specify spectrum component characteristics in gamma spectrum analysis, employing the C programming language, which may be used in a wide range of computer environments. The performance of the system was evaluated using test standard source group and activation analysis measurements, and also composite spectra were used, and the results of these tests showed that the expert system works very well, even for difficult spectra.

In 1997, a simulation technique was developed by (Hovgaard and Grasty) [11] to analyze and process gamma-ray data to determine the nuclear spectrum. The technique contains 256 channels of a survey data set. Data analysis simulations for uranium and thorium have shown that statistical noise reduction is equivalent to increasing the detector size by a typical factor between 3 and 4. This technique can be applied to any series of gamma spectrum measurements.

(Gontchar, *et al.*) in 1997 [12], calculated the decay of highly excited nuclei by splitting the nucleus using a giant-quanta statistical model in the C language by coupling the Monte Carlo algorithm with the fission dynamics, where the program calculates the fission probabilities, mean distributions, variances, correlation of observations, and the average energies of these particles. The code also provides the possibility to investigate the effect of different nuclear friction shape factors on the quantities that can be observed.

In 1999, (Theisen, *et al.*) [13], improved the processing of gamma ray high-efficiency data using germanium detectors. It was tested on statistical datasets and found that this method leads to an increase in the weakness of the spectrum quality and efficiency. It is also found that the uncertainty is affected by an increase or decrease in the width of the gates.

(Aarnio, *et al.*) in 2001 [14], used UNISAMPO's extensive gamma-spectrum processing program, analyzing 32,000 spectrums, i.e., up to 2,500 peaks and containing 1024 channels and peak analysis according to strict statistical criteria in addition to the interface of the SHAMAN system used. For peak identification and large-scale radionuclide identification.

In 2003 (Simonits, *et al.*) [15], studied the development of a versatile gamma spectroscopy program using object-oriented design that provides a comprehensive environment for acquisition and analysis of gamma spectra in personal computers. The method uses the base form of DAVIDON6 with modified FLETCHER, which greatly increases the optimization efficiency of the Ge detector. HyperLab also uses the Broyden-Fletcher-Goldfarb Hanno (BFGS) algorithm, which is generally considered superior to the Davidon-Fletcher-Powell approach.

In 2005 (Jiamei, *et al.*) [16], studied the effect of reducing the statistical fluctuations of gamma spectra by simulating wavelet analysis in which several hundreds of gamma spectra were randomly generated for a statistical computation. They found that the statistical fluctuation of the enumerations in each channel can be reduced many times by removing the wave noise, but the correlation of the data between the channels should be noted.

In 2006, (Pattabirama, *et al.*) [17], developed a new analytical method for estimating and subtracting random coincidences in X-ray spectroscopy: It uses enumerations to perform back subtraction automatically to obtain multiple times the gamma-ray data to estimate events arising from random coincidences.

While (Neti and Howell) in 2008 [18], worked a statistical study to see how Poisson's statistics affect the interpretation of spontaneous radiometric data. Each cell's measured distributions were submitted to Poisson, LN, and Poisson-lognormal statistical tests (P-LN). This statistical research backs up the idea of utilizing LN distributions to describe radioactivity absorption. When examining data from spontaneous radioactive distributions, extreme caution is essential to guarantee that Poisson processes do not alter the main LN distribution.

(John, *et al.*) used in 2009 [19], developed a set of Poisson statistical tools using the area of direct interest approach (ROI) to analyze gamma ray spectra, based on the assumption that the Poisson distribution can be approximated to the Gaussian distribution, and because Gaussian approximation fails when the standard deviations are far from the mean. So, they created a set of Poisson statistical tools, to detect and quantify signals in spectroscopy, as these tools provide improved accuracy compared to traditional Gaussian methods in both quantitative evaluation and qualitative detection of small peaks, determining the net peak area and its

uncertainties, and expecting Poisson statistics to be applied in enumeration experiments. Neutrons, alpha and beta.

In 2010 (Mathkour, *et al.*) [20] studied radioactive decay using an algorithm based on a simulation in which the Monte Carlo method was used as a stochastic process to determine when radioactive decay appears exponential and when it appears random while, the simulation is based on the analytical equation with clarification of charts and graphs.

In the same year, (Wasim, *et al.*) [21] conducted a statistical analysis of gamma spectroscopy data by identifying background components in a gamma spectrophotometric laboratory using MATLAB and Microsoft Excel software. The results of the analysis showed the compatibility of the data presented with the background spectra, and indicated that the increase in the number of peaks after 24 hours from the time of acquisition becomes insignificant and these tools will be applied to quality control in gamma ray measurements the others.

While (Shumakov and Kasatkin) compared in 2010 [22] statistical methods for radiation detection using Monte Carlo simulation algorithms for statistical analysis of information received from radiation monitoring devices. The results of the comparative analysis showed that the best results can be obtained from the detection method by combining Poisson distribution with probability methods in a Gaussian distribution.

In 2012, (Dam, *et al.*) [23] studied the statistical distribution of the number of scintillation photons computed in dSiPMs where a probabilistic model of the number of calculated scintillation photons was developed. Relationships of rate and variance values in the number of cells fired were inferred and suggested as an

accurate method for correcting the energy spectra measured by dSiPM-based scintillation detectors.

(Kawano, *et al.*) in 2012, [24] based on the Monte Carlo Hauser-Feshbach (MCHF) hypothesis, a code for simulating a Monte Carlo emission of neutrons and gamma rays from a composite nucleus was developed. Nuclear reactions can be examined at a tiny level. As long as the compound nucleus' excitation energy is greater than the neutron separation energy, CGM can emit multiple neutrons.

Also in 2012, (Adam and Eltaye)[25] used several statistical methods to study radionuclides in phosphate deposits. Pearson's coefficient showed that the distribution in  $^{238}\text{U}$  phosphate is controlled by varying the concentration of  $^{40}\text{K}$ , and the Q-Q plots showed that the radioactive variables. This observed abnormal feature may be attributed to the influence of complex geological factors.

In 2013 (Hauf, *et al.*) [26] studied radioactive decay measurement using HPGe detector and compared the Geant4 simulation with the experimental setup HYPERMET software. Two different approaches were used to model the radioactive decay, the simulation showed that the general features of the measurements could be reproduced appropriately, statistical sampling produces a more precise simulation of the photopeak and its position, according to the statistical analysis of the experimental data for each decay.

Also, in 2013, (Jinzhao and Xianguo) [27] proposed a new algorithm to remove noise from the gamma ray spectrum that was measured by the HPGe detector with high accuracy, which measures the statistical oscillation and scattering properties for accuracy, and found that the algorithm does not only overcome noise and the Gibbs phenomenon. Pseudo is in the spectrum, but it also maintains its characteristic peak shape.



In the same year, (Ahmed, *et al.*) [28] presented a statistical model to determine the formation factor of the alpha decay process in the radioactive nuclei. This model was tested for  $^{212}\text{Po}$  for the decay of the alpha group and the results obtained showed the presence of an alpha particle and thus can be used to predict the cluster radioactivity, and this model can give further insight into understanding the nuclear structure in radioactive nuclei.

While in 2014 (Ravisankar, *et al.*) [29] analyzed and statistically treated the radiometric data measured for the gamma ray spectrum in radionuclides and to determine the similarities and correlations between the different samples. The resulting tree diagram was classified into Hierarchical Mass Analysis (HCA) divided into four groups. Each group contains 15 variables. And by using the Pearson correlation coefficient, it was found that the distribution of  $^{226}\text{Ra}$  in building materials is controlled by the contrast concentration of 40 thousand .

In 2015, (Yoon *et al.*) [30] conducted a statistical analysis of instantaneous gamma activity using a Monte Carlo statistical simulation. Through simulations, they were able to distinguish between nine gamma ray peaks resulting from 14.1 MeV neutron particles for each of the detector materials .

In the same year, studied (Batmunkh, *et al.*) [31] the pathways of particles emitted by radionuclides and their radioactive decay within the DNA in the cell nucleus using Monte Carlo simulations, they computed the deposited energy's radial distribution as well as the kinetic energy spectrum of electrons produced by decaying elementary particles. Radiation to different radionuclides in the cell nucleus. The G4-RadioactiveDecay and low energy electromagnetic pulses from the Geant4 Monte-Carlo package were used to accomplish this.

(Sitek and Celler ) noted in 2015, [32] the imprecision of Poisson's statistics in describing nuclear decomposition, when data acquisition times exceed the half-life of radioisotopes in a sample, this method becomes worthless. Poisson statistics are erroneous in such instances, according to the study, and should not be used to calculate decay statistics for radioactive materials.

In 2016 ( Kalfas ,*et al.*) [33] introduced a software package for use in nuclear spectroscopy and sample analysis, spectroscopy simulation, assessment of detection system performance, background assessment, and identification of possible elements and isotopes so that SPECTRW can analyze and display up to 8 spectra simultaneously.

Also, in 2017, (Lorusso, *et al.*) [34] using Monte Carlo simulations to address the difficulties in radiological analysis, and presented the first experimental model to measure the half-life of a radioisotope ( $^{211}\text{Pb}$ ). where work focused on the comparison between statistical sampling and exponential regression analysis, and concluded that exponential regression gives results with higher accuracy.

In the same year (Schlattauer, *et al.*) [35] developed a gamma ray spectroscopy system for recording and processing spectra using Gaussian photopeak synthesis in multichannel spectra with a LabVIEW-based digital system. The application of the developed system has been successfully tested in the design of spectrometry systems in the laboratories of the experimental physics department.

Whereas (Dayman and Weber) [36] presented, in 2018, a study on analyzing the gamma ray spectrum using an experimental database extracted from the composition of spent nuclear fuel isotopes. A statistical method called the quantitative comparator was developed and analyzed using simulation of radioactive

nuclear fuel. The study led to Development of classification and analysis methods for known and used data library to analyze unknown data.

Also, in 2018, (Lindell *et al.*) [37] presented a study on how to distinguish MOX from UOX fuels based on the consistency of specified fission products and the resulting gamma ray emissions, through statistical analysis of the gamma ray spectrum with high accuracy using MathWorks MATLAB. Theoretically, the findings of the nuclear fuel simulations showed that the nuclear fuel elements can be classed as UOX or MOX. To distinguish between MOX and UOX PWR fuel groups, gamma-ray spectroscopy and multivariate statistical techniques have shown to be efficient.

In 2019, (Lam and Zhang) [38] created an algorithm to analyze and measure  $^{22}\text{Na}$  &  $^7\text{B}$  spectra and determine the FWHM peak using the Python programming language. By using HPGe detector, and linear regression model to remove any background and residual noise, where determining the maximum and minimum peak is critical to achieving the accuracy of the gaussian distribution of the peak, the study has proven that the algorithm and the software provide a reliable and effective method for analyzing radioactivity for radionuclides .

Also, in 2019, (F. Li, *et al.*) [39] determined the accuracy of the qualitative and quantitative analysis of radionuclides through the gamma spectrum detection, through the development and application of gamma spectrum algorithms and technology in reducing noise, subtracting background, separating overlapping peaks.

In 2020 (Kejzlar, *et al.*), used [40], a number of statistical methods and diagnostic tools, including bayesian model rate calibration, chi-square correlation analysis, also used BMA to improve predictions and uncertainty estimation of the LDM model, and the results showed that the use of standard statistical software and

tools called for by this work would be useful in further studies of nuclear models, in particular-the quasi-experimental mass formula and the realistic parameter Skyrme density function energy.

In the same year, (Longo, *et al.*) [41] used algorithms describing the performance and shape of the CsI(Tl) pulse and then compared with the newly developed CsI(Tl) luminescence response simulation. It was observed that when combined with GEANT4 simulation, it would allow modeling of the adopted scintillation response. On particles to CsI(Tl) pulse. Comparisons between data and simulations show that pulse shape recognition could be a new tool for identifying sources of improvement in simulating hadronic reactions in nuclear materials

Also, in 2020, created (Fanto, *et al.*) [42] a statistical model describing the decay of the compound nucleus. According to this statistical model, the partial decay width of the composite nucleus' resonance will be subject to significant fluctuations in the Porter-Thomas distribution (PTD) inside a random matrix model. They discovered that, as expected by the statistical model, PTD accurately depicts the distribution of partial widths of all decay channels. They discovered that the distribution of total-decay widths is relatively narrow, and that it is unaffected by large changes in the strength function parameters, as well as partial width distribution deviations from PTD. As a result, the results rule out an explanation of current experimental data within the composite nucleus statistical model's description.

(Amado, *et al.*) [43] presented in 2021, a theoretical formula for determining the total peak power by calculating the total efficiency and peak and calculating the total area which is widely used in gamma ray spectroscopy, using five different detectors, two iodide detectors NaI (Tl) and three HPGe detectors with different

crystal sizes and energies. The compatibility of this theory with Monte Carlo simulations and available experimental data .

In 2021, (Fernandez, *et al.*) [44] introduced a program to analyze gamma detector response using NaI(Tl) (3"x3") and radiation source neutron detector (GADRAS-DRF) using spectroscopy simulation for isotope identification, photopeak and Compton calculation, and estimation of source energy distributions. The isotopes presented in the ANSI standard are analogues commonly used for medical, industrial and military purposes, and it is recommended for inclusion in mobile devices with which device libraries function as input to the deep learning model .

In the same year, (Belgya and Szentmiklósi) [45], modeled the response function of the HPGe detector at the Budapest PGAA station was modeled using the GEANT4 Monte Carlo approach. The experimentally measured  $^{60}\text{Co}$  spectrum was found to be quite near to the Monte Carlo response function for the 1173 and 1332 keV peaks. After the impurity spectra are removed, and the resulting spectrum uncertainty is calculated, according to the study, the results of the used detection methods are consistent with spectroscopy.

In 2021, the idea of study presented by (Vraničar, *et al.*) [46], was to test the applicability of one of two mathematical calculation software EFFTRAN and Angle for the purpose of accurately determining the radioactivity concentrations compared to the simulation method (GEANT 4).T study showed that the results obtained are useful in measures gamma spectrum and does not contain commercial programs designed to analyze nuclear radioactive materials for nuclear energy.

Whereas (Bukartas, *et.al.*) estimate in 2021, [47] the location and activity of the point gamma source by performing a Bayesian algorithm on the measurement

data and using two detectors (HPGe and NaI (Tl)) was found that the introduction of angular efficiency differences for the detection devices improved the accuracy of the activity estimation slightly, while the input of data from additional detectors significantly reduced the system's noise ratio increasing the stability and accuracy of detection of source location and activity.

Also, in the same year, (André, *et al.*) [48], determine radionuclide and quantitative investigation of beta-emitting radionuclides in natural background radiation by analyzing the overall spectrum in scintillation detectors NaI(Tl) and estimating standard deviations using Fisher information matrix and Monte Carlo simulations. The Gaussian approximation is confirmed for coverage periods and a satisfactory evaluation of standard deviations is produced, the suggestion method can be used to do automatic spectrum analysis and to aid specialists in making decisions when dealing with complex emitter spectra.

### **1.3 Aims of The Work**

The purpose of this project is to employ statistical models and codes to try to obtain a more comprehensive and clear understanding of the random behavior of nuclear phenomena, because we believe that there is no such thing as randomness, but existence of accurate laws. As a result, the field of statistics and probability is unable to come up with interpretations, and the only way can do it is to use our practical results and the latest codes in this field such as language R programming statistical.

# **Chapter Two**

## **Theoretical Part**

### **2.1 Introduction**

The application of computer science to statistics was known as statistical computing [49]. It's used in a variety of fields, sciences, and statistics, including biometrics, data analysis, graphics, simulations, algorithms, and Bayesian computing. In addition to mathematically intensive statistical methods including reduction methods, Markov chain Monte Carlo methods and linear regression and others. Computational statistics tries to build an algorithm for implementing statistical procedures on computers [50]. There are many statistical programs that may distinguish one from the other by simple treatment or may not differ except in its name [49]. Among the programs specialized in statistical computing are (MATLAB, Minitab, R, S, Excel, SPSS) [50].

### **2.2 Statistical Computing in Programming Language R**

R is an open-source programming language that is widely used as a statistical software and data analysis tool. R generally comes with the command-line interface. R is available across widely used platforms like Windows, Linux, and macOS [51]. Also, the R programming language is the latest cutting-edge tool.

It was designed by Ross Ihaka and Robert Gentleman at the University of Auckland, New Zealand, and is currently developed by the R Development Core Team. R programming language is an implementation of the S programming

language. It also combines with lexical scoping semantics inspired by Scheme [50]. The main interface of the program is shown in figure (2-1).

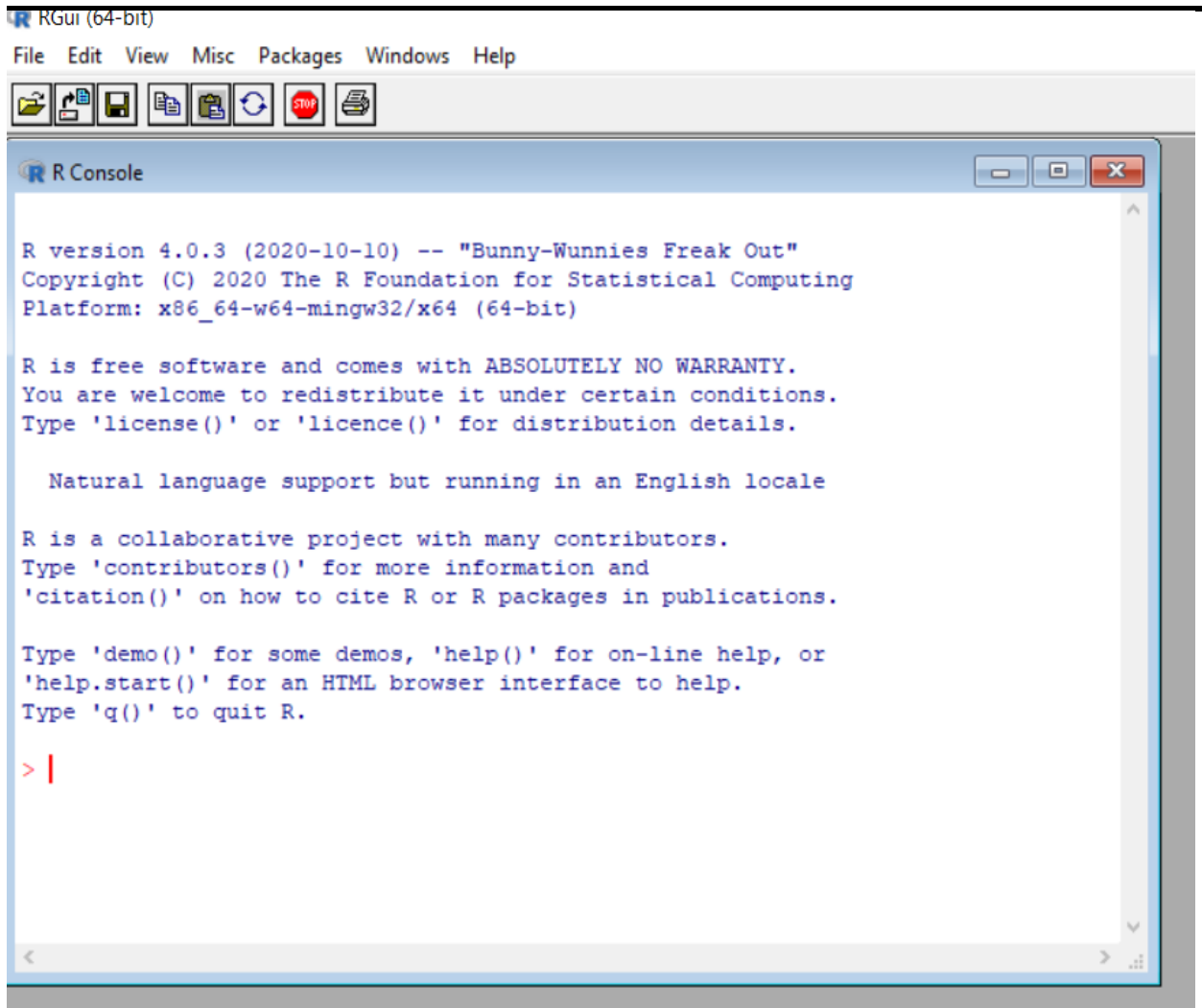


**Figure (2-1) R Graphical user interface.**

## 2.2.1 Statistical Features of R

Basic Statistics: The most common basic statistics terms are the mean, mode, and median. These are all known as "Measures of Central Tendency".



Static graphics: R is rich with facilities for creating and developing interesting static graphics. R contains functionality for many plot types including graphic maps, mosaic plots, biplots, and the list goes on [52].

Probability distributions: Probability distributions play a vital role in statistics and by using R we can easily handle various types of probability distribution such as Binomial Distribution, Normal Distribution, Chi-squared Distribution and many more [53].

Data analysis: It provides a large, coherent and integrated collection of tools for data analysis [54].

## **2.2.2 Programming Features of R**

R Packages: One of the major features of R is it has a wide availability of libraries. R has CRAN (Comprehensive R Archive Network), which is a repository holding more than 10,000 packages [53].

Distributed Computing: Distributed computing is a model in which components of a software system are shared among multiple computers to improve efficiency and performance. Two new packages used for distributed programming in R were released in November 2015 [54].

## **2.2.3 Programming in R**

Since R is much similar to other widely used languages syntactically, it is easier to code and learn in R. Programs can be written in R in any of the widely used IDE (Integrated development environment) like R Studio, Rattle, etc. After writing the program save the file with the extension R [52].

## **2.2.4 Advantages of R**

- 1- R is the most comprehensive statistical analysis package. As new technology and concepts often appear first in R [54].
- 2- As R programming language is an open source. Thus, you can run R anywhere and at any time [55].
- 3- R programming language is suitable for GNU/Linux and Windows operating system [53].
- 4- R programming is cross-platform which runs on any operating system.
- 5- R everyone is welcome to provide new packages, bug fixes, and code enhancements.

## **2.2.5 Applications of R**

- 1- R use for Data Science gives a broad variety of libraries related to statistics. It also provides the environment for statistical computing and design [52].
- 2- R is used by many quantitative analysts as its programming tool. Thus, it helps in data importing and cleaning [6].
- 3- R is the most prevalent language. So, many data analysts and research programmers use attach giants like Google, Facebook, Bing, Twitter, Accenture, Wipro and many more using R nowadays [53].

In this study, the latest available version R system, version 4.0.3,2020 was used. R-Studio use as an alternative to R as it is an open-source tool that provides Ide to use R language, and enterprise-ready professional software for data science teams to develop share the work with their team. In the case of running the

RStudio program, the screen appears as in figure (2-2), which is divided into four windows, and in each window, there are several tabs [54].

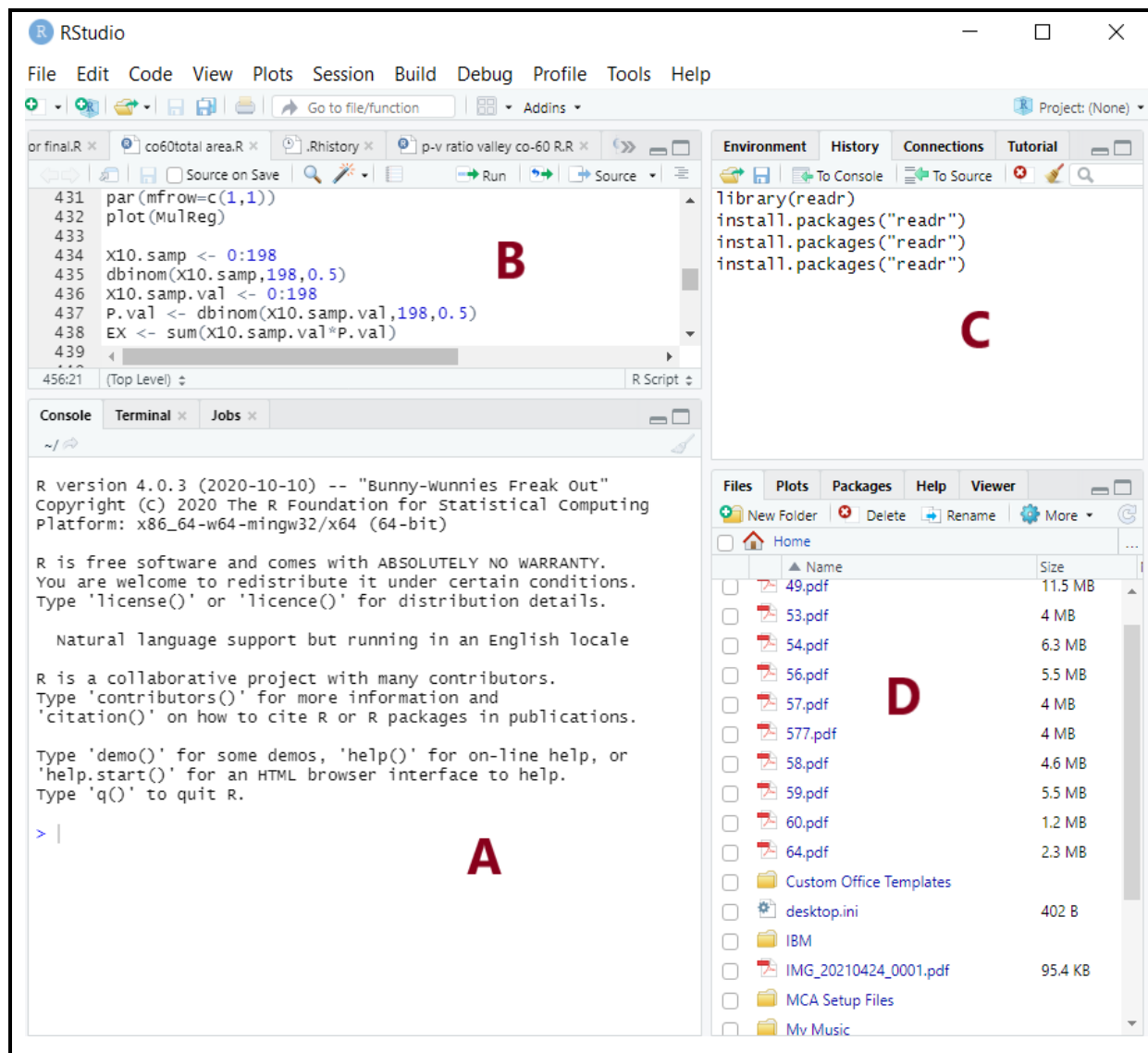


**Figure (2-2) The interface of R-Studio.**

A: Console, in which the commands are executed, and you can type the code or command that want to execute and then press Enter to be executed [55].

B: Editor Source, its commands can be written, modified, and saved to benefit from them later, and the line want can be executed by pressing Enter +

Ctrl and you can execute any part of the code by selecting it using the mouse and then also pressing Ctrl + Enter [55].

C : Workspace, Folder, Files History, can view the variables that have been defined, and in the clipboard the commands that have been executed appear, and can re-execute any instruction by simply clicking on it two clicks. As for files, the location from the hard disk that is being worked on is displayed [54].

D: Plots, Packages and Help, all drawings that drew in plots are displayed and can navigate between these drawings and save them. As for the package, it is a set of predefined methods, and R contains a lot of readymade packages that did not leave any aspect of the statistic until and entered it, and in this list can download the packages from the Internet and make updates and so on, while the help list provides with help on any matter type it into the search box[55].

## **2.3 Statistical Applications**

The statistical applications using R program are the aspect they show clearly the importance of this language in most important statistical operations by preparing easy to write the syntax or code phrase to get clear results and detailed. Statistical analysis in R is performed by using many in-built functions. Most of these functions are part of the R base package. These functions take R vector as an input along with the arguments and give the result. The following are a number of functions used in this study.

### 2.3.1 Mean and Standard Deviation

It is calculated by taking the sum of the values and dividing with the number of values in a data series, as Eq. [56]. The function **mean()** is used to calculate this in R.

$$\bar{x} = \frac{1}{n} \sum_{i=1}^n x_i = \sum_{x_i} (x_i * P(x_i)) \quad (2-1)$$

Where:

$\bar{x}$  : the sample mean

$x_i$  : numerical value

n : the number of data values in a sample

$\Sigma$  : means to add or to find the sum

$P(x_i)$ : the probability of x. (values multiplied by their respective relative).

The basic syntax for calculating mean in R is –

```
mean(x, trim = 0, na.rm = FALSE, ...)
```

where: **x** : the input vector.

**trim** : used to drop some observations from both end of the sorted vector.

**na.rm** : used to remove the missing values from the input vector.

### Median

The middle most value in a data series is called the median. The **median()** function is used in R to calculate this value.

The basic syntax for calculating median in R is

```
median(x, na.rm = FALSE)
```

where:

**x** : the input vector. , **na.rm** : used to remove the missing values from the input vector.

The variance Mean of the squared deviations from the mean. Square of the standard deviation. as Eq. [56].

$$s^2 = \frac{1}{n-1} \sum_{i=1}^n (x_i - \bar{x})^2 = \frac{n}{n-1} \sum_x ((x_i - \bar{x})^2 * P(x_i)) \quad (2-2)$$

Where:

$s^2$  : is variance.

$x_i - \bar{x}$ : deviations from the mean (how far a value is from the mean).

The standard deviation number that is equal to the square root of the variance and measures how far data values are from their mean, as Eq. [56].

$$s = \sqrt{s^2} \quad (2-3)$$

Where: s is standard deviation.

These equations have been programmed in the R program as follows.

## 2.4 Random Variables

It is a variable that represents the future numerical results of a random phenomenon. The set of possible values for a random variable is known as the sample space [57], and the probability of obtaining any of the values in the sample space is known as the probability of the value.

A variable provides us with named storage that our programs can manipulate. A variable in R can store an atomic vector, group of atomic vectors or a combination of many R objects. A valid variable name consists of letters, numbers and the dot or underline characters. The variable name starts with a letter or the dot not followed by a number.

There are two types of random variables: [56]:

## 1- Discrete Random Variables

## 2- Continuous Random Variable

Thus, a probability distribution is a description of a specific random phenomenon in terms of the probability of events occurring. This means that a random variable can follow a certain probability distribution [55]. There are two types of probability distributions [56]:

1- Discrete probability distributions such as: The Binomial distribution. It can be described as the probability mass function, which is represented by Eq. [57]:

$$f(x) = P(X = x) \quad (2 - 4)$$

Where:

$f(x)$ : is the probability function, value of  $x$ . Among its characteristics [53]

$P(X = x)$  is the probability that the random variable  $X$  takes a given  $x$ .

$$a) \quad f(X_i) \geq 0, \text{ for } i = 1, \dots, n$$

$$b) \quad \sum_{i=1}^n f(X_i) = 1$$

The discrete probability distribution can also be described by the cumulative distribution function, which is represented by the Eq. [51]

$$F(x) = P(X \leq x) = \sum_{u \leq x} f(u) \quad (2 - 5)$$

Where:

$F(x)$  is cumulative distribution function

$f(u)$  is probability function, it is its characteristics:

$$f(x_i) \geq 0, \text{ for } i = 1, \dots, n$$

2- Continuous probability distributions, such normal distribution and exponential distribution. It can be described by the probability density function, which is represented as the Eq. (2-5), where  $x$  denotes the probability that the random variable  $X$  will take a specific value. It has the following characteristics [52]:

$$a) \quad f(X_i) \geq 0, \text{ for } i = 1, \dots, n$$

$$b) \quad \int_{-\infty}^{\infty} f(x)dx = 1$$

The continuous probability distribution can also be described by the cumulative distribution function, which is represented by the Eq. [53]:

$$F(x) = P(X \leq x) = \int_{-\infty}^{\infty} f(u)du \quad (2 - 6)$$

## 2.5 Probability Distributions in the R Statistical Program

For each distribution there are four functions in the program. where the name of the distribution is preceded by the letter  $d$  to obtain the probability density function. The name of the distribution is preceded by the letter  $p$  to obtain the cumulative distribution function. The name of the distribution is preceded by  $q$  to obtain the quantile function. The name of the distribution is preceded by the letter  $r$  for the random sample function.

### 2.5.1 Binomial Distribution

The binomial distribution model deals with finding the probability of success of an event which has only two possible outcomes in a series of experiments the appearance of an event (head) and the absence of an event (tail) [1].



If the experiment was repeated  $n$  times, and the probability of success was considered to be  $p$ , and the probability of failure was expected to be  $q = 1 - p$ . If assume that  $x$  is a random variable that indicates the number of experiments that were successful. As a result, can calculate the probability density function for  $X$ . If  $X \sim \text{Binomial}(n, p)$  then, Eq. [1].

$$P(x) = \frac{n!}{(n-x)!x!} p^x (1-p)^{n-x}, \text{ for } x = 0, 1, 2, 3, \dots, n \quad (2-7)$$

where:

$n$  : The number of atoms recorded for the counting rate.

$p$  : The probability of radioactive decay.

$q$ : probability of no radioactive decay.

$x$ : size of samples

The expectation and the variance reduce to the formula, as Eq.

$$\bar{x} = np \quad , \quad \sigma^2 = np(1-p) \quad (2-8)$$

The square root of variance is the standard deviation ( $\sigma$ ), as Eq. [1]

$$\sigma = \sqrt{\sigma^2} = \sqrt{\bar{x}(1-p)} \quad (2-9)$$

R has four in-built functions to generate binomial distribution. They are described:

**dbinom(x, size, prob)**

**pbinom(x, size, prob)**

**qbinom(p, size, prob)**

**rbinom(n, size, prob)**

where: **x** : a vector of numbers.

**p** : a vector of probabilities.

**n** : number of observations.

**size** : the number of trials.

**prob** : the probability of success of each trial.

### **dbinom()**

This function gives the probability density distribution at each point [56-57].

```
# Create a sample of 200 numbers which are incremented by 1.  
x <- seq(0,200,by = 1)  
# Create the binomial distribution.  
y <- dbinom(x,200,0.5)
```

### **pbinom()**

This function gives the cumulative probability of an event. It is a single value representing the probability.

### **qbinom()**

This function takes the probability value and gives a number whose cumulative value matches the probability value.

### **rbinom()**

This function generates required number of random values of given probability from a given sample.

## **2.5.2 Poisson Distribution**

The Poisson distribution can be used to describe a wide range of scientific events. It defines the probabilities of random events and it can be extended to "intervals" on the space or time axes [1]. When the maximum number of

occurrences of the events is very big, the Poisson random variable is a helpful model is a rough estimate of the number of times a rare event will occur, where the predicted number of occurrences is  $\lambda$  [55].

The Poisson distribution may be constructed from the binomial distribution by setting  $n \rightarrow \infty$  and fixing the mean  $\bar{x} = np$ , it can also set  $p \rightarrow 0$ , as an alternative because there is no longer a fixed number of possible events, and each new event is statistically independent of the number of events that have already occurred, the binomial distribution reduces to Eq. [56].

If  $X \sim \text{Poisson}(\lambda)$ , then

$$P(x) = \frac{(pn)^x e^{-pn}}{x!}, \quad x = 0, 1, 2, 3, \dots, n \quad (2-10)$$

where,  $\bar{x} = pn$  is represent in R program  $\lambda$  is distribution parameter

The expectation and the variance reduce to the formula, as Eq. [57].

$$E(X) = \bar{x} = \text{Var}(X) = pn = \lambda \quad (2-11)$$

$$\sigma = \sqrt{\text{Var}(X)} = \sqrt{\lambda} \quad (2-12)$$

The general mathematical equation for Poisson regression is  
 $\log(y) = a + b_1x_1 + b_2x_2 + b_nx_n \dots$

where: **y** is the response variable.

**a** and **b** : the numeric coefficients.

**x** : the predictor variable.

The function used to create the Poisson regression model is the **glm()** function.

### 2.5.3 The Uniform Distribution

The uniform distribution is used to simulate measurements where all values in a particular interval  $[a, b]$  have an equal chance of occurring [56].

A uniform distribution's probability density function is shown in Eq. [57].

If  $X \sim \text{Uniform}(a, b)$  then the density is

$$f(x) = \frac{1}{(b-a)} \quad , \text{for } a \leq x \leq b. \quad (2-13)$$

Where:

$a$  is the lowest value ,  $b$  is the highest value

$x$  is the interval field , for  $x : 0, 1, 2, \dots, n$  .

The expectation and the variance reduce to the formula, as Eq. [58].

$$E(X) = \frac{a+b}{2} \quad , \quad \text{Var}(X) = \frac{(b-a)^2}{12} \quad (2-14)$$

### 2.5.4 The Exponential Distribution

The Exponential distribution is used to simulate the length of time between events. If  $X \sim \text{Exponential}(\lambda)$ , as Eq. [58]:

$$f(x) = \lambda e^{-\lambda x} \quad (2-15)$$

Where:  $\lambda$  is the rate of the distribution [59].

The exponential distribution is usually used to represent the lifetime of a phenomenon if it has a constant rate  $\frac{1}{\lambda}$  , and if this phenomenon is not subject to obsolescence, that is, it is not affected by the duration that the phenomenon lasted before.[59].

When  $X \sim \text{Exponential}(\lambda)$ , as the Eq.

$$E(X) = \frac{1}{\lambda} \quad (2-16)$$

the variance is shown in Eq.

$$\text{Var}(X) = \frac{1}{\lambda^2} \quad (2-17)$$

The standard deviation is the square root of the variance, i.e.,

$$\sigma = 1/\lambda. \quad (2-18)$$

where expectation and standard deviation decrease as the mean increases.

### 2.5.5 The Normal Distribution

One of the most important continuous distributions is the normal distribution. It is used to describe the repetitive patterns of many statistical phenomena by studying the shape of the normal distribution curve.

According to mathematical theories, the normal distribution is an approximation of the distribution of the numerical properties of the data produced by these measurements, where the binomial distribution can be approximated by the normal distribution and the Poisson distribution can be approximated by the normal distribution [58].

If  $X \sim \text{Normal}(\mu, \sigma^2)$  then the density of  $X$  is given by the Eq. [59].

$$f(x) = \frac{\exp\left\{-\frac{(\mu-x)^2}{2\sigma^2}\right\}}{\sqrt{2\pi\sigma^2}} \quad , \text{ for all } x \quad (2-19)$$

Where:  $\mu$  is the mean,  $\sigma^2$  is standard deviation.

In a random collection of data from independent sources, it is generally observed that the distribution of data is normal. Which means, on plotting a graph

with the value of the variable in the horizontal axis and the count of the values in the vertical axis we get a bell shape curve. The center of the curve represents the mean of the data set. In the graph, fifty percent of values lie to the left of the mean and the other fifty percent lie to the right of the graph. This is referred as normal distribution in statistics.

R has four in built functions to generate normal distribution [56-57].

**dnorm(x, mean, sd)**

**pnorm(x, mean, sd)**

**qnorm(p, mean, sd)**

**rnorm(n, mean, sd)**

where: **x** : a vector of numbers.

**p** : a vector of probabilities.

**n** : number of observations(sample size).

**mean** : the mean value of the sample data. It's default value is zero.

**sd** : the standard deviation. It's default value is 1.

**dnorm()**

This function gives height of the probability distribution at each point for a given mean and standard deviation.

**pnorm()**

This function gives the probability of a normally distributed random number to be less that the value of a given number. It is also called "Cumulative Distribution Function".

**qnorm()**

This function takes the probability value and gives a number whose cumulative value matches the probability value, as figure (2-3) [58].

### **rnorm()**

This function is used to generate random numbers whose distribution is normal. It takes the sample size as input and generates that many random numbers. We draw a histogram to show the distribution of the generated numbers.

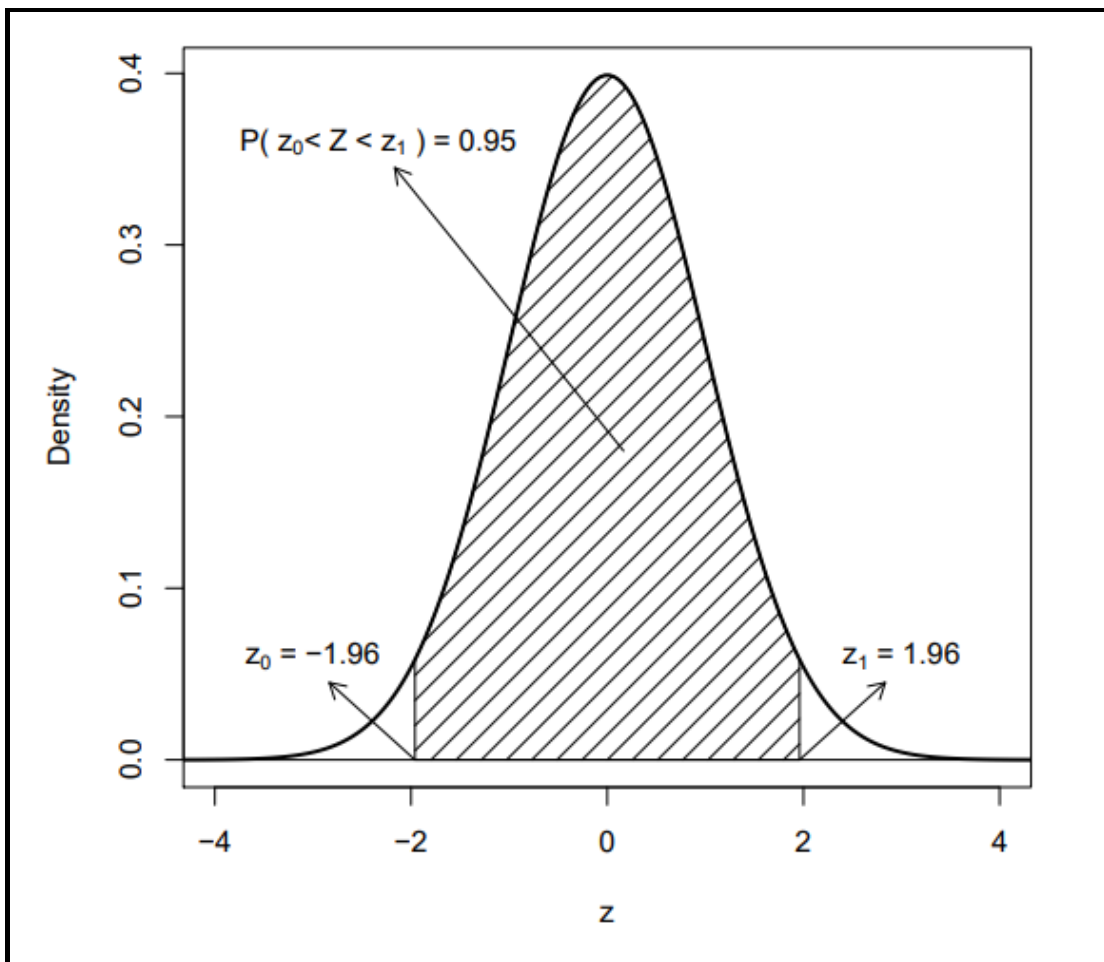


**Figure. (2-3) Central 95% of the standard normal distribution [58].**

## 2.6 Normality Tests and Homogeneity of Variances Tests

Hypothesis testing is defined as a guess or claim related to the mediators of the statistical community it bears true and false [57]. When testing any hypothesis, it must be formulated as two hypotheses, called hypothesis (Hypothesis Null), symbolized  $H_0$ , the second hypothesis is (Hypothesis Alternative), symbolized by  $H_1$ , and the goal of testing the hypothesis is to study the possibility of rejecting the primary hypothesis at a specific level of significance. The alternative and determining the level of importance, usually 0.05 [57]. So, it calculates the appropriate test and calculating the significance p-value, then comes a stage take a statistical decision by comparing the test's significance with the level of importance, if it is valuable the p-value less than the level of significance  $H_0$  reject the initial hypothesis, and if the p-value is greater from the level of importance it accepts the initial hypothesis [58].

There are several tests that can be used to ensure that the data adheres to a normal distribution, and we will try to show the most important of them.

### 2.6.1 Kolmogorov-Smirnov Test and Shapiro-Wilk Test

The hypothesis test is used as Eq. [59].

$$H_0: X \sim N(\mu, \sigma^2)$$

opposite (2-20)

$$H_1: X \neq N(\mu, \sigma^2)$$

It can be applied using R : **ks.test(X, "pnorm", mu, sigma)**.

It can be also applied using R : **shapiro.test(X)**

If  $P < 0.05$  then data are distributed according to a normal distribution [59].



## 2.6.2 Q-Q Plot

It is a less accurate descriptive method than the two previous methods. This method is based on drawing a spread diagram for the data after arranging them in ascending order with their standard values. If the propagation has a linear shape around a normal straight line, the data is normal, and whenever the data moves away from the normal distribution line, this indicates a lack of commitment the data is in a normal distribution [57]. It used to make sure the imposition is whether the data given follows the natural distribution. We will use, which can be obtained using the following code [58]:

```
qqnorm(x, main="x")  
qqline(x, col = 2, lwd=2)
```

There are several tests for the Homogeneity of variances, the most popular of which are the Bartlett test and the Levin test.

## 2.6.3 Bartlett's Test

It is used when the data are distributed according to a normal distribution and divided into several groups according to a specific factor and to test the hypothesis, as Eq. [58].

$$H_0: \sigma_1^2 = \sigma_2^2 = \dots = \sigma_r^2$$

opposite (2-21)

$$H_1: \sigma_i^2 \neq \sigma_j^2 \quad , \text{for some } i, j$$

It can be also applied using R : **bartlett.test(Y ~ X, data = myData)**.

## 2.6.4 T-Test Independent Samples

Mean can be compared to two sets of data or two samples  $x, y$  independent, using a T-Test, depends on assumption that this data represents a normal distribution society. Thus, the Hypothesis test is, as Eq. [59]:

$$H_0: \bar{x} - \bar{y} = m$$

opposite

$$H_1: \bar{x} - \bar{y} \neq m \quad (2-22)$$

Which studies the significance of the difference between  $\bar{x}-\bar{y}$  equals a fixed amount such as  $m$ .

That is, to test the difference of the sample mean  $\bar{x}$  from the sample mean  $\bar{y}$ , i.e., to see if the difference is between  $\bar{x}, \bar{y}$  is a difference of statistical significance or it is just a coincidence [57].

It can be also applied using R by **T.Test (x, y, mu=m)** .

## 2.6.5 Wilcoxon Test

It is a nonparametric alternative to the one-sample T-Test, and is used to test the mean difference of a sample for a specified value.

## 2.7 Correlation and Regression

The Pearson correlation coefficient is used to investigate the existence and intensity of a relation between two quantitative variables  $X$  and  $Y$ , where the correlation coefficient falls within the interval  $[1, -1]$  and whenever its absolute value approaches one, this indicates that the relation is stronger, but when its absolute value approaches the half, it is the relation is medium, and when its value approaches

zero, the relation is weak, and the positive sign is The correlation coefficient indicates that the relation is direct, while the negative sign indicates that the relation inversely, after computing the coefficient of correlation R the hypothesis is tested, as Eq. [59]:

$$H_0: R = 0$$

opposite (2-23)

$$H_1: R \neq 0$$

Conditions for applying the linear Pearson correlation coefficient

- 1- The study variable be quantitative.
- 2- Data are distributed for each of the two samples according to a normal distribution.
- 3- The two variables have a linear relation.
- 4- Homoscedasticity the spread should be roughly cigar-shaped
- 5- The absence of an outlier value.
- 6- The sample size constitutes at least 5% of the population size.

## 2.8 Simple Linear Regression

Simple linear regression is the study of the effect of the variable X (variable independent) on the variable Y (variable dependent) [58]. The linear regression model is given as Eq. [58]:

$$Y = \beta_0 + \beta_1 X + \epsilon, \epsilon; \epsilon \sim N(0, \sigma^2) \quad (2-25)$$

where  $\epsilon$  is residual random.

$\beta_0$  : Reflects the value of the dependent variable y in the case of the value of the independent variable.

$\beta_1$ : Slope of a straight line

The regression analysis aims to find estimations for each of  $\beta_0, \beta_1$ , this makes the sum of the squares of sediments as small as possible apply simple linear regression using r by the instruction **lm(y~x)** [59]. Conditions for applying simple linear regression.

- 1- All variables must be quantitative.
- 2- The absence of a non-linear relation between the residue and the estimated value of Y.
- 3 - Residue is independence variable.
- 4- The residue follows to normal distribution.
- 5 - Homogeneity of variance.
- 6- There are no outliers.
- 7- The sample size is rather large.

## 2.9 Multiple Linear Regression

The effect of various variables  $X_1, X_2, \dots, X_P$  is studied using multiple linear regression. On a y variable termed the variable dependent. The multiple linear regression model is given as, Eq. (2-25). [58]

$$Y = \beta_0 + \beta_1 X_1 + \beta_2 X_2 + \dots + \beta_P X_P + \epsilon; \epsilon \sim N(0, \sigma^2) \quad (2-24)$$

Apply multiple regression with R, by code:

**lm(y~x1+x2+...+xp).**

Conditions for applying multiple linear regression [59].

- 1- All variables must be quantitative.

- 2- The absence of a non-linear relation between the residue and the estimated value of Y.
- 3 - Residue is independence variable.
- 4- The residue follows to normal distribution.
- 5 - Homogeneity of variance.
- 6- There are no outliers.
- 7- The sample size is rather large.

# Chapter Three

## Experimental Part

### 3.1 Introduction

This chapter deals with a description of the electronic nuclear counting and analysis system used to measure the gamma spectrum emitted from radioactive isotopes, and studying its parts and preparing them for the purpose of obtaining the best and most accurate experimental results instead of using the results of other researchers. This work also includes an explanation of all region of the spectrum.

### 3.2 Gamma Spectroscopy System

This work, was used SPECTCH UCS-30 gamma ray measurement system associated with a scintillation detector NaI(Tl). This system consists of a primary amplifier, main amplifier, with equipped H.V, and a multi-channel analyzer [60]. This system is connected to a computer for the purpose of operating it, analysing the resulting spectrum (MCA) and reading the measurements, as figure (3-1) shows the block diagram of a NaI(Tl) detector system, and the following is an explanation of the parts of this system .

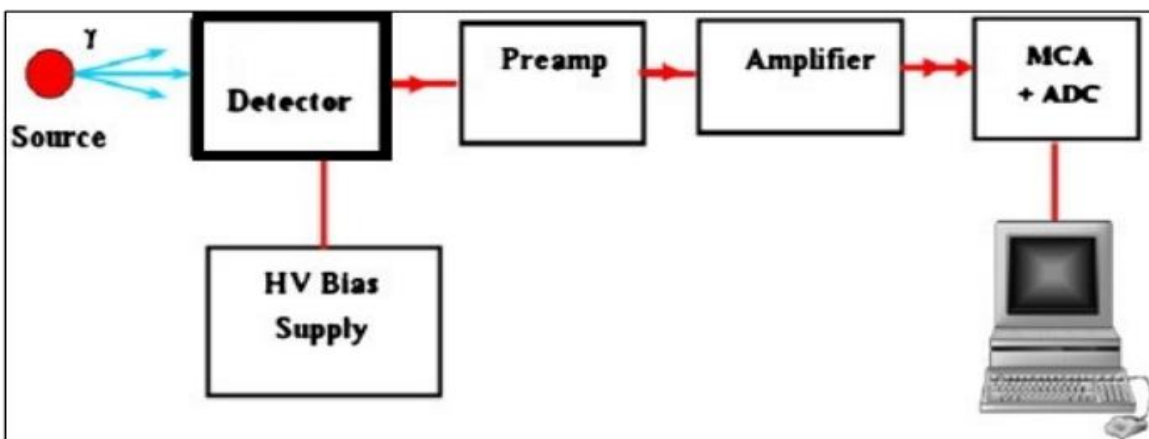


Figure (3-1). Electronic system used [61].

### **3.2.1 The NaI (Tl) Detector**

In this study, the scintillation detector of iodide sodium activated with Thallium NaI(Tl), manufactured by (Alpha Spectra, Inc) [60], it was used and it consists of two main parts, the scintillation material and the photomultiplier, the scintillator material is (inorganic) at size (3"x3"), it is characterized by the production of photons (scintillation) when absorbing the gamma rays, and they are fed with Thallium, whose presence is necessary for the activation process to occur [62].

As the photoelectric multiplier, it consists of a photo cathode and a group of dynodes [4], the resulting photon in the crystal when it falls on the photo cathode leads to the production of an electron. Then the dynamics amplify the number of electrons produced from the photo cathode, which interacted with scintillation material [61].

### **3.2.2 Preamplifier**

The primary amplifier works on shaping the pulse to distinguish it from electronic noise, as correct modulation leads to reduced noise and improved pulse shape, resulting thus improving energy resolution [62].

### **3.2.3 Main Amplifier**

The main amplifier is responsible for amplifying the electronic pulses coming out of the primary amplifier after modulating them and then analyzes them with a multichannel analyzer (MCA), where by the signal is amplified proportional to the amplitude of the incoming pulse [62].

### **3.2.4 High Voltage Power Supply**

The detector is supplied with the appropriate voltage for operation, as the appropriate voltage in this study was 900 V. which is within the relative stability region of the detector.

### **3.2.5 Multichannel Analyzer**

The multi-channel analyzer (MCA) is supplied by (SPECTRUM TECHNIQUES, LLC) records and processes pulses according to their capacity and that each storage is called a channel and contains 4096 channels, as the pulse amplitude is proportional to the energy of the photon incident on the detector, and that each of these pulses are stored in a specific channel according to their energy. It can be considered that distribution of the pulses in the channels is a picture of the distribution of the energy of the incident photons on the detector [1-62].

### **3.2.6 Computer**

The personal Computer (Dell), which is connected to the measurement system, was used to collect information and analyze it through the USC-30 program. This program is considered an integrated program for qualitative analyzes of the gamma spectrum and dealing with all parts of the energy spectrum.

## **3.3 Radioactive Sources**

Three radioactive sources are used in this study ( $^{137}\text{Cs}$ ,  $^{60}\text{Co}$ , ,  $^{22}\text{Na}$ ). It was in the form of a plastic disk (2.5 cm). table (3-1) shows the radioactive sources used, half-life, and the energies of the gamma ray photons.



**Table (3-1) Radioactive Sources Used in This Study.**

Radioactive Source	Half life	Activity	Energy decay MeV	I <sub>γ</sub> %	Production Date
<sup>60</sup> Co	5.2714 year	0.205 μci	1.1732 1.3325	99.857	Apr 2008
<sup>137</sup> Cs	30.07 year	0.7574 μci	0.6617	85.1	Jan 2009
<sup>22</sup> Na	2.602 year	0.04 μci	1.274 0.511	90	Dec 2008

### 3.4 Gamma-Ray Spectra

The gamma ray spectrum emitted from radioactive sources was measured at a distance of (7 cm) between the radiating source and the scintillation detector, where the collection time was (200 seconds), and the amplification at 1. Given that the gamma rays are single-energy, so their spectrum is linear, and thus the areas of the spectrum can be distinguished for the gamma rays, as shown in figure (3-2).

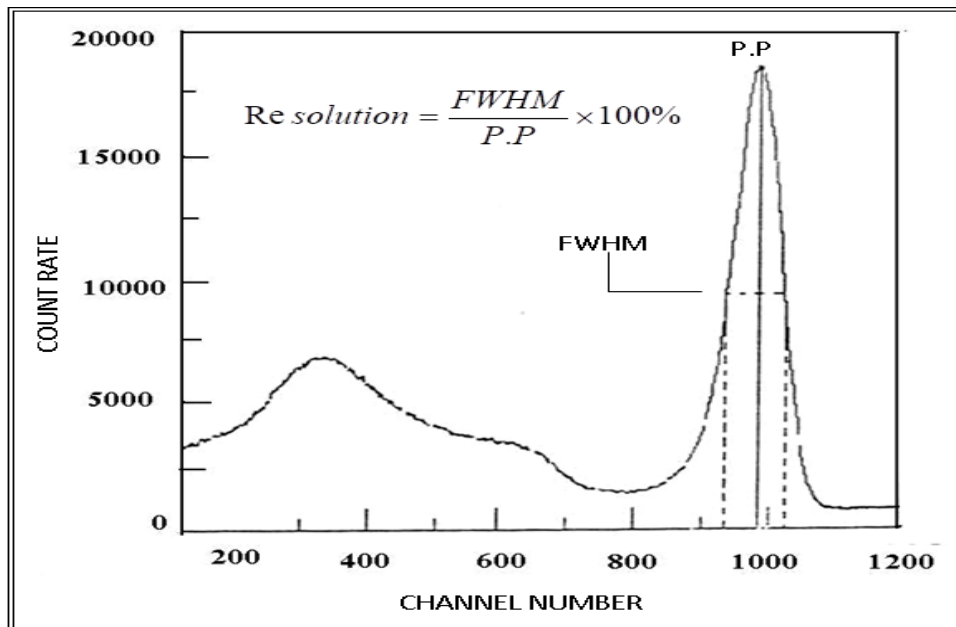


**Figure (3-2). Gamma spectrum [61].**

The peak is the position of the maximum count, and the peak area is the complete response signal for a specified gamma ray transition or is the difference between its entire area and the respective background [63]. The background includes all pulses not belonging to the photopeak but recorded by the multi-channel analyzer in the peak channels [64].

#### **3.4.1 Total Area of Spectrum (T.A.)**

It represents the number of pulses for all channels, as the area equals the sum of the count rate for all channels and is measured in units (C/ s).

#### **3.4.2 Net Total Area (N.T.A.)**

The total area under the spectrum minus the additional contributions as the Compton continuation area, measured in units (C/ s).

#### **3.4.3 Cross Total Area (C.T.A.)**

It represents the total area under the whole spectrum of the spectrum, measured in units (C/ s).

#### **3.4.4 Photopeak Area (P.P.A.)**

This represents the complete absorption of the energy of a gamma ray photon into the detector crystal and the reaction that gives rise to that peak is the photoelectric reaction, measured in units (C/ s).

#### **3.4.5 Photopeak Net Area (P.N.A.)**

Represents the area from the start to the end of the photoreceptive minus the area of the Compton continuation, measured in units (C/ s) , as figure (3-3).

#### **3.4.6 Photopeak Cross Area (P.C.A.)**

It represents the total area of the spectrum, measured in units (C/ s), as figure(3-3).

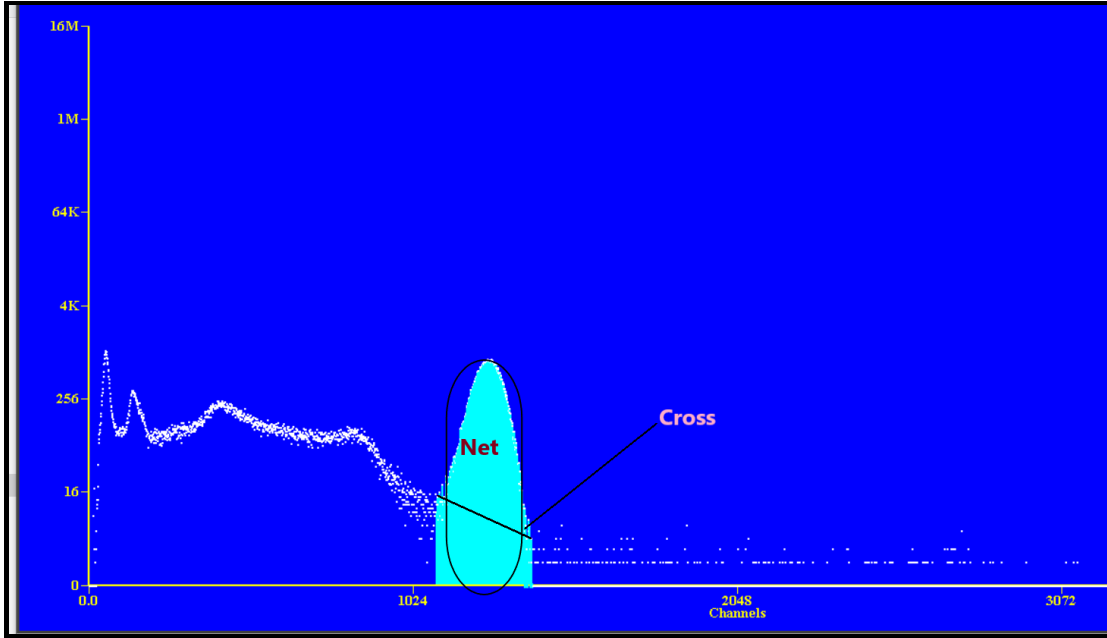


**Figure (3-3) Net and Cross Photopeak.**

### 3.4.7 Peak to Valley Ratio

A criterion used to check the quality of the spectrum shape, by dividing the highest value to the lowest value at the peak spectrum, and whenever the ratio is large, this indicates the quality of the spectrum.

### 3.4.8 Energy Resolution

It is a measure of the ability of the counter to differentiate between two closely energies [64]. The quantum line width at its mid-peak height (FWHM) (Full Width at Half Maximum), to measure the energy separation of the NaI(Tl) detector, Eq. (3-1) was use [65], as figure (3-4)

$$\text{Energy Resolution (E. R)} = \frac{FWHM}{P.P} \times \% \quad (3-1)$$

where:

FWHM: the full width at half maximum. It's defined as the width of the distribution at half the peak level.

P.P : indicates centroid at the photopeak.

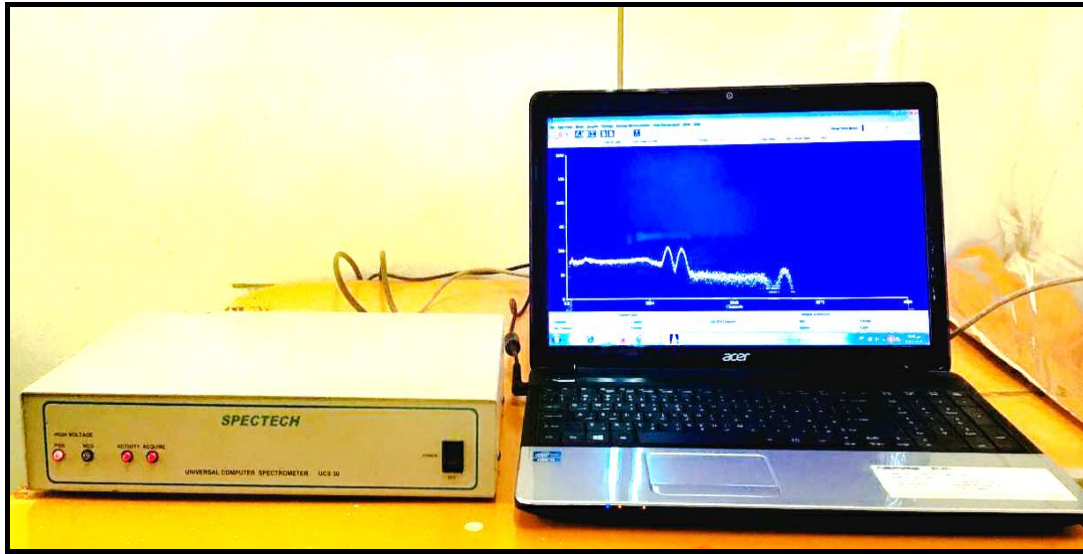


**Figure (3-4) Gamma spectrometer system, UCS-30.**

### **3.5 UCS-30 Universal Computer Spectrometer**

The Universal Computer Spectrometer System (UCS-30) is a complete spectrum system designed for nuclear science education equipped by Spectrum Techniques company that offers a wide range of radiation spectrometers and detectors [60]. Built as a direct replacement for the famous UCS-20, the UCS-30 offers many upgrades and additional functionality to improve versatility.

UCS-30 uses software for Spectrum Techniques, as well as the special isotope recognition function of Spectrum Techniques- ISOMATCH. This helps the consumer to scan the spectrum and assess the emission components for each nuclide present. UCS-30 is operated by a (PC or Mac) via a USB connection [64].

The UCS-30 includes an auto calibration function that automatically sets the HV and amplifier gain to 1 kV / channel using a  $^{137}\text{Cs}$  source, and is available in three different versions, each with a different number of switch gain channels - 1024 (1K), 2048 (2K) and 4096 (4K) [65].

UCS-30 uses an internal amplifier that enables direct connection of luminescence detectors. The bipolar amplifier requires polarity determination and several modulation times when various types of detectors are used for external amplifiers. [62], as figure (3-5).

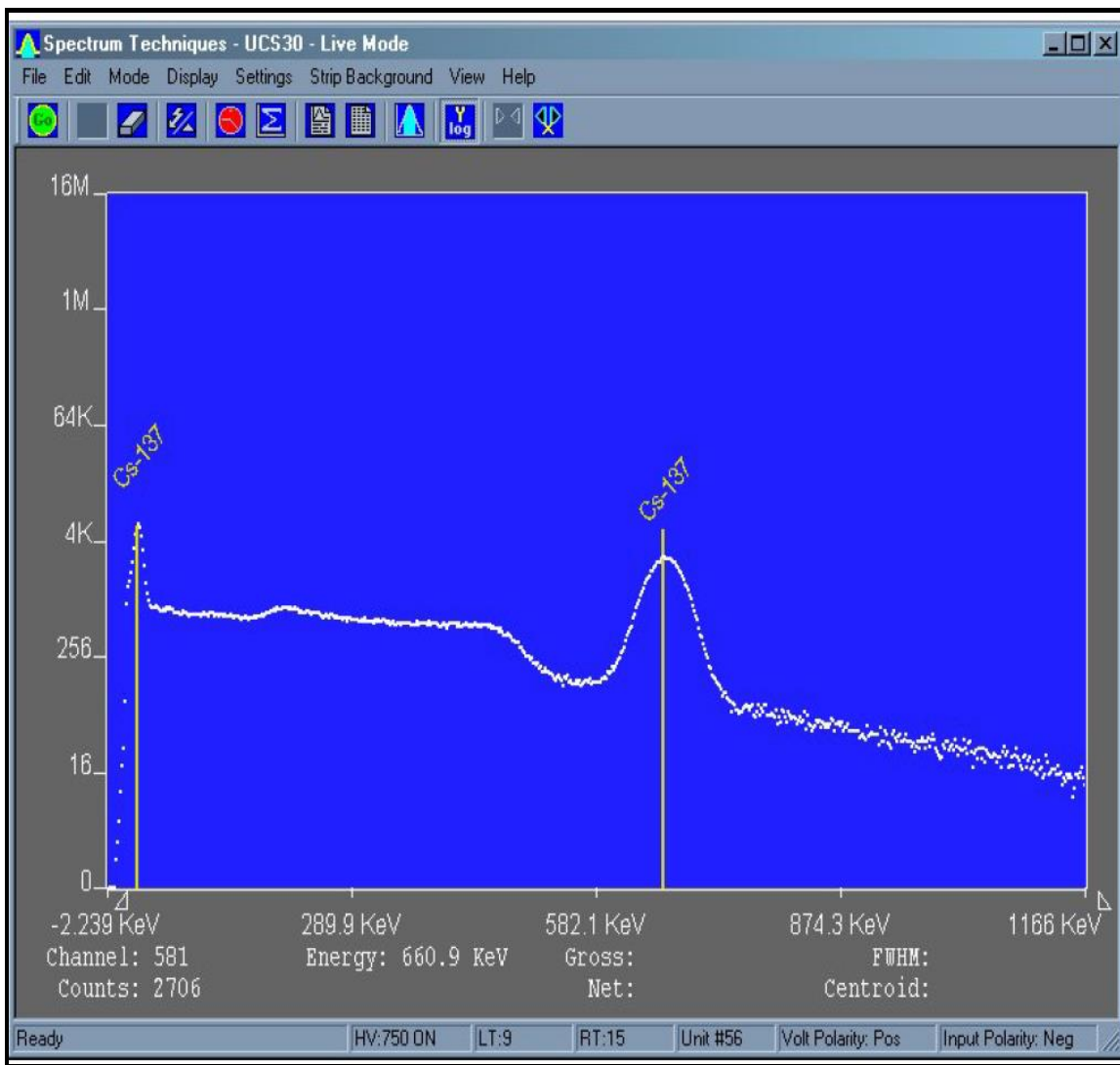


**Figure (3-5) Demonstrates a model of a gamma-ray spectrum in the USC-30 program window.**

# Chapter Four

## Results and Discussion

### 4.1 Spectrum for Total area and Photopeak.

Three radioactive sources were used in this study, where 400 spectra were collected for each source. The spectrum was measured before and after subtraction background radiation in Total area (T.A.), photopeak area (P.P.A.) of the Cesium ( $^{137}\text{Cs}$ ), Cobalt ( $^{60}\text{Co}$ ), and Sodium ( $^{22}\text{Na}$ ) sources as shown in Appendices (1), (2) and (3). The Energy resolution (E.R) and Peak to valley ratio (P/V) of the  $^{137}\text{Cs}$ ,  $^{60}\text{Co}$  and  $^{22}\text{Na}$  were also calculated, as shown in Appendices (4) and (5). These appendices were abbreviated in Tables (4-1) to (4-6) for  $^{137}\text{Cs}$ ,  $^{60}\text{Co}$  and  $^{22}\text{Na}$ , respectively.

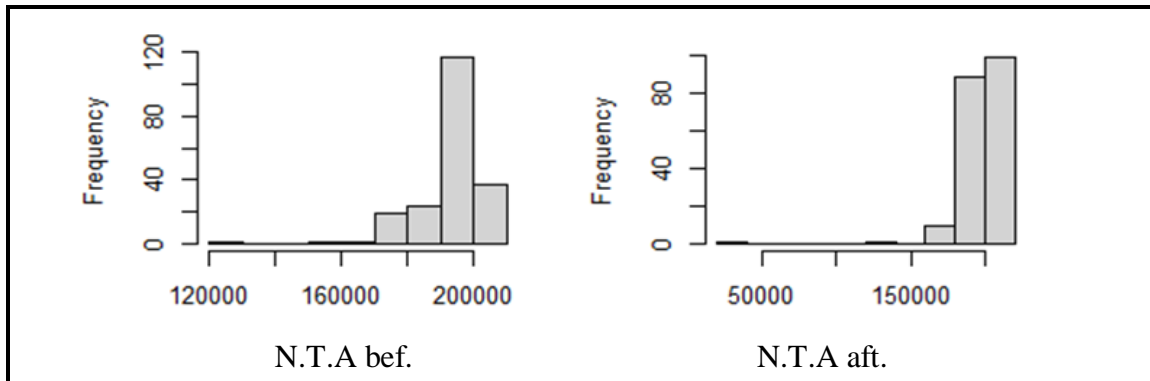
Table (4-1) is summary of the studied models of the total spectrum area and the photopeak area for  $^{137}\text{Cs}$  source, as figures (4-1).

**Table (4-1) Summary Spectrum  $^{137}\text{Cs}$  for Total Area and Photopeak.**

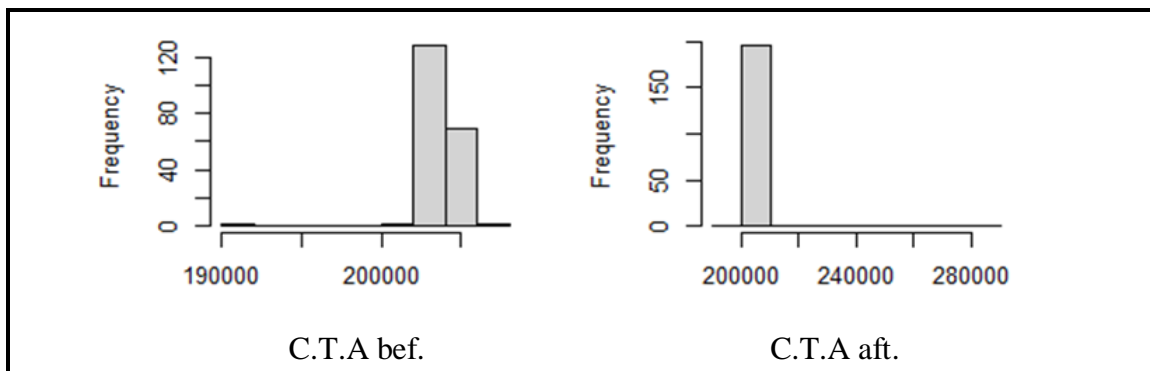
Summary		N.T.A.		C.T.A.		P.N.A.		P.C.A.	
		Before	After	Before	After	Before	After	Before	After
Population Study	Min	129577	20947	191508	195879	44164	76371	77384	78007
	Max	203201	208842	206568	280591	78628	78881	80371	80737
	1st Qu	190902	195588	203530	207933	76912	77415	79077	79474
	Median	195238	199934	203856	208271	77365	77682	79245	79664
	3rd. Qu	198992	203792	204195	208600	77715	77965	79479	79840
	IQR	8090	8204	665	667	803	550	402	366
	O- up	215336	221148	207565.5	281591.5	79832.5	79706	81575.5	81562
	O.down	117442	8641	190510.5	194878.5	42959.5	75546	76179.5	77182
	Mean	192716.3	196973	203766.9	208844.5	77118.9	77680.35	79249.7	79658.6
	Var	94315759	23944735	1068344	46687988	5830936	239283.5	106047.6	94108.6
$\sigma$	9711.63	15474.09	1033.607	6832.861	2414.733	489.1662	325.6494	306.773	

		Contain table (4-1)							
<b>Sample</b>	<b>(EX)</b>	192787	196914	203767.8	208848.4	77113.97	77683.22	79251.71	79661.8
	<b>Var</b>	95070345	24149623	1078587	47156958	5885934	237898.7	106620.6	93395.8
	<b>sd.</b>	9750.402	15540.15	1038.55	6867.092	2426.094	487.7486	326.5282	305.607
	<b>Median</b>	195343	199993	203856	208271	77365	77682	79245	79671
	<b>IQR</b>	8191	7671	672	659	794	568	406	365
	<b>O- up</b>	215487.5	220348.5	207576	281579.5	79819	80072	81562	81928
	<b>O.down</b>	117290.5	9440.5	190500	194890.5	42973	75180	76193	76816
<b>Sample standard Bar</b>	<b>X.bar</b>	192719	196976	203766.6	208847.7	77121.39	77680.6	79249.66	79658.5
	<b>Var</b>	4712.951	10887.87	30.932	1396.552	724.6645	12.12063	4.750035	4.59692
	<b>Sd.</b>	68.65093	104.3449	5.561654	37.37046	26.91959	3.48147	2.179458	2.14404
	<b>Median</b>	192703	196961	203766	208851	77117	77680	79249	79658
	<b>IQR</b>	91	88	5	5	6	4	3	3
	<b>O-up</b>	193175.5	197965	203786.5	208922.5	78482	78882	80442	80858
	<b>O.down</b>	192485.5	196731	203740.5	208477.5	75915	76481	78067	78459

Table (4-1) is a summary of the studied sample of the total spectrum area and the photopeak area of  $^{137}\text{Cs}$  source, where the table is divided into three groups, the first group is the study population represented by radioactive sources, the second group is the random samples selected by the R program, and the third group represents expected samples if there were other samples taken from the same study population. The Table also included a picture of the data distribution, as shown in the figure (4-1).



a

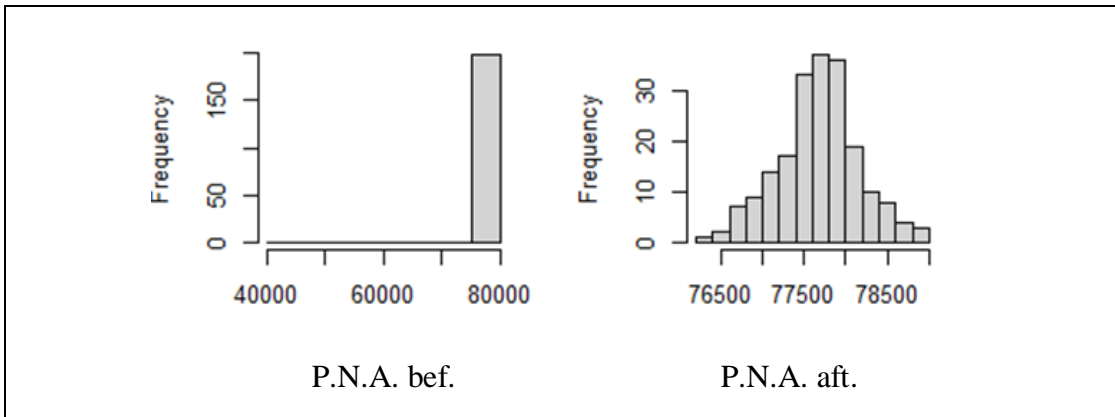


b

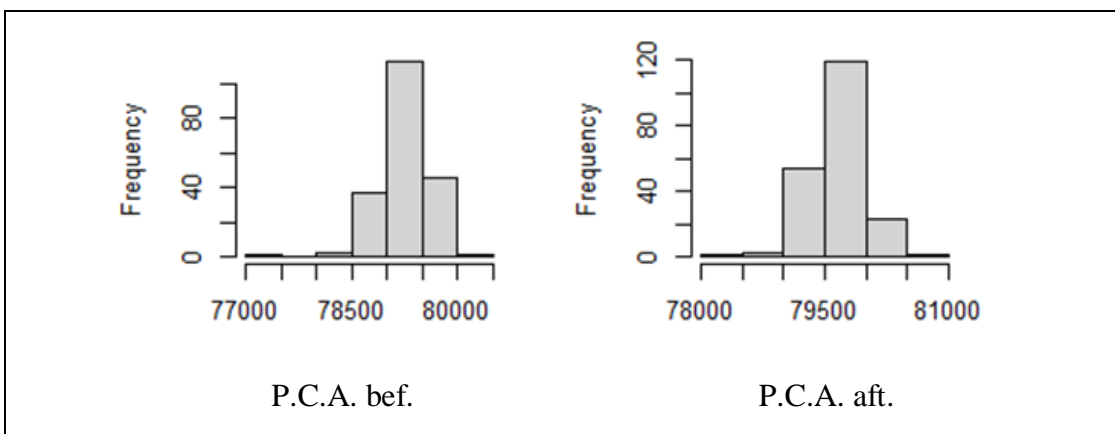
**Figure (4-1) The general behavior of total area before and after subtraction B.G for  $^{137}\text{Cs}$  source a-Net. b- Cross.**

Histogram (4-1) represents the behavior the total area of  $^{137}\text{Cs}$  source where the x-axis refers to total area and the y-axis is the frequency which the number of times a given datum occurs in a data set. where that note the difference between the net and the cross for the total area of the  $^{137}\text{Cs}$  source where the cross contains fewer columns than what is in the net area, depending on the estimate of data distribution and spread near the mean, figure (4-2) shows the general behavior of the photopeak samples of  $^{137}\text{Cs}$  source.





a



b

**Figure (4-2) The general behavior of photopeak before and after subtraction**

**B.G for  $^{137}\text{Cs}$  source    a-Net.   b- Cross.**

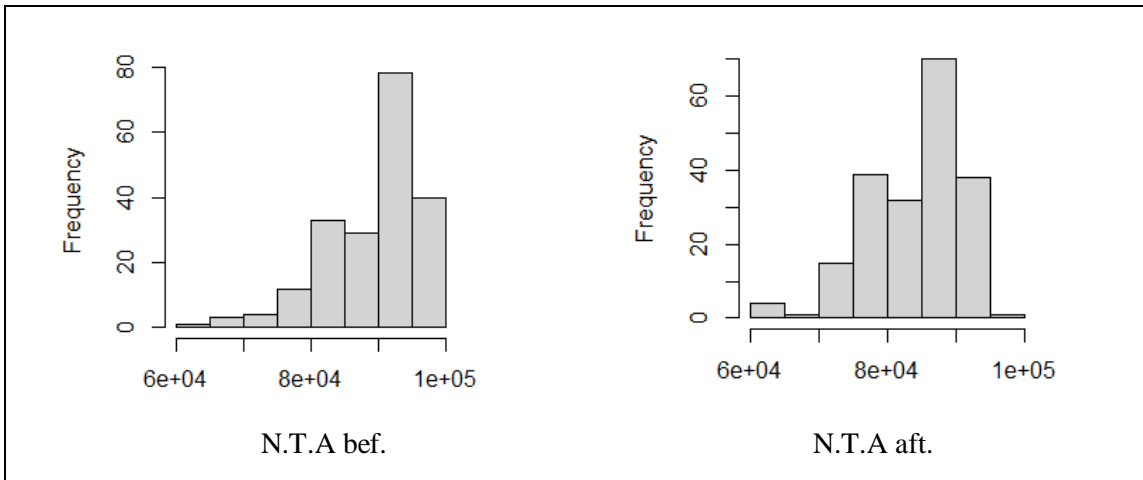
The histogram (4-2) is a behavior of photopeak for  $^{137}\text{Cs}$  source, where photopeak area on the x-axis, and the data on y-axis is the number of times of data set, which show the difference between net photopeak area before subtraction background radiation and net photopeak area after subtraction background radiation depending on the number of columns, which helps to know the compatibility of the real data distribution with the normal distribution.

Table (4-2) is summary of the studied models of the total spectrum area and the photopeak area for  $^{60}\text{Co}$  source.

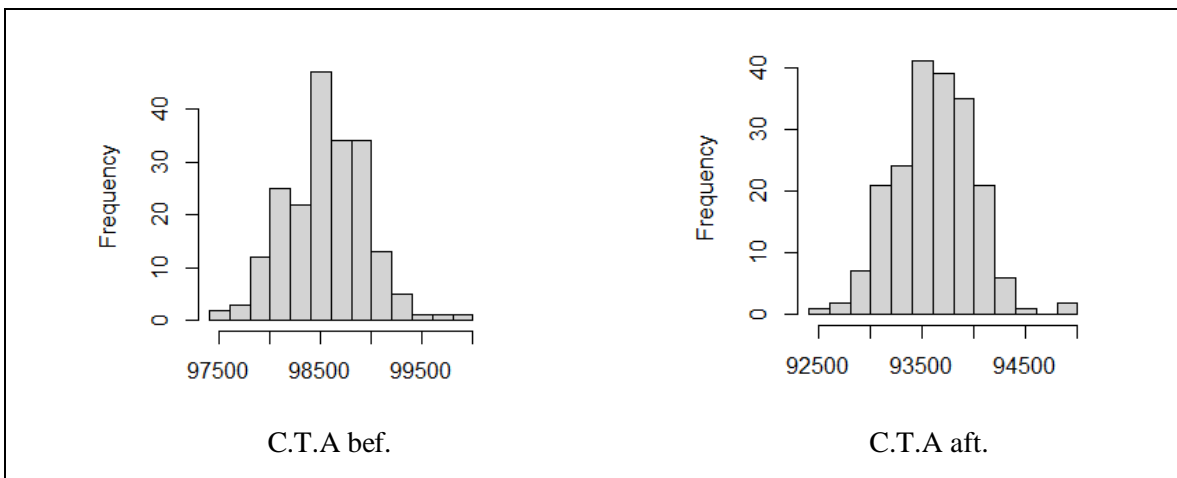
**Table (4-2) Summary Spectrum <sup>60</sup>Co for Total Area and Photopeak.**

Summary		N.T.A.		C.T.A.		P.N.A.1		P.N.A.2		P.C.A.1		P.C.A.2	
		Before	After	Before	After	Before	After	Before	After	Before	After	Before	After
Population	Min	61740	63195	97495	92539	10462	10147	6659	9186	13385	14154	12037	11707
	Max	99863	98983	99864	98983	12486	12279	11415	11183	15934	15499	14423	12661
	1st Qu	84384	79056	98292	79056	11129	10951	10346	9919	15234	14819	12382	12185
	Median	92097	85646	98550	85646	11336	11214	10568	10236	15383	14963	12487	12267
	3rd. Qu	94805	89787	98823	89787	11567	11524	10790	10515	15506	15074	12577	12379
	IQR	10451	10437	535	493	438	573	444	596	272	255	195	194
	O- up	115539	115518	100667	110987	13143	13138.5	12081	12077	16342	15881	14715.5	12952
	O-down	46063.5	46084.5	96692.5	76442.5	9805	9287.5	9680	8292	12977	13772	11744.5	11416
	Mean	89372.2	83916.4	98552.7	93613.8	11350.15	11226.3	10544	10224.6	15362	14946	12487.7	12272
	Var	515051	486441	154002	145633	149785	165128.	193073	162293	62921	45694	40809.7	23894
$\sigma$	7176.71	6974.53	392.431	381.62	387.0206	406.359	439.45	402.856	250.84	213.76	202.014	154.57	
Sample	(EX)	89374.9	83877.8	98552.1	93613.3	11346.28	11230.5	105457	10225.9	15361	14944	12489.6	12273
	Var	518038	489445	1555048	147038	149529.5	165037	194084	161406	63441	45723	40899.9	23801
	sd	7197.49	6996.04	394.341	383.456	386.6904	406.248	440.55	401.754	251.84	213.83	202.237	154.28
	Median	92019	85646	98547	93613	11334	11216	10568	10236	15378	14961	12488	12268
	IQR	10451	10776	535	509	437	563	445	594	273	257	193	199
	O- up	115539	115147	100666	110566	13141.5	13123.5	12082	11838.5	16343	15884	14712.5	13071
	O-down	46063.5	47031	96692.5	76862.5	9806.5	9302.5	5991.5	8530.5	12975	13768	12096.5	11298
Sample standard Bar	X.bar	89373.7	83915.4	98552.8	93613.7	11350.04	11226.1	10543	10224.4	15361	14946.	12487.8	12272
	Var	2248.7	2719.09	6.84401	6.85900	8.701051	7.78477	8.2732	8.12812	2.8573	1.9437	1.89436	1.1534
	sd	47.4205	52.1449	2.61611	2.61897	2.949754	2.79012	2.8764	2.85099	1.6904	1.3942	1.37636	1.0741
	Median	89370	83909	98553	93614	11350	11226	10544	10224	15362	14946	12488	12272
	IQR	72	68	4	4	4	4	3	4	2	2	2	2
	O-up	105182	99759.5	114237	109298	12012.5	11889.5	11217	10887.5	15779	15358	12900.5	12684
	O-down	73612.5	68125.5	82869.5	77930.5	10685.5	10563.5	9881.5	9560.5	14948	14532	12068.5	11859

Table (4-2) is shown summary of the studied samples of the total spectrum area and the photopeak area for <sup>60</sup>Co source, as figures (4-3) and (4-4) which describe the general behavior of the data distribution for total area and photopeak.



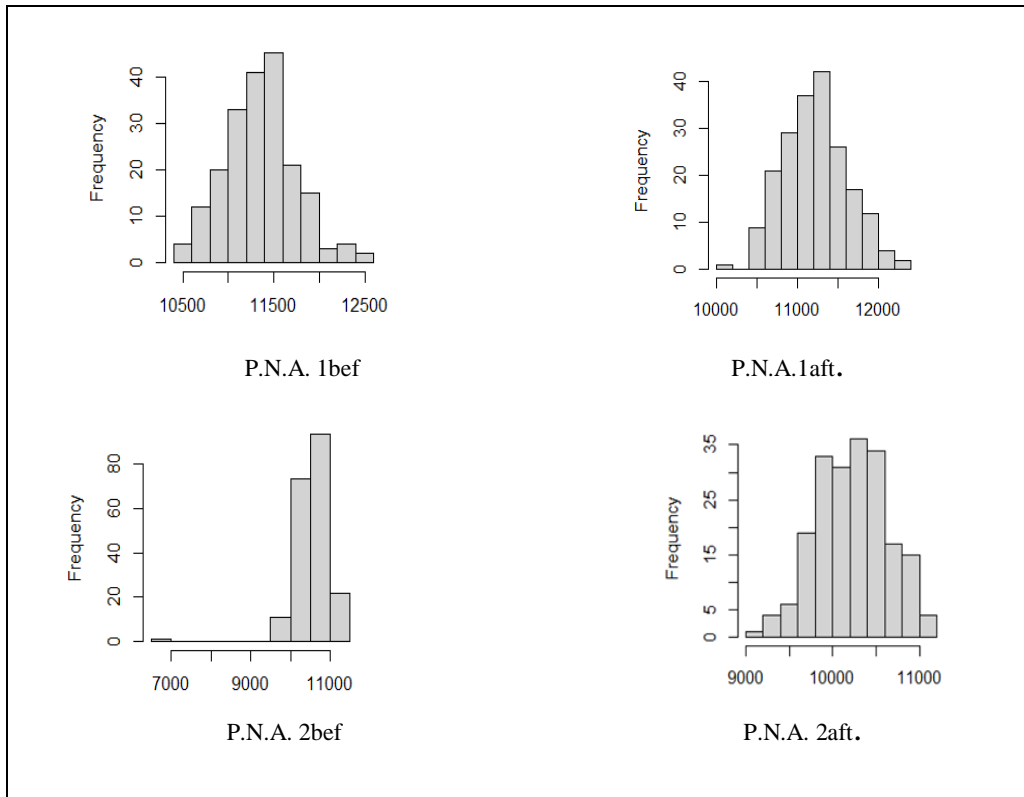
a



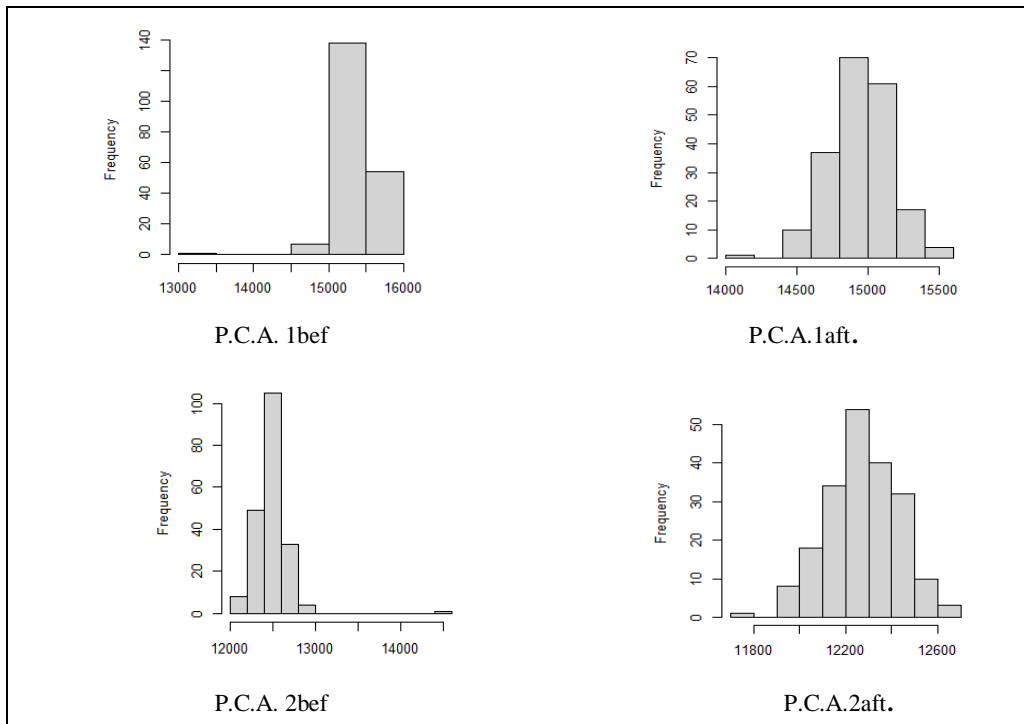
b

**Figure (4-3) The general behavior of total area before and after subtraction B.G for  $^{60}\text{Co}$  source a-Net. b- Cross.**

Figure (4-3) shows the histogram of the behavior of total area of the  $^{60}\text{Co}$  source before and after the subtraction background radiation, where it notes that the behavior of the N.T.A was a close to the exponential form, while the behavior of the C.T.A was close to the shape of the bell or close to the normal distribution because C.T.A represents the total area under the whole spectrum, meaning it represents the gaussian shape of the peak, figure (4-4) shows the general behavior of the p.p.A. samples of  $^{60}\text{Co}$  source.



a



b

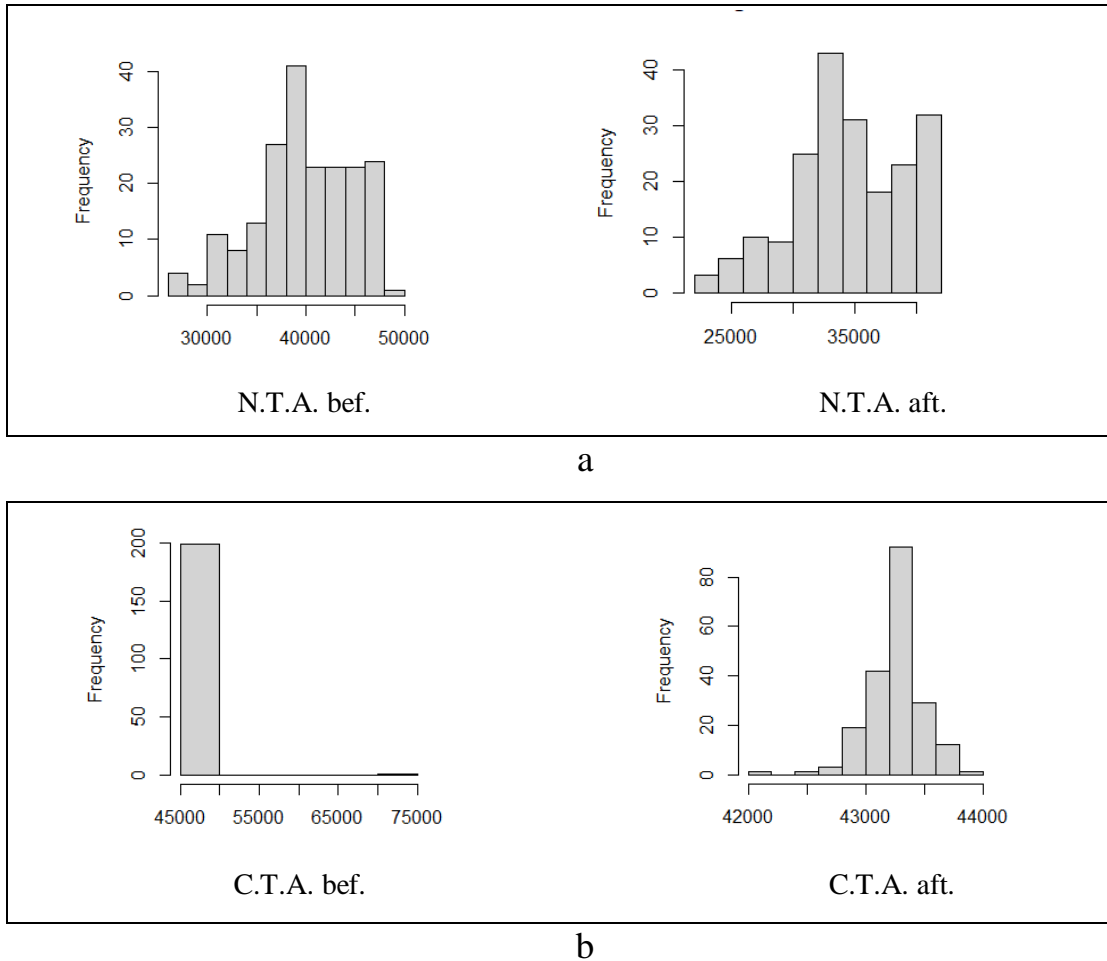
**Figure (4-4) The general behavior of photopeak before and after subtraction B.G for  $^{60}\text{Co}$  source a-Net. b- Cross.**

Figure (4-4) shows the behavior of the (net and cross) photopeak, where it notices a difference in the histogram of the photopeak before subtraction B.G from its shape after subtraction B.G, in addition to the clear difference between the first photopeak and the second photopeak. This led to not giving clear vision of the mechanism of data distribution and dispersal, table (4-3) is summary of the studied samples of the T.A. and the P.P.A. for  $^{22}\text{Na}$  source.

**Table (4-3) Summary of Spectrum  $^{22}\text{Na}$  for Total Area and Photopeak.**

summary		N.T.A.		C.T.A.		P.N.A.		P.C.A.	
		Before	After	Before	After	Before	After	Before	After
Population Study	Min	27317	22589	46994	42163	12929	12689	15212	14801
	Max	48980	42000	74714	43945	14983	18389	16142	15860
	1st. Qu	36795	31653	47949	43147	13768	13579	15546	15151
	Median	39653	34706	48081	43278	13993	13823	15651	15264
	3rd. Qu	43917	38559	48181	43381	14236	14027	15774	15370
	IQR	7122	6906	232	234	468	448	228	219
	O- up	59663	52359	75062	44296	15685	19061	16484	16188
	O-down	16634	12230	46646	41812	12227	12017	14870	14472
	Mean	39652.54	34705.78	48192.12	43255.9	13992.9	13823.34	15661	15267
	Var	22927386	2129422	3608355	52181.3	122493.	231988.6	29090	2496.1
$\sigma$	4788.255	4614.567	1899.567	228.432	349.991	481.652	170.55	157.99	
Sample	(EX)	39613.39	34678.36	48193.65	43255.8	13993.5	13824.99	15661	15268
	Var	23002797	2127006	3644724	52704.1	123633	234062.3	29323	24981.
	sd.	4796.123	4611.948	1909.116	229.573	351.614	483.7998	171.24	158.05
	Median	39654	34524	48081	43278	14018	13785	15651	15264
	IQR	7241	6661	237	239	473	453	230	218
	O- up	59841.5	51991.5	75069.5	54806.5	15692.5	19068.5	16487	16187
	O-down	16455.5	12597.5	46638.5	31301.5	12219.5	12009.5	14867	14474
Sample standard Bar	$\bar{X}$	39648.98	34708.52	48192.66	43255.9	13992.9	13823.13	15661	15267
	Var	1088.641	1009.924	95.42251	2.68626	6.02542	16.7524	1.1911	1.2109
	sd.	32.99456	31.7793	9.768444	1.63898	2.45467	4.09297	1.0914	1.1004
	Median	39648	34708	48193	43256	13993	13824	15661	15268
	IQR	42	46	2	2	3	3	2	2
	O-up	50608.5	45641.5	59062.5	54123.5	14709.5	14538.5	16010	15616

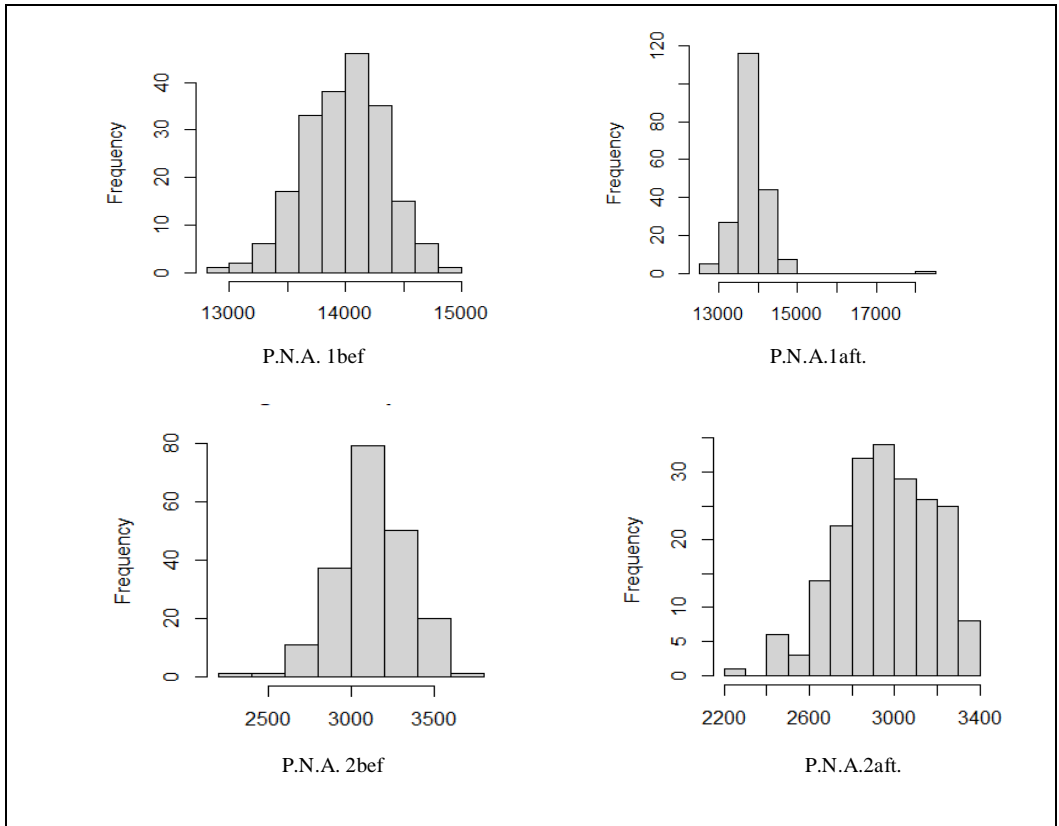
Table (4-3) presents a summary of  $^{22}\text{Na}$  source for the T.A. and P.P.A. samples before and after subtracting B.G., table shows the lowest and highest readings, the mean, median, variance, standard deviation, and the quartiles' values, in addition to the outliers values if found in the studied sample, as figure (4-5) which describe the general behavior of the data distribution for total area.



**Figure (4-5) The general behavior of total area before and after subtracting B.G for  $^{22}\text{Na}$  source a-Net. b- Cross.**

The histogram (4-5) represents the behavior of total area of the  $^{22}\text{Na}$  spectrum, it notes the difference between the shape for N.T.A.bef. and C.T.A.bef. B.G., as well as the presence of a small difference in the shape of the histogram for the N.T.A.bef.

and N.T.A.aft. subtracting B.G., while it notices a significant difference in the shape of the histogram for the C.T.A.bef. and C.T.A.aft. This indicates the absence of a basic principle on which the mechanism of distributing data about mean is based, figure (4-6) represents the general behavior of the photopeak samples of  $^{22}\text{Na}$  source.



a

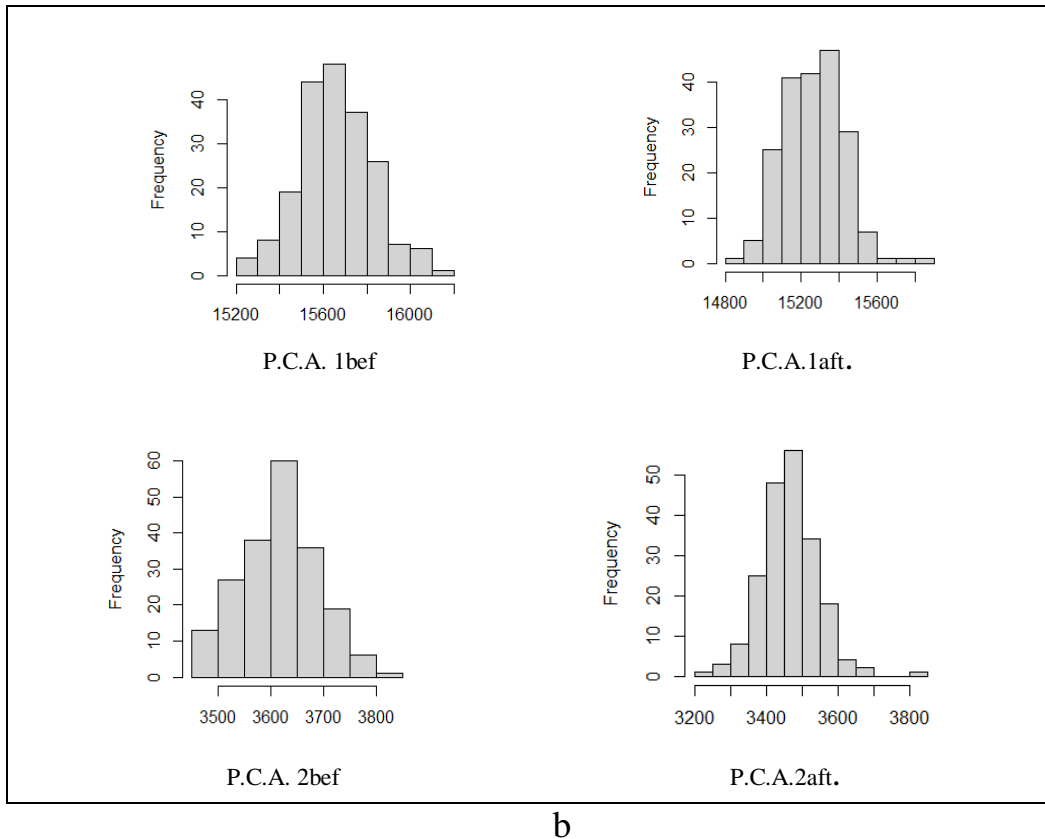


**Figure (4-6) The general behavior of photopeak before and after subtracting B.G for  $^{22}\text{Na}$  source a-Net. b- Cross.**

Histogram (4-6) represents the area of the photopeak of the  $^{22}\text{Na}$  source, and its note that there is a difference between the shape of the P.N.A.bef and P.N.A.aft. after the background, while the cross-photopeak it notices a slight convergence between the shapes of the P.C.A.bef. and P.C.A.aft. This result differs from the previous forms, which supports the view that there is no unified mechanism for distributing data statistically.

## 4.2 Spectrum for Energy Resolution and P/V Ratio

For the E.R. and the P/V Ratio, there are shown in the tables (4-4) to (4-6) for  $^{137}\text{Cs}$ ,  $^{60}\text{Co}$  and  $^{22}\text{Na}$  source, respectively.



**Table (4-4) Summary of Spectrum <sup>137</sup>Cs for Energy Resolution and P/V Ratio.**

summary		E.R.		P/V	
		Before	After	Before	After
Population	Min	0.04777	0.06613	77.64	12.57
	Max	0.07772	0.07446	208.75	295
	1st Qu	0.06943	0.06926	120.54	141.29
	Median	0.07049	0.07043	139.00	172.00
	3rd. Qu	0.07178	0.07171	143.17	211.81
	IQR	0.00235	0.00245	22.63	70.52
	O- up	0.081245	0.078135	242.695	400.78
	O-down	0.044245	0.069805	43.695	118.35
	Mean	0.07048518	0.07043431	133.9234	174.8603
	Var	6.062001e <sup>-06</sup>	2.888173e <sup>-06</sup>	454.4595	2035.041
	σ	0.002462113	0.001699463	21.31806	45.11143
Sample	EX	0.07050699	0.07042285	133.8258	174.1392
	Var	6.075703e <sup>-06</sup>	2.903885e <sup>-06</sup>	458.0791	1991.874
	sd	0.00246489	0.00170408	21.40278	44.63041
	Median	0.07085	0.07051	139.00	172.00
	IQR	0.00233	0.00246	22.71	70.57
	O- up	0.081215	0.077955	242.815	329.065
	O-down	0.044275	0.062635	43.575	-21.495
Sample standard Bar	X.bar	0.07048523	0.07043308	133.9257	174.8783
	Var	3.442291e <sup>-10</sup>	1.519468e <sup>-10</sup>	0.0222194	0.09711117
	sd	1.855341e <sup>-05</sup>	1.232667e <sup>-05</sup>	0.1490618	0.3116267
	Median	0.07048	0.07043	133.9	174.9
	IQR	1e <sup>-05</sup>	3e <sup>-05</sup>	0.2	0.4
	O-up	0.074095	0.074095	168.365	209.765
	O-down	0.066955	0.066955	99.435	140.035

Table (4-4) shows summary of the studied samples of the E.R and P/V ratio for <sup>137</sup>Cs source before and after subtracting B.G., table presents min and max readings, the mean, median, variance, standard deviation, and the quartiles' values,

as figure (4-7) which describe the general behavior of the data distribution for E.R. sample.

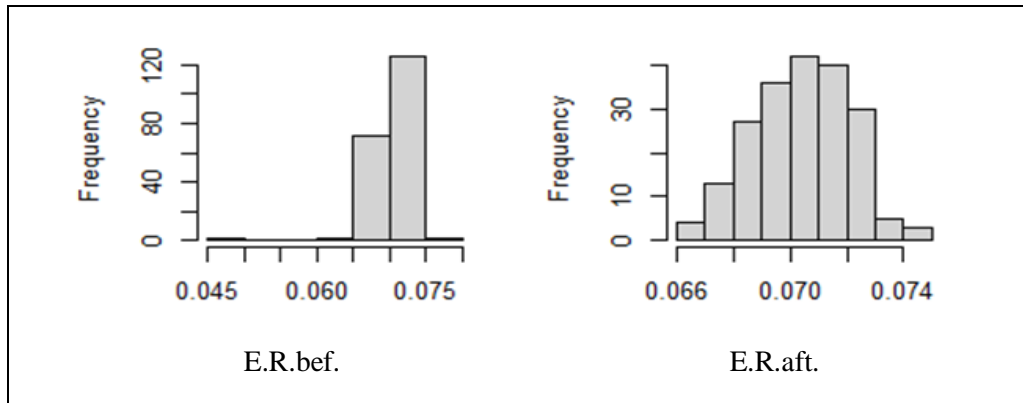


**Figure (4-7) The general behavior for energy resolution before and after subtracting B.G for  $^{137}\text{Cs}$  source.**

The histogram (4-7) presents the general behavior of the E.R. of the  $^{137}\text{Cs}$  spectrum, it notes a difference in shape between E.R.bef. from E.R.aft. , accordingly it can use histograms to estimate the distribution and spread of data around the mean, as we note that the x-axis (data range) is divided into equal periods while the height of each square represents the number of observations that fall within the mean ,table (4-5) shows the summary of the studied models of the E.R. and P/V ratio for  $^{60}\text{Co}$  source.

**Table (4-5) Summary of Spectrum <sup>60</sup>Co for Energy Resolution and P/V Ratio.**

Summary		(E.R.)1		(E.R.)2		(P/V)1		(P/V)2	
		Before	After	Before	After	Before	After	Before	After
Population	Min	0.02010	0.03214	0.001874	0.02361	2.13	8.40	9.80	9.09
	Max	0.05285	0.05030	0.064894	0.23721	26.60	21.17	47.00	26.00
	1st Qu	0.03753	0.04006	0.040293	0.03683	13.32	11.27	16.13	14.00
	Median	0.04040	0.04271	0.043065	0.03972	15.00	12.33	19.00	15.86
	3rd. Qu	0.04262	0.04486	0.045335	0.04188	17.71	13.78	23.06	17.67
	IQR	0.00509	0.0048	0.005042	0.00505	4.39	2.51	6.93	3.67
	O- up	0.060485	0.0575	0.072457	0.244785	33.185	24.935	57.395	31.505
	O-down	0.012465	0.02494	-0.005689	0.016035	-4.455	4.635	-0.595	3.585
	Mean	0.03986406	0.04241644	0.04265783	0.04027563	15.8268	12.59047	19.5023	16.05614
	Var	1.947939e-05	1.308436e-05	2.338671e-05	0.000214429	11.97626	4.087218	24.68808	10.16238
$\sigma$	0.004413547	0.003617231	0.00483598	0.01464341	3.460673	2.021687	4.96871	3.187849	
Sample	EX	0.03980277	0.04241024	0.04265862	0.04030798	15.81424	12.58781	19.52035	16.0668
	Var	1.924542e-05	1.321196e-05	2.351405e-05	0.000216478	12.07783	4.063478	24.8981	10.23127
	sd.	0.00438696	0.003634826	0.00484913	0.01471317	3.475318	2.015807	4.98146	3.198636
	Median	0.04027	0.04271	0.043065	0.03980	15.00	12.33	19.00	15.86
	IQR	0.00499	0.00485	0.005021	0.0051	4.37	2.51	6.96	3.67
	O- up	0.060335	0.057575	0.0724255	0.244695	33.155	24.935	57.44	32.555
O-down	0.012615	0.024865	-0.0056575	0.016125	-4.425	4.635	-0.64	2.535	
Sample standard Bar	X.bar	0.03986823	0.04241664	0.04266048	0.04028166	15.8286	12.59037	19.5021	16.05499
	Var	9.627217e-10	7.480784e-10	1.63196e-09	6.018681e-09	0.000663	0.0001857	0.0011757	0.0006211
	sd.	3.102776e-05	2.735102e-05	4.039753e-05	7.758016e-05	0.02575	0.013629	0.034288	0.024922
	Median	0.03987	0.04241	0.04265	0.04028	15.83	12.59	19.50	16.06
	IQR	4e-05	4e-05	3e-05	5e-05	0.04	0.02	0.04	0.03
	O-up	0.047445	0.049985	0.050365	0.047885	22.465	19.175	26.135	22.665
	O-down	0.032305	0.034865	0.035035	0.031795	9.205	5.995	12.765	9.415

Table (4-5) is shown summary of the studied samples of the E.R and P/V ratio for <sup>60</sup>Co source, where the table is divided into three groups, the first group is the study population represented by radioactive sources, the second group is the random samples selected by the R program, and the third group represents expected samples

if there were other samples taken from the same study population. The Table also included a of data distribution, as shown in the figure (4-8).

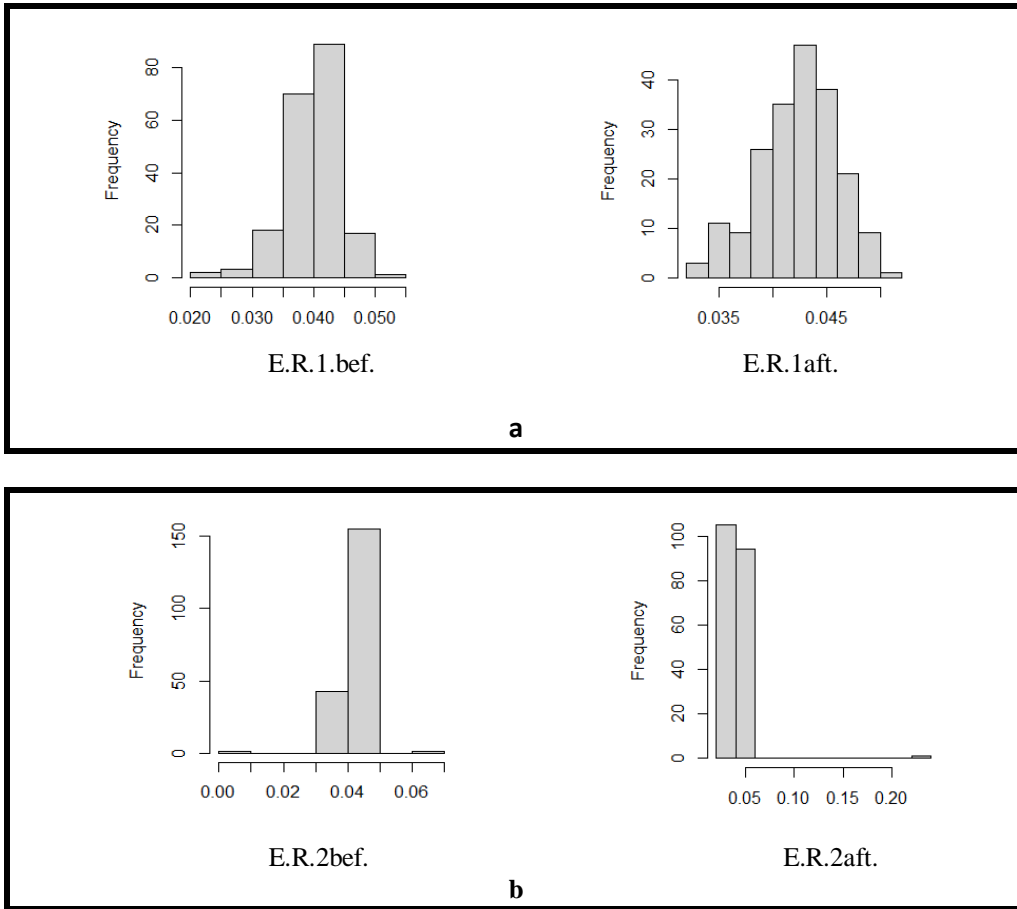


**Figure (4-8) The general behavior for energy resolution before and after subtracting B.G for  $^{60}\text{Co}$  source. a-E.R.1 b-E.R.2.**

It had been noticed from the figure (4-8) the dispersion of the E.R. values of the  $^{60}\text{Co}$  source before and after subtracting B.G. It had been noticed that there is a clear difference between the E.R.1 value of the first photopeak from the E.R.2 values of the second photopeak. Also, table (4-6) shown summary of the studied samples of the E.R. and P/V ratio for  $^{22}\text{Na}$  source.

**Table (4-6) Summary Spectrum <sup>22</sup>Na for Energy Resolution and P/V Ratio.**

Summary		E.R.		P/V	
		Before	After	Before	After
Population Study	Min	0.05895	0.05889	15.50	16.12
	Max	0.07903	0.07895	40.80	40.80
	1st. Qu	0.06886	0.06848	22.44	23.75
	Median	0.07106	0.07069	24.65	26.12
	3rd. Qu	0.07361	0.07305	27.28	30.00
	IQR	0.00475	0.00457	4.84	6.25
	O- up	0.086155	0.085805	48.06	50.175
	O-down	0.051825	0.052035	8.24	6.745
	Mean	0.0711175	0.07065205	25.2044	26.9545
	Var	1.274763e <sup>-05</sup>	1.330377e <sup>-05</sup>	21.0708	21.4894
	σ	0.0035703	0.00364743	4.59029	4.63567
Sample	EX	0.0710915	0.07066547	25.2625	26.9590
	Var	1.280449e <sup>-05</sup>	1.342067e <sup>-05</sup>	20.93724	21.53792
	sd	0.003578336	0.003663423	4.575723	4.640896
	Median	0.07106	0.07072	24.67	26.12
	IQR	0.00481	0.00461	4.76	6.2
	O- up	0.086245	0.085865	47.94	50.1
	O-down	0.051735	0.051975	8.36	6.82
Sample standard Bar	X.bar	0.07111877	0.07065025	25.20298	26.95836
	Var	6.58427e <sup>-10</sup>	5.963769e <sup>-10</sup>	0.0009903977	0.001042847
	sd	2.565983e <sup>-05</sup>	2.442083e <sup>-05</sup>	0.031470	0.032293
	Median	0.07112	0.07065	25.20	26.96
	IQR	3e <sup>-05</sup>	4e <sup>-05</sup>	0.04	0.04
	O-up	0.078425	0.077955	32.41	34.17
	O-down	0.063845	0.063385	17.93	19.73

Table (4-6) presents a summary of <sup>22</sup>Na source for the E.R. and P/V ratio samples before and after subtracting B.G., the table shows the min and max value of data probability, mean, median, variance, standard deviation, and the quartiles' values, the figure (4-9) which describe the general behavior of this data distribution.

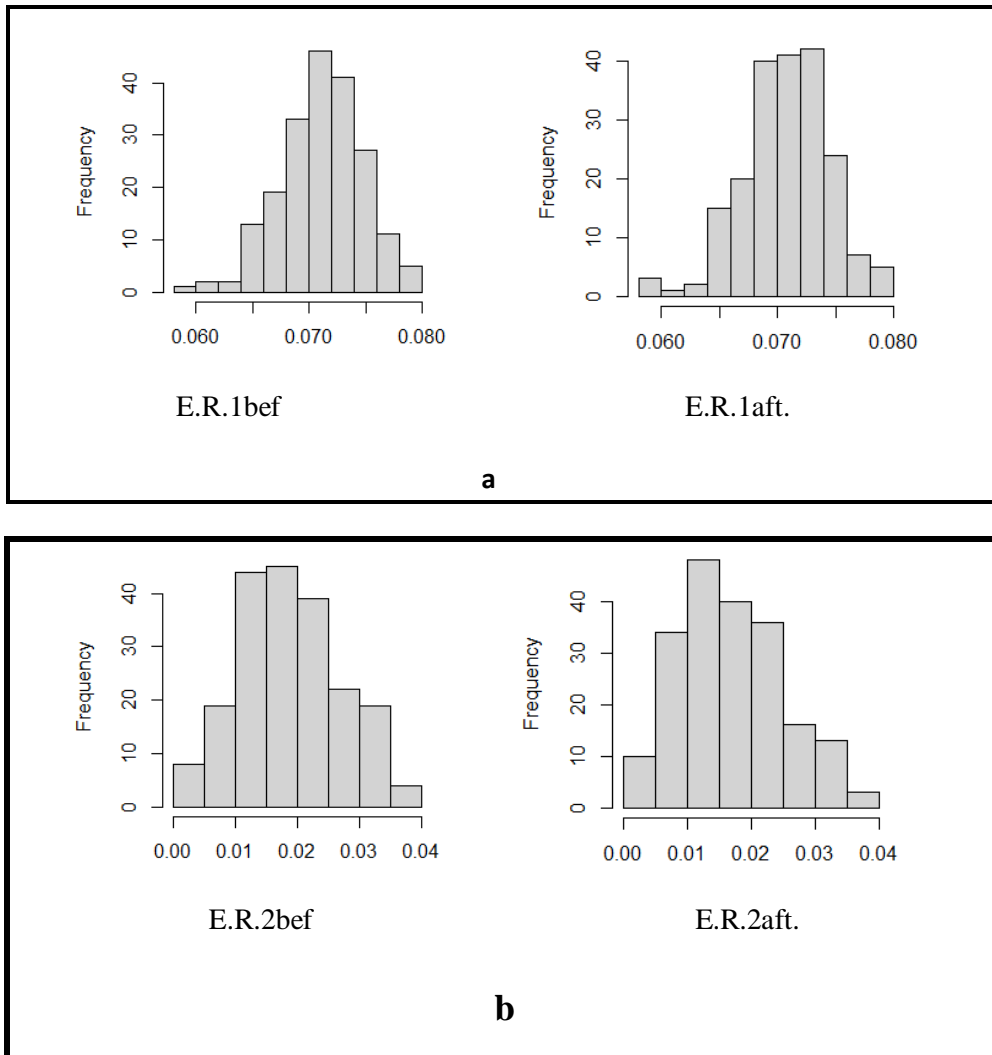


**Figure (4-9) The general behavior for energy resolution before and after subtracting B.G for  $^{22}\text{Na}$  source. a-E.R.1 b-E.R.2.**

It had been noticed from the figure (4-9) that there is convergence in the dispersion of data for the E.R. samples of the first and second photopeak before and after subtracting B.G., despite the fact that the E.R.2 sample of the second photopeak is greater than the E.R.1 sample of the first photopeak, whether before or after subtracting B.G.

As for the P/V ratio, there are shown in the figures (4-10) to (4-12) for  $^{137}\text{Cs}$ ,  $^{60}\text{Co}$  and  $^{22}\text{Na}$  source, respectively.

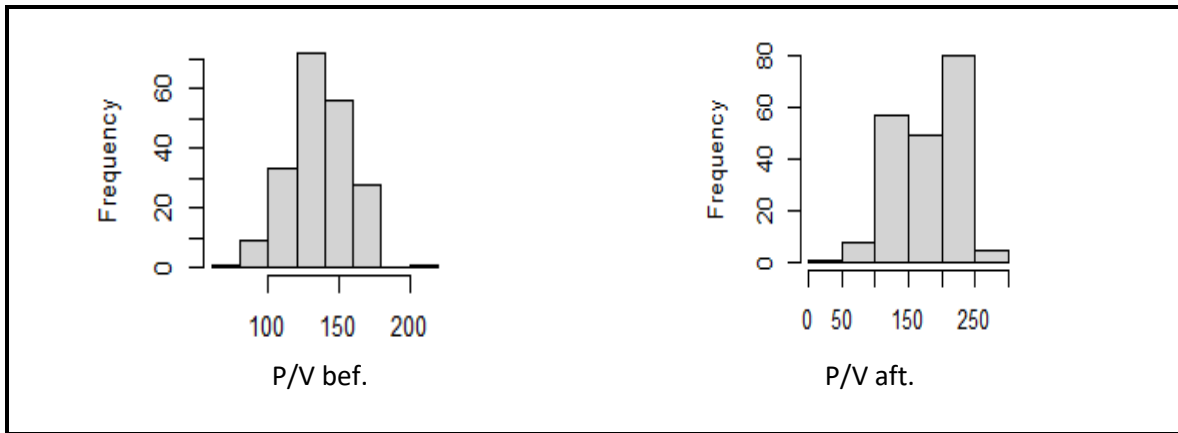


**Figure (4-10) The general behavior for p/v ratio before and after subtracting B.G. for  $^{137}\text{Cs}$  source.**

From figure (4-10), it notices that there is a very small difference between the P/V ratio before and after subtracting B.G. for  $^{137}\text{Cs}$  source, this means that there is little dispersion in the data around the mean, unlike what is found in the previous samples, and this indicates the difficulty of relying on the histogram to explain the mechanism of data dispersion. This applies to all other sources and forms in figures (4-11) and (4-12) for  $^{60}\text{Co}$  and  $^{22}\text{Na}$  source, respectively.

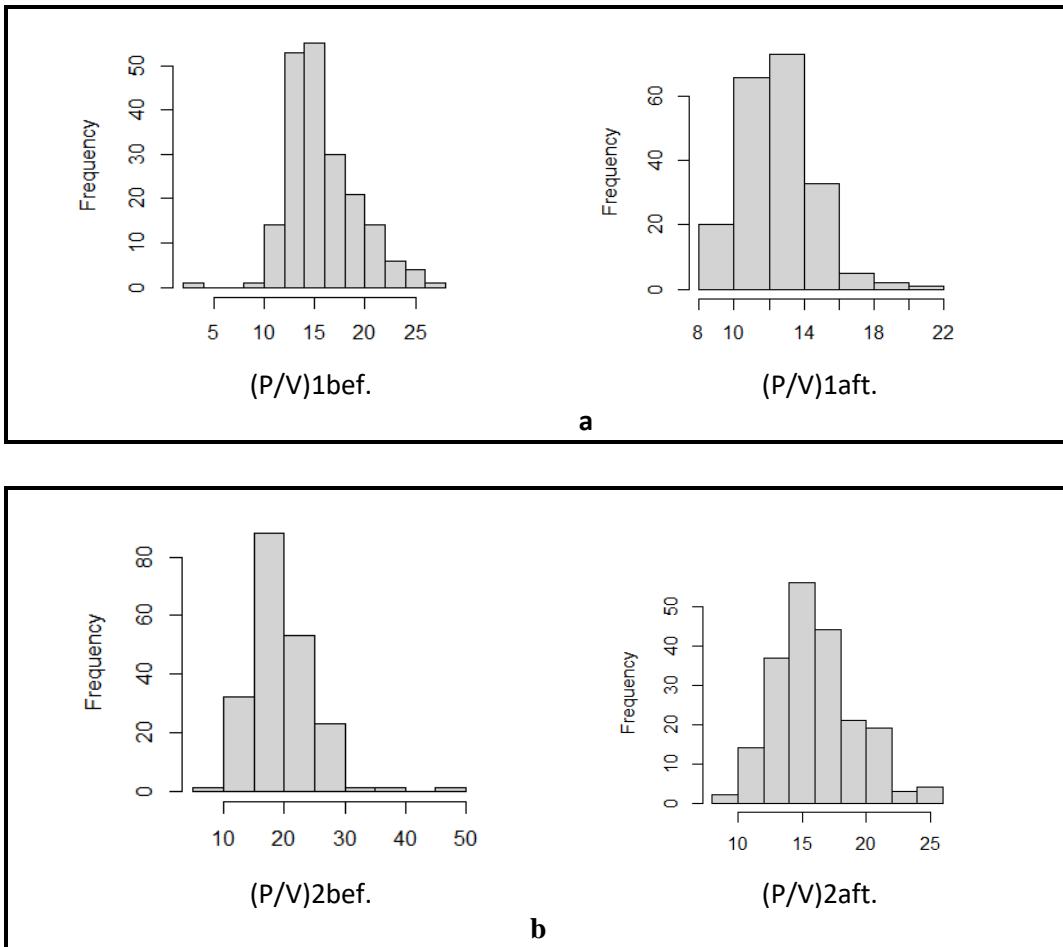


**Figure (4-11) The general behavior for P/V ratio before and after subtracting B.G. for  $^{60}\text{Co}$  source. a-(P/V) 1 b-(P/V)2 .**

Histogram (4-11) shows there is convergence in the dispersion of data for the values of the P/V ratio of the first and second photopeak area before and after the subtracting B.G. for  $^{60}\text{Co}$  source, despite the fact that the values of the P/V ratio for the second photopeak is greater and the number of columns is more than the values of the P/V ratio of the first photopeak after subtracting B.G.



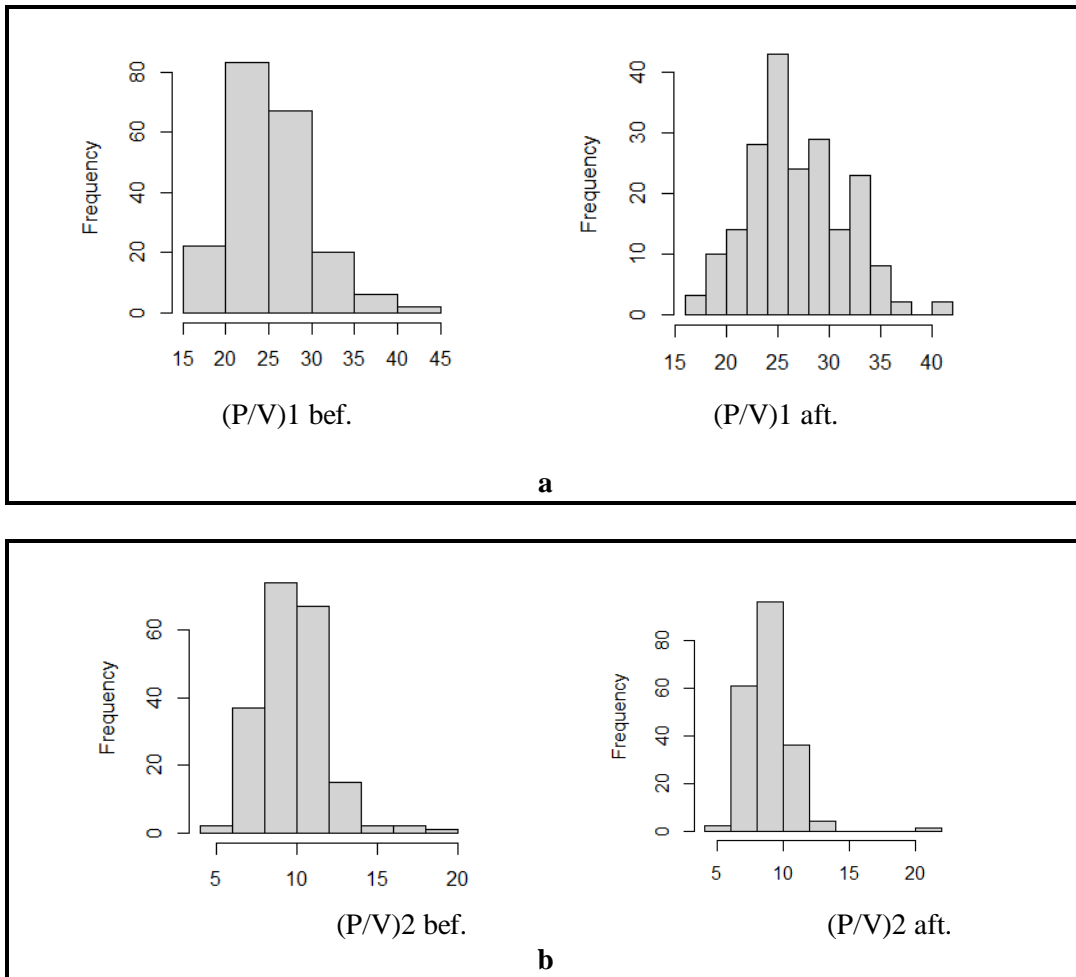


**Figure (4-12) The general behavior for P/V ratio before and after subtracting B.G. for  $^{22}\text{Na}$  source. a-(P/V) 1 b-(P/V)2**

It had been noticed from the figure (4-12) there is a difference between the P/V ratio before and after subtracting B.G. for first and second photopeak area for  $^{22}\text{Na}$  source. This contradicts what was stated in the previous figures, which confirms the difficulty of relying on this statistical method in understanding and reading data is scattered about the mean.

### 4.3 Normality Test.

To find out the homogeneity of the variance we use Normality Test which contains the Kolmogorov-Smirnov Test, Shapiro. Test, T-Test, Wilcoxon Test and Bartlett for the data samples, as table (4-7).

**Table (4-7) Normality for Total Area and Photopeak Area of Three Sources.**

Source	Type of test	N.T.A.		C.T.A.		P.N.A.1		P.N.A.2		P.C.A.1		P.C.A.2	
		Before	After	Before	After	Before	After	Before	After	Before	After	Before	After
<sup>137</sup> Cs	Kolmogorov-Smirnov test	0.5774	0.4701	2.2e-16	1.89e-13	2.2e-16	1.108e-07			4.26e-10	6.35e-07		
	Shapiro. Test	2.498e-05	1.38e-06	0.1392	2.2e-16	2.2e-16	2.2e-16			2.2e-16	7.99e-16		
	bartlett. test	0.564	0.7143	0.6244	0.03948	0.4652	0.8373			0.7249	0.9209		
	t-test	0.9943	0.9991	0.9942	0.9883	0.9979	0.9556			0.9956	0.9468		
	Wilcoxon. test	0.9665	0.8555	0.9903	7.87e-07	2.2e-16	0.06			5.897e-11	2.88e-08		
<sup>60</sup> Co	Kolmogorov-Smirnov test	0.000194	0.000664	0.9189	0.8336	0.7939	0.7957	0.0765	0.9149	0.2451	0.7686	0.0116	0.7678
	Shapiro. Test	1.445e-10	8.907e-09	0.4834	0.4065	0.1708	0.5901	1.49e-15	0.6363	6.11e-13	0.4439	2.2e-16	0.3562
	bartlett. test	0.995	0.6303	0.7082	0.6727	0.5139	0.5757	0.7314	0.0669	0.5997	0.07595	0.0493	0.2478
	t-test	0.9975	0.9985	0.9983	0.9971	0.9967	0.9938	0.9923	0.9946	0.9938	0.9929	0.9985	0.998
	Wilcoxon. test	0.2547	0.6921	0.983	0.9645	0.7645	0.8077	0.4578	0.9664	0.4563	0.7571	0.5454	0.9771
<sup>22</sup> Na	Kolmogorov-Smirnov test	0.2434	0.1384	2.2e-16	0.1503	0.7604	0.00953	0.2642	0.8898	0.8659	0.9098	0.8446	0.7901
	Shapiro. Test	5.289e-05	4.62e-05	2.2e-16	0.000143	0.9127	2.2e-16	0.2265	0.0385	0.7456	0.1311	0.3976	0.00083
	bartlett. test	0.5172	0.3	0.8631	0.3408	0.4784	0.6109	0.9328	0.9386	0.5386	0.6069	0.2087	0.6742
	t-test	0.9916	0.9933	0.9968	0.9984	0.9985	0.995	0.9993	0.9964	0.9947	0.9992	0.9953	0.9991
	Wilcoxon. test	0.6363	0.9586	5.62e-13	0.4497	0.7785	0.224	0.9489	0.7299	0.849	0.8744	0.9218	0.8342

Table (4-7) shows the test of normality i.e., whether the samples studied follow a normal distribution or not follow a normal distribution of three radioactive sources, for the total area and photopeak samples, by noting the p-value (significant level) if the p-value is higher than 0.05, it accepts the null hypothesis ( $H_0$ ), or if the p-value is less than (0.05), it rejects the null hypothesis and take the alternative hypothesis ( $H_1$ ) according to the (Eq. 2-19), it means that the two groups are different on the mean.

Therefore, it had been found that in Kolmogorov-Smirnov test for the  $^{137}\text{Cs}$  source in T.A. samples, the N.T.A. after and before subtracting B.G. was p-value greater than 0.05 (follow to a normal distribution), while the p-value was less than the C.T.A. before and after subtracting B.G. for the same source. i.e., this sample is not following a normal distribution.

While test result was exactly the opposite in the  $^{60}\text{Co}$  source, where p-value in N.T.A. before and after subtracting B.G. was less than 0.05 (not follow normal distribution), and C.T.A. before and after subtracting B.G. was p-value greater than 0.05.(follow normal distribution).

In  $^{22}\text{Na}$  source, the p-value of N.T.A. before and after subtracting B.G. and C.T.A. after subtracting B.G. were greater than 0.05 (follow normal distribution) except in C.T.A. before subtracting B.G. was p-value much less than 0.05 which means that this sample is not follow normal distribution.

For P.P.A. samples the Kolmogorov-Smirnov test in P.N.A. and P.C.A. before and after subtracting B.G. were p-value less than 0.05 for the  $^{137}\text{Cs}$  source which means that samples not follow to a normal distribution.

In  $^{60}\text{Co}$  source, a Kolmogorov-Smirnov test showed that all P.P.A. samples before and after subtracting B.G. were follow to a normal distribution because p-value is greater than 0.05.

For  $^{22}\text{Na}$  source, the P.P.A. samples before and after subtracting B.G. were follow to a normal distribution, except P.N.A.1 after subtracting B.G. was not follow to a normal distribution because p-value was less than 0.05.

In Shapiro Test for  $^{137}\text{Cs}$  source of T.A. samples, and P.P.A. samples were not following to normal distribution because p-value was more less than 0.05.

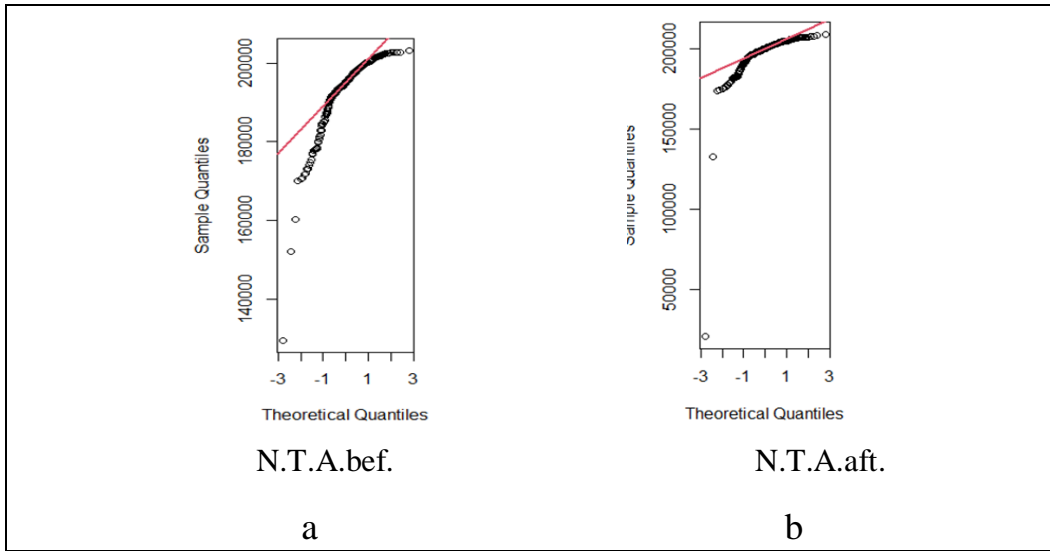
In  $^{60}\text{Co}$  source the Shapiro. Test for T.A. samples were N.T.A. not follow to a normal distribution unlike the C.T.A. was p-value greater than 0.05, therefore the samples are following to a normal distribution.

As for the P.P.A. samples were oscillating between follow and not follow to normal distribution, where the P.N.A.1 sample ware followed while the P.N.A.2 after was not follow normal distribution, while P.C.A.1 before subtracting B.G. was not follow normal distribution, but the P.C.A.1 sample after subtracting B.G. was follow, and the same of the P.C.A.2 sample.

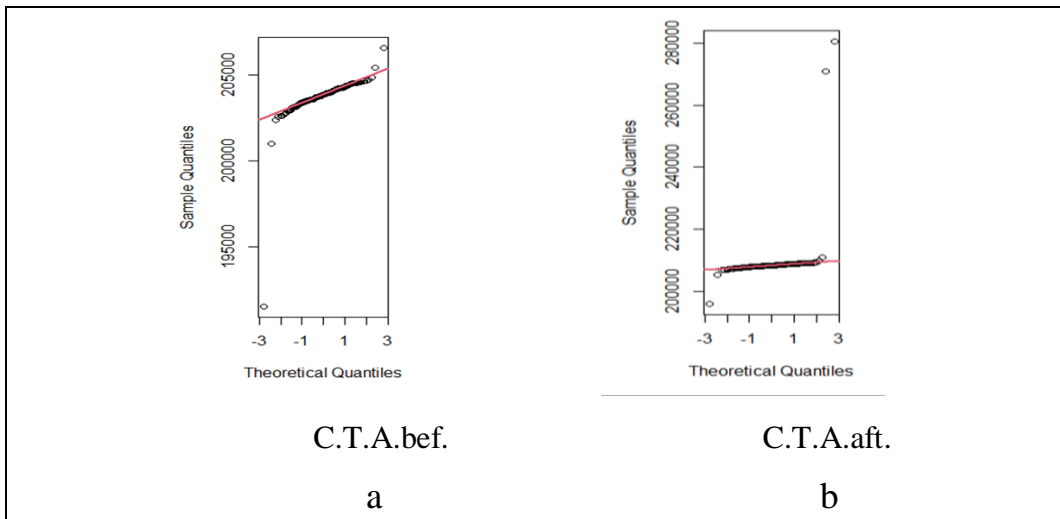
In  $^{22}\text{Na}$  source the Shapiro Test for T.A. samples before and after subtracting B.G. were not follow normal distribution. But in P.P.A. samples were all samples before subtracting B.G. follow the normal distribution unlike the samples after subtracting B.G. was not follow normal distribution depend on p-value less than 0.05.

In bartlett. test for three sources ( $^{137}\text{Cs}$ ,  $^{60}\text{Co}$  and  $^{22}\text{Na}$ ) for T.A. and P.P.A. samples are following normal distribution because p-value was greater than 0.05, according (Eq.2-19).

The T-Test was used to compare the mean between two groups to find out homogeneous the variance of the studied samples is by noting the p-value greater than 0.05, so it have been found all samples in T.A. and P.P.A. are homogeneous because p-value was greater than 0.05 for ( $^{137}\text{Cs}$ ,  $^{60}\text{Co}$  and  $^{22}\text{Na}$ ), as figures (4-13) to (4-18) .

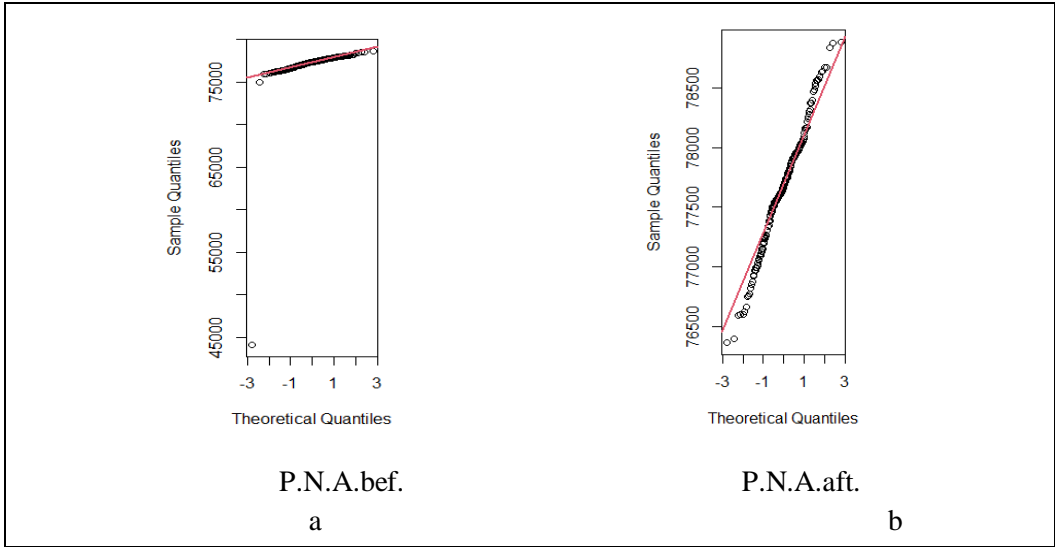


**1. Net area (a-before and b-after)**

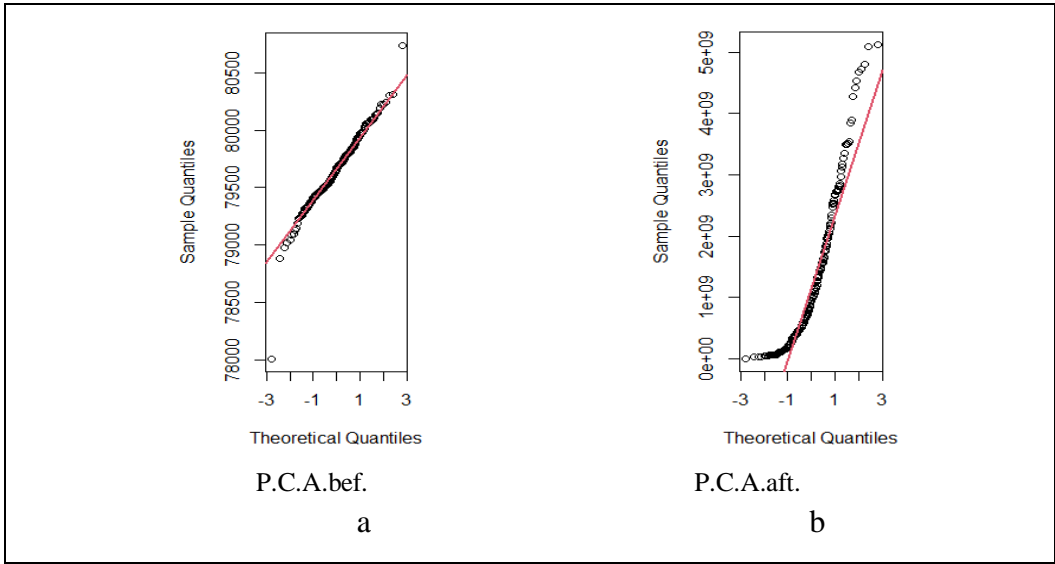


**2. Cross area (a- before and b-after)**

**Figure (4-13) Comparative of sampling mean by T-Test for total area of  $^{137}\text{Cs}$  source. 1- N.T.A. 2- C.T.A.**



**1. Photopeak net area (a- before and b- after)**

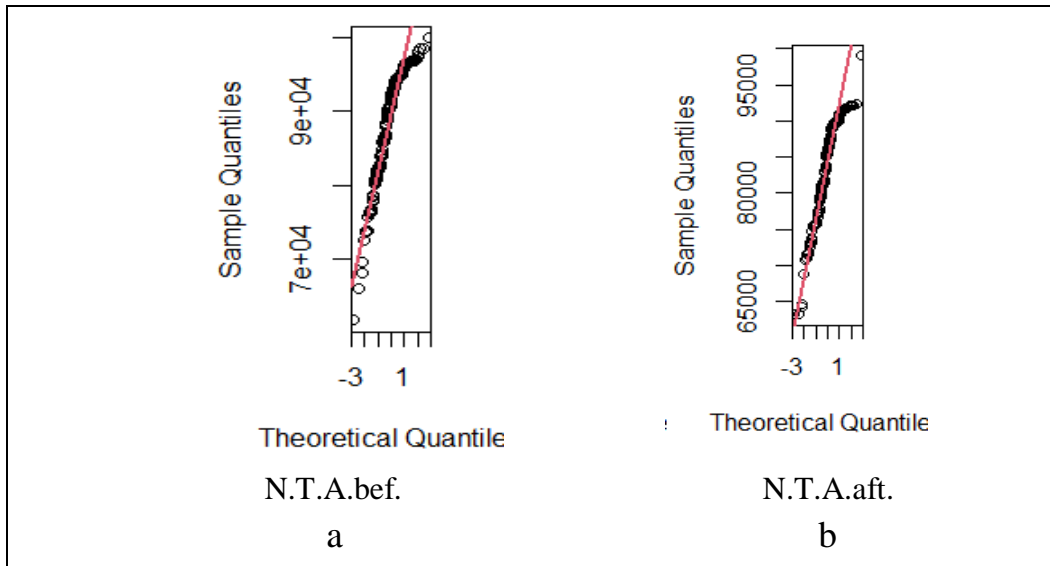


**2. Photopeak cross area (a- before and b- after)**

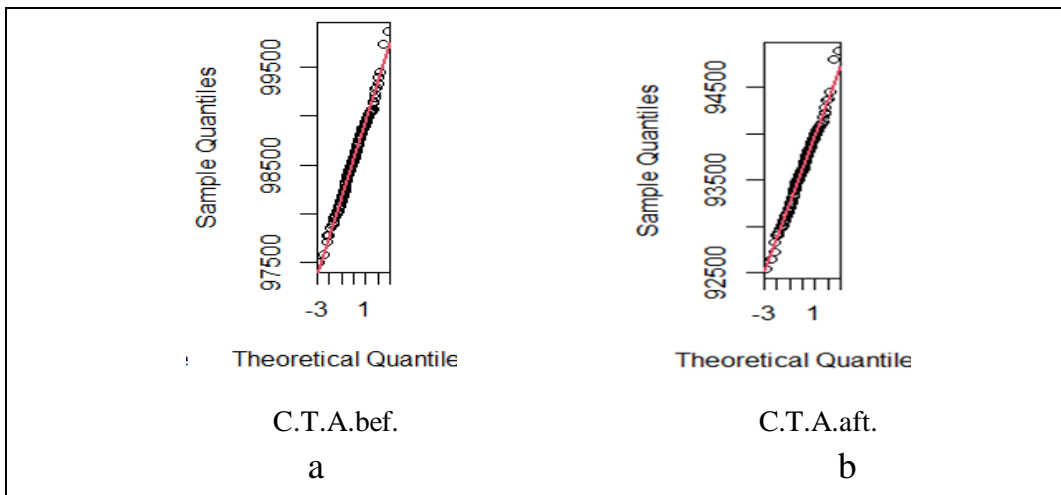
**Figure (4-14) Comparative of sampling mean by T-Test for photopeak area of <sup>137</sup>Cs source. 1. P.N.A. 2. P.C.A.**

Figures (4-13) and (4-14) show the T-Test for T.A. and P.P.A. samples for <sup>137</sup>Cs source, it found that the variance samples are homogeneous which indicates

that there is no significant difference between the mean of the samples, i.e., the samples are statistically regular. T.Test for  $^{60}\text{Co}$  source is shown at figure (4-15).



**1. Net area (a-before and b-after)**



**2. Cross area (a-before and b-after)**

**Figure (4-15) Comparative of sampling mean by T-Test for total area of  $^{60}\text{Co}$  source. 1- N.T.A. 2- C.T.A.**

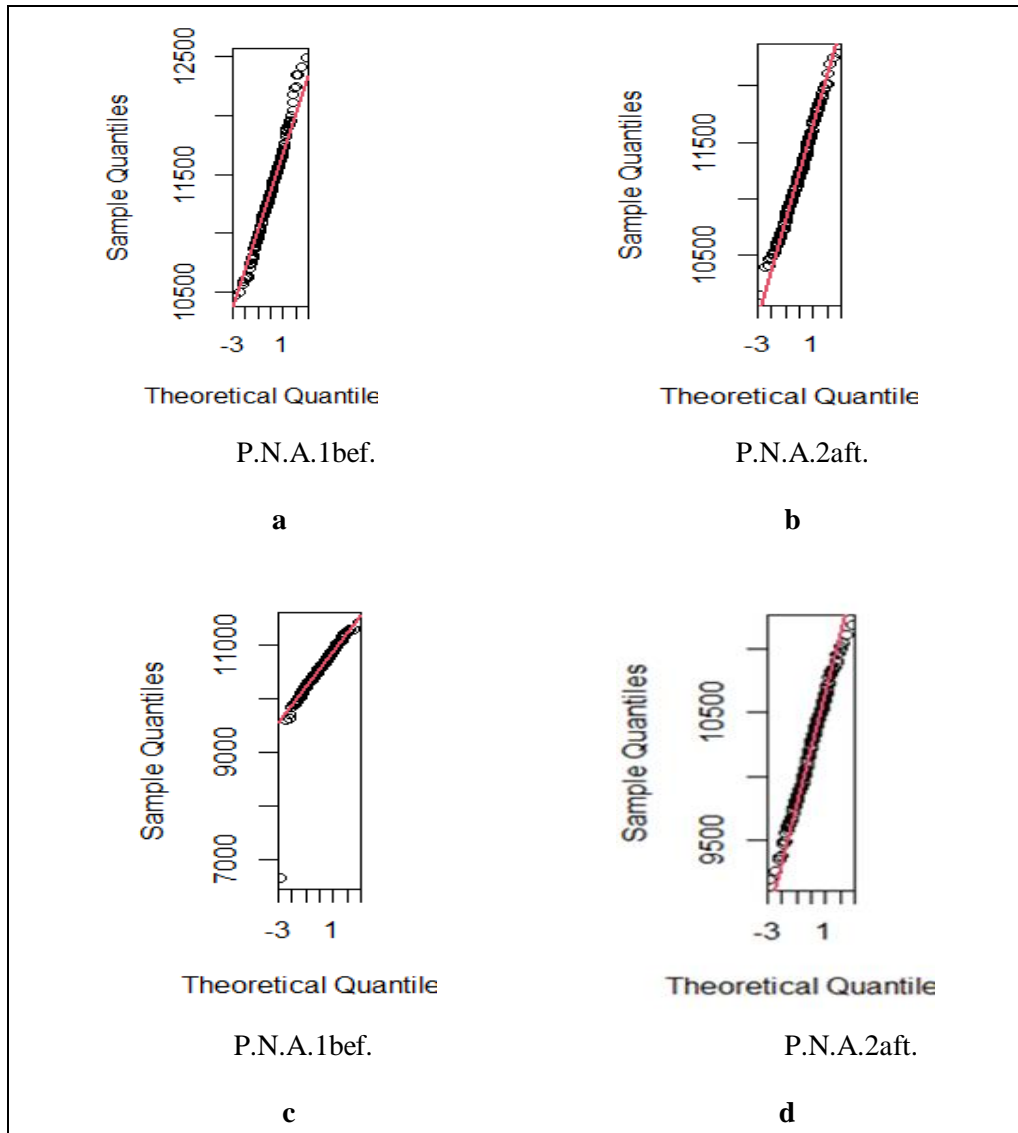
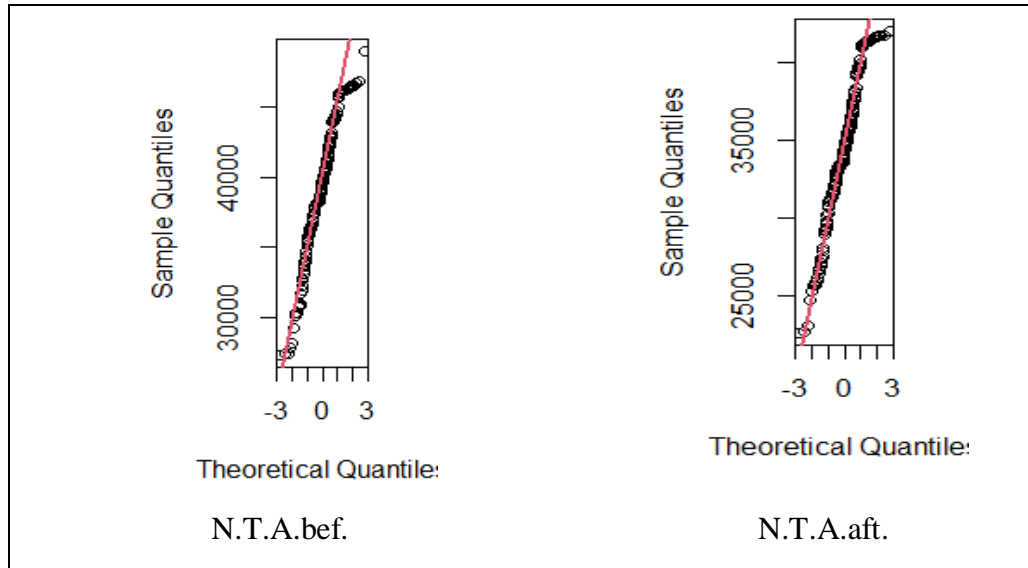


**Figure (4-16) Comparative of sampling mean by t-test for photopeak area of  $^{60}\text{Co}$  source. a & b P.N.A. 1 (before and after subtracting B.G.) c & d P.N.A. 2 (before and after subtracting B.G.).**

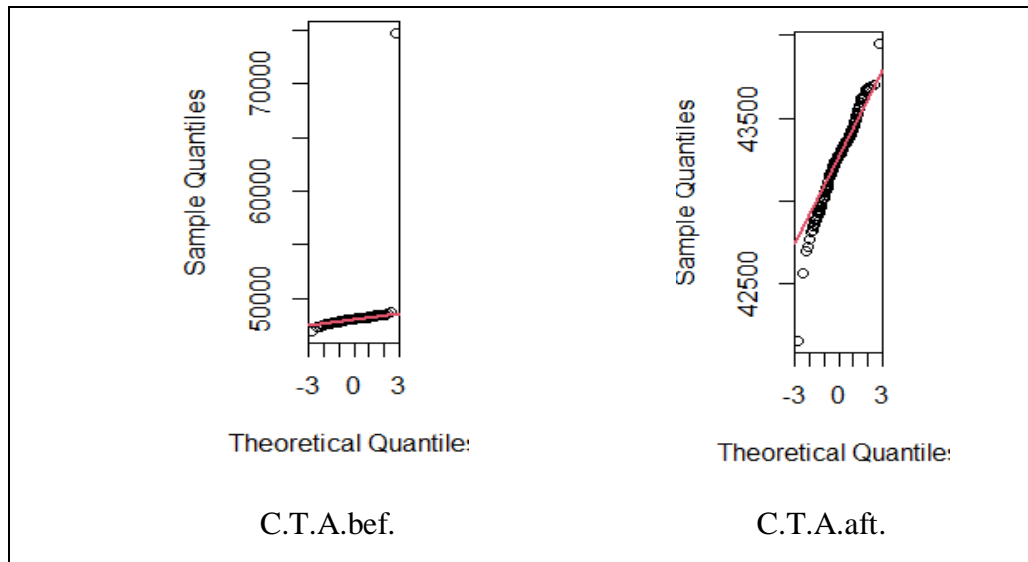
Figures (4-15) and (4-16) show the T-Test of the photopeak for  $^{60}\text{Co}$  source before and after the subtracting B.G., which note that the samples are homogeneous by matching the red straight line to the points of the studied samples, where the congruence is high in the samples except for the c sample, which has an abnormal shape from the rest of the samples.



The same case applies to the  $^{22}\text{Na}$  source in the use of T-Test to compare the mean between the two groups of samples, as figures (4-17) and (4-18).



a



b

**Figure (4-17) Comparative of sampling mean by T-Test for total area of  $^{22}\text{Na}$  source. a- N.T.A. b- C.T.A.**

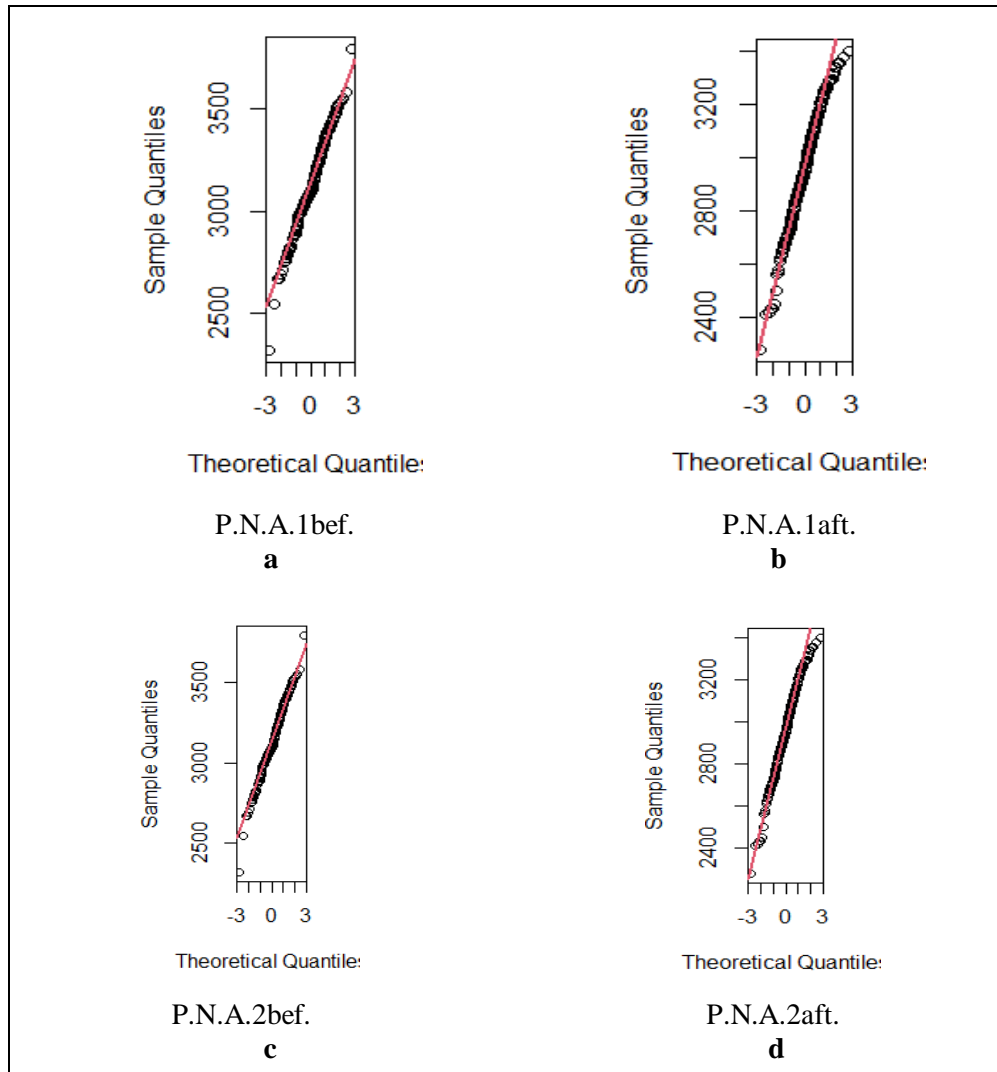


**Figure (4-18) Comparative of sampling mean by t-test for photopeak area of  $^{22}\text{Na}$  source. a & b P.N.A. 1 (before and after subtracting B.G.) c & d P.N.A. 2 (before and after subtracting B.G.).**

Figures (4-17) and (4-18) show the T-Test of the photopeak for  $^{22}\text{Na}$  source before and after the subtracting B.G., where note that the samples are homogeneous in all samples except for the b sample, which has an abnormal shape from the rest of the samples.

In Wilcoxon Test for  $^{137}\text{Cs}$  source, most of the samples were follow to a normal distribution because p-value is greater than 0.05, while P.C.A. was unfollowing normal distribution before and after the subtracting B.G. because p-value is  $<0.05$

As for the Wilcoxon Test for the source of  $^{60}\text{Co}$  and  $^{22}\text{Na}$ , all studied samples were follow to normal distribution depending on p-value.

The normality and homogeneity tests for the E.R. samples and the P/V ratio of the three sources were also calculated as shown in the table (4-8).

**Table (4-8) Normilty for E.R and P/V Ratio for Three Sources.**

Source	Type of test	(R.E.)1		(R.E.)2		(P/V)1		(P/V)2	
		Before	After	Before	After	Before	After	Before	After
$^{137}\text{Cs}$	Kolmogorov-Smirnov Test	7.317e-06	0.007866			0.4173	0.03841		
	Shapiro. Test	3.009e-07	2.736e-05			0.1888	2.2e-16		
	bartlett. Test	0.2091	0.9931			0.5917	0.7552		
	T-Test	0.9955	0.9988			0.9989	0.9908		
	Wilcoxon. Test	0.57	0.2203			0.8001	0.3173		
$^{60}\text{Co}$	Kolmogorov-Smirnov Test	0.2467	0.4762	0.04036	2.2e-16	0.002964	0.5315	0.09303	0.06228
	Shapiro. Test	2.598e-05	0.04941	7.06e-16	2.2e-16	6.075e-07	0.0001471	1.222e-07	0.0004735
	bartlett. Test	0.7312	0.1933	0.5117	0.5563	0.6066	0.756	0.2422	0.3536
	T-Test	0.9893	0.9994	0.9938	0.9954	0.9907	0.9992	0.9911	0.9967
	Wilcoxon. Test	0.4395	0.5842	0.3097	0.01023	0.3191	0.4652	0.5325	0.3988
$^{22}\text{Na}$	Kolmogorov-Smirnov Test	0.9325	0.87	0.4029	0.2513	0.04307	0.03548	0.1034	0.009483
	Shapiro. Test	0.278	0.06552	0.02991	0.001728	8.001e-05	0.04014	5.646e-06	4.709e-13
	bartlett. Test	0.4382	0.9905	0.883	0.2787	0.655	0.9412	0.9572	0.1767
	T-Test	0.996	0.9944	0.9973	0.9996	0.9964	0.9906	0.9955	0.998
	Wilcoxon. Test	0.7377	0.6948	0.7021	0.6087	0.2843	0.7992	0.4308	0.1827

In Kolmogorov-Smirnov test of R.E. samples for the  $^{137}\text{Cs}$  source, the p-value was smaller than 0.05, therefore it not follows to a normal distribution, in

contrast at E.R.aft. the p- value was larger than 0.05 and so it follows to a normal distribution. As for P/V ratio it was follow to a normal distribution in all samples.

The Kolmogorov-Smirnov test of the  $^{60}\text{Co}$  source for the sample E.R.bef subtracting B.G. was following to the normal distribution, but E.R.bef subtracting B.G. was unfollow to normal distribution. While the P/V ratio of the  $^{60}\text{Co}$  source was following to a normal distribution both before and after subtracting B.G.

For the  $^{22}\text{Na}$  source, the E.R. and P/V ratio samples in the Kolmogorov-Smirnov test were follow to a normal distribution before and after subtracting B.G., depending on the p- value, which was greater than 0.05 in all samples.

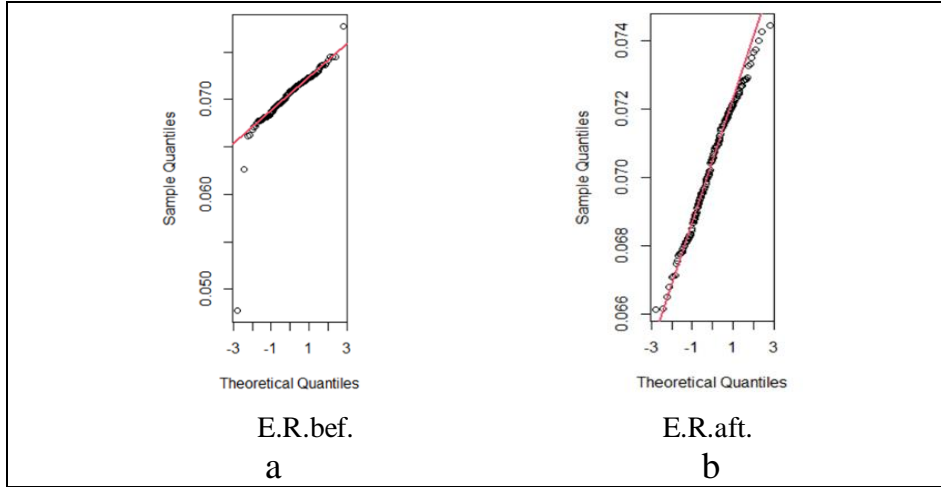
In the Shapiro Test of the  $^{137}\text{Cs}$  source of the E.R. sample was p-value less than 0.05 therefore not follow to the normal distribution, as well as the case for the  $^{60}\text{Co}$  source. As for  $^{22}\text{Na}$  source, p-value was greater than 0.05, so it follows a normal distribution.

For the P/V ratio in the Shapiro Test for  $^{137}\text{Cs}$  source before subtracting B.G. was follow to normal distribution, but it's after subtracting B.G p-value was less than 0.05 so, it not follows the normal distribution. Also, the P/V ratio samples for the  $^{60}\text{Co}$  and  $^{22}\text{Na}$  sources before and after background were not follow to normal distribution.

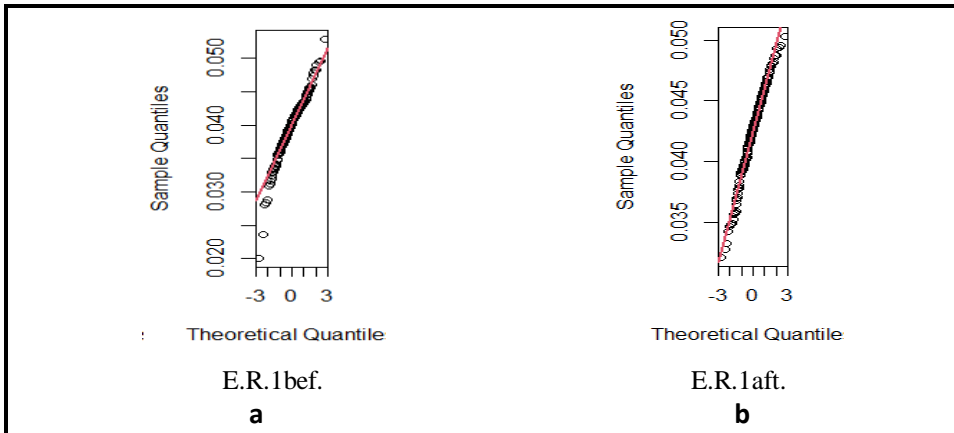
In bartlett. test for three sources ( $^{137}\text{Cs}$ ,  $^{60}\text{Co}$  and  $^{22}\text{Na}$ ) for E.R. and P/V ratio samples are following normal distribution because p-value was greater than 0.05.

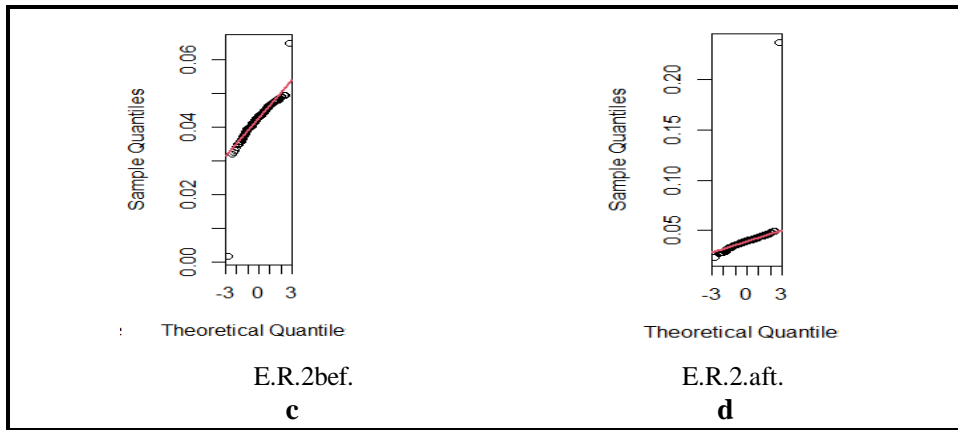
In Wilcoxon test for three sources ( $^{137}\text{Cs}$ ,  $^{60}\text{Co}$  and  $^{22}\text{Na}$ ) for E.R. and P/V ratio samples are following normal distribution because p-value was greater than 0.05.

The T-Test was used to find out the homogeneity of the variances of the studied samples when comparing mean between two groups. It had been found in the E.R. samples and the P/V ratio of the radioactive sources used that all data are homogeneous as shown in the figures (4-19) to (4-21).

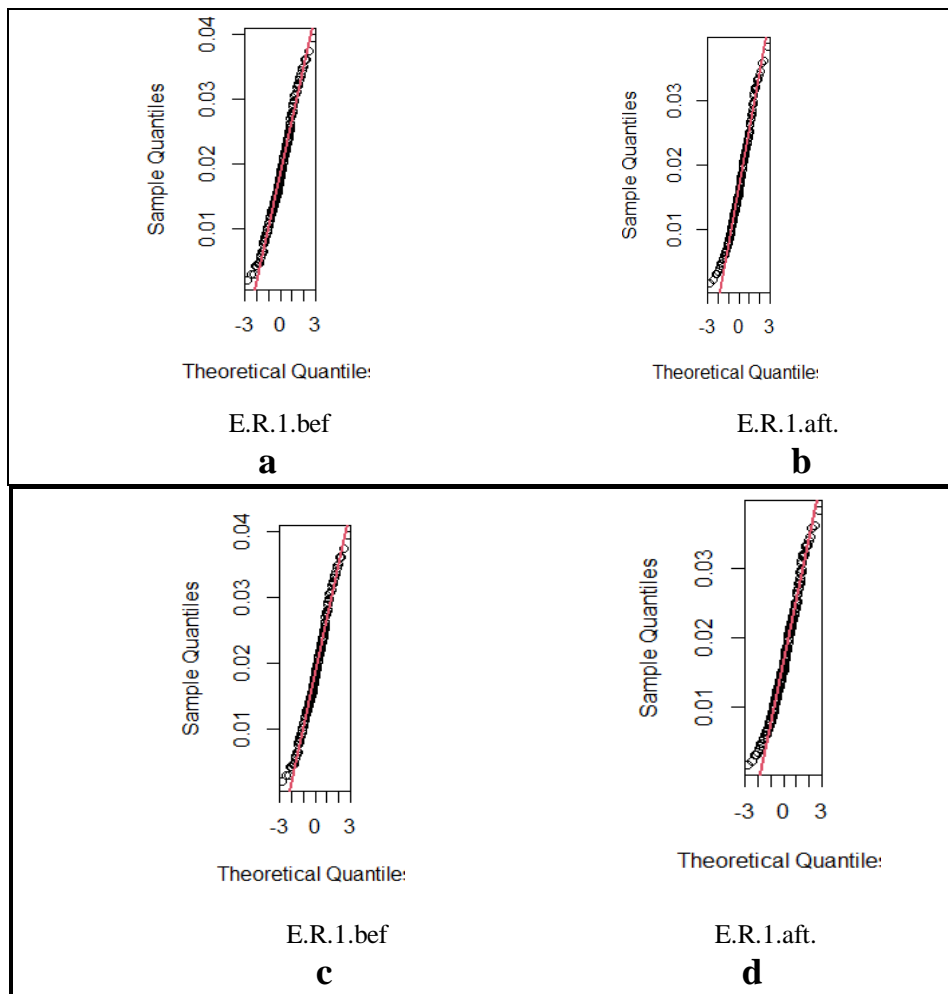


**Figure (4-19) Comparative of sampling mean by T-Test for energy resolution of  $^{137}\text{Cs}$  source. a- before b- after subtracting B.G.**





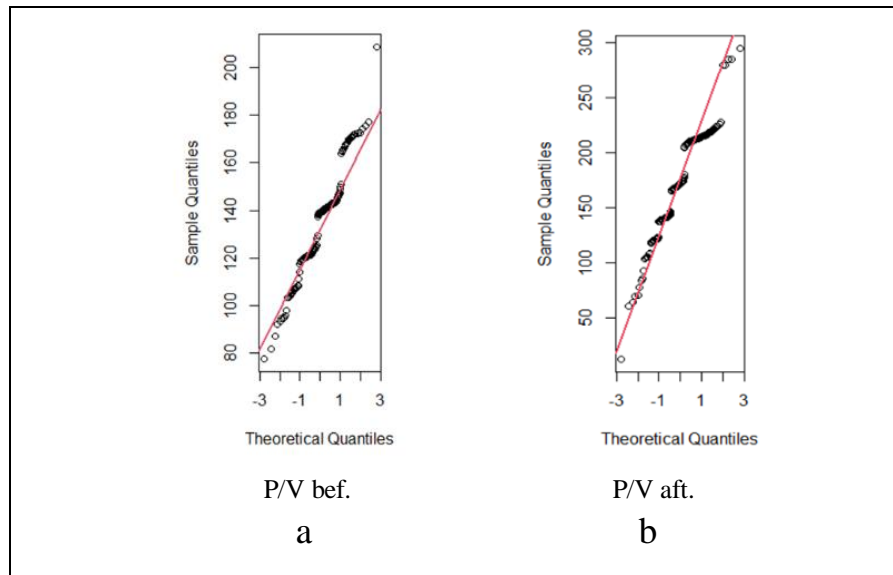
**Figure (4-20) Comparative of sampling mean by T-Test for energy resolution of  $^{60}\text{Co}$  source. a & b E.R. 1 c & d E.R. 2.**



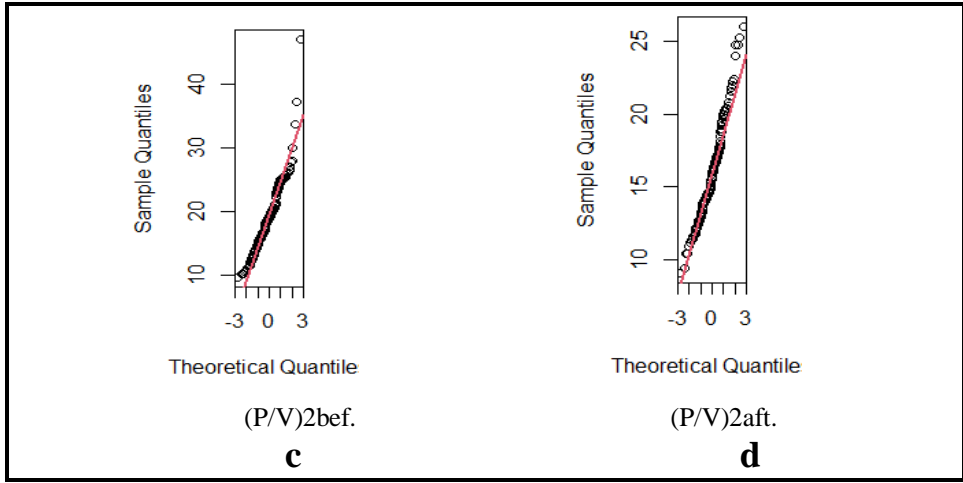
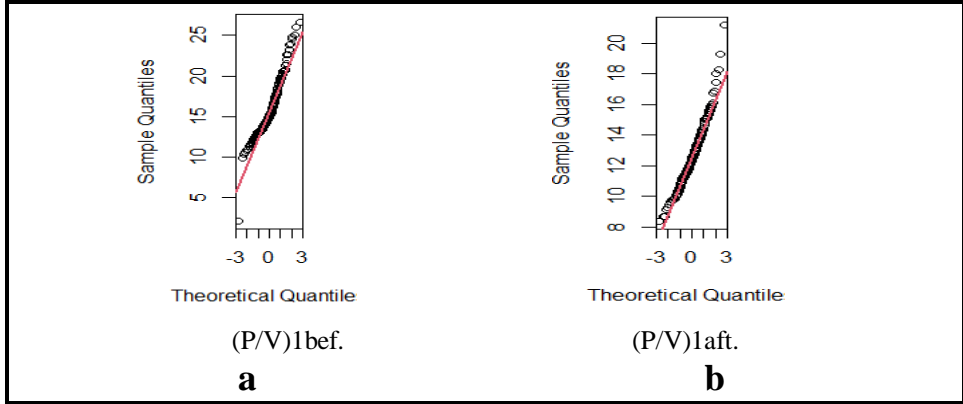
**Figure (4-21) Comparative of sampling mean by T-Test for energy resolution of  $^{22}\text{Na}$  source. a- before b- after subtracting B.G.**

Figures (19 to 21) show the T-Test of the E.R. sample for three sources before and after the subtracting B.G., it notes that the samples are homogeneous in all samples for  $^{22}\text{Na}$  source also  $^{60}\text{Co}$  source samples homogeneous except the c samples which has an abnormal behavior from the rest of the samples. As the same case in  $^{137}\text{Cs}$  where E.R. before subtracting B.G. samples are not clear behavior while E.R. after subtracting B.G. samples are homogeneous.

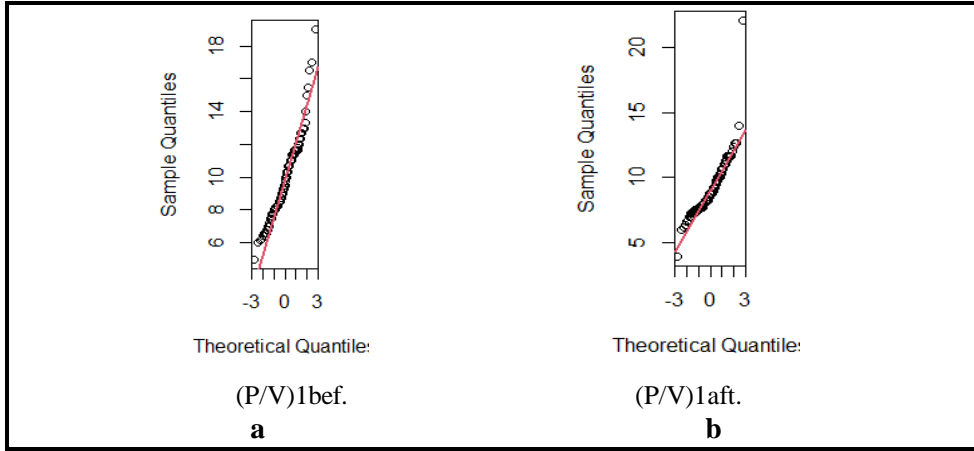
As for the P/V ratio of the T-Test for the studied samples, it was shown in figures (4-22) to (4-24), respectively.



**Figure (4-22) Comparative of sampling mean by T-Test for P/V ratio of  $^{137}\text{Cs}$  source. a- before b- after subtracting B.G.**



**Figure (4-23) Comparative of sampling mean by T-Test for P/V ratio of <sup>60</sup>Co source. a- &b (P/V)1 ratio c- &d (P/V)2 ratio.**





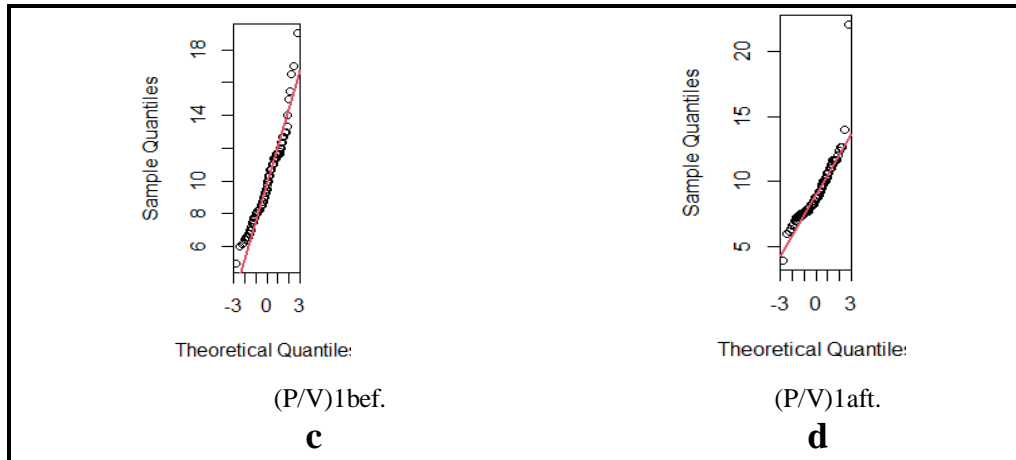
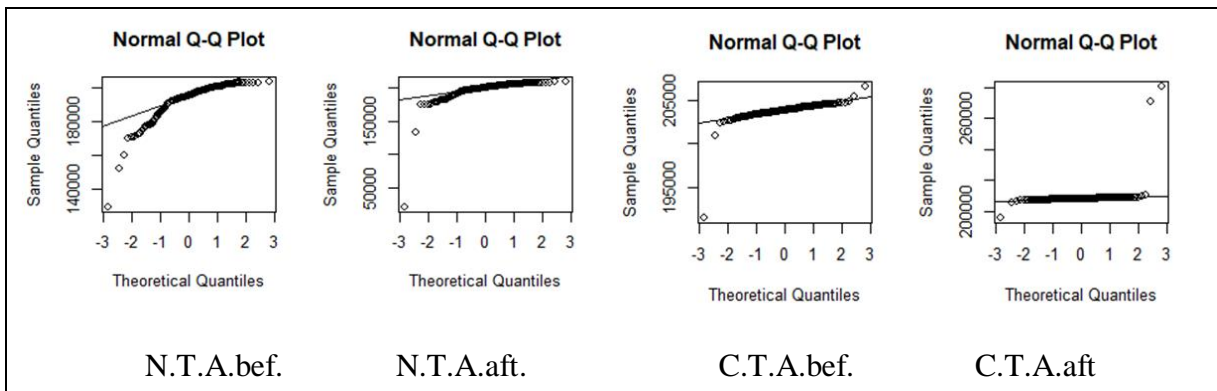


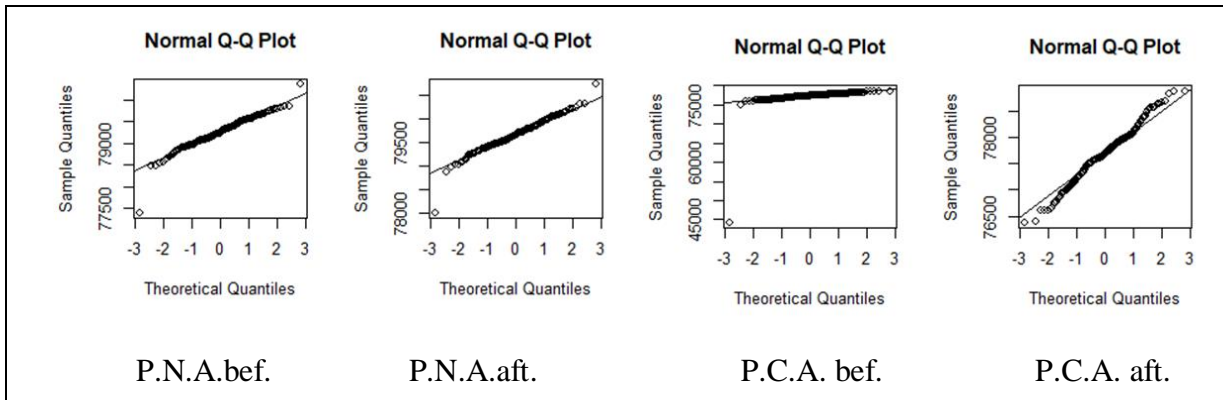
**Figure (4-24) Comparative of sampling mean by T-Test for P/V ratio of <sup>22</sup>Na source. a- &b (P/V)1 ratio c- &d (P/V)2 ratio.**

Figures (4-22 to 4-24) show that T-Test of the P/V ratio for (<sup>137</sup>Cs, <sup>60</sup>Co and <sup>22</sup>Na) source samples before and after subtracting B.G. are homogeneous in all samples, so the mean of the samples does not differ substantially, meaning that the samples are statistically regular and homogeneous so, the 95 percent confidence the others samples will exhibit the same behavior.

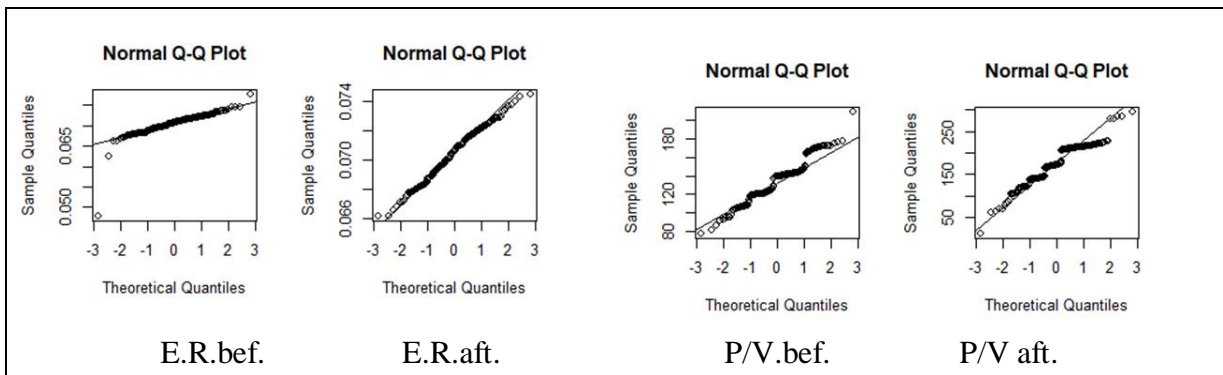
For make sure the imposition the data samples for three sources if follows the normal distribution or not, we will use Q-Q Plot, as shown in figures (4-25)- (4-27).



**a- T.A.**



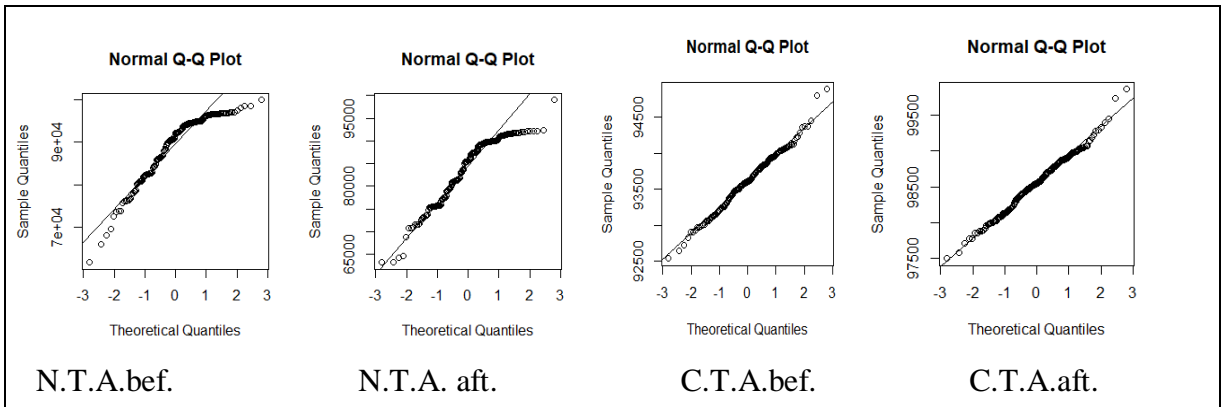
**b- P.P.A.**



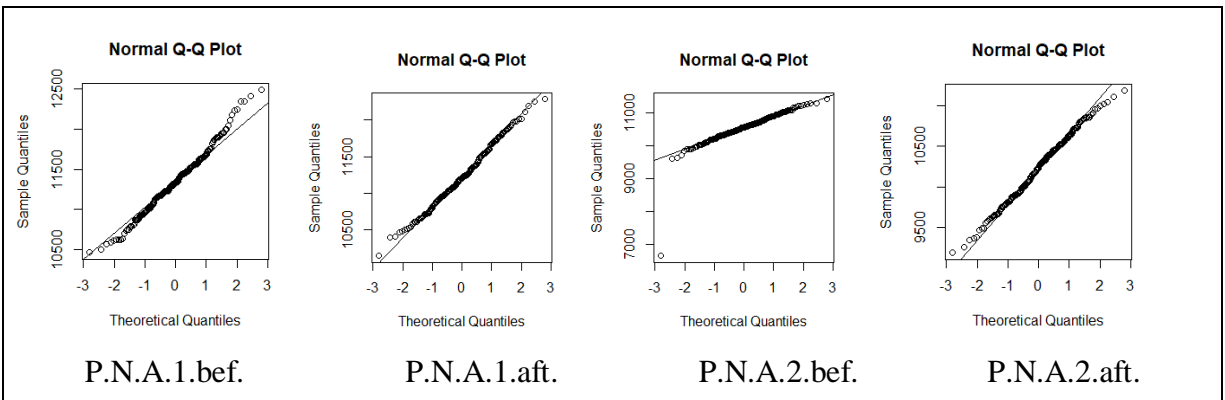
**c-E.R. and P/V ratio.**

**Figure (4-25) Q-Q-Norm to spread of data for samples for  $^{137}\text{Cs}$  source.**

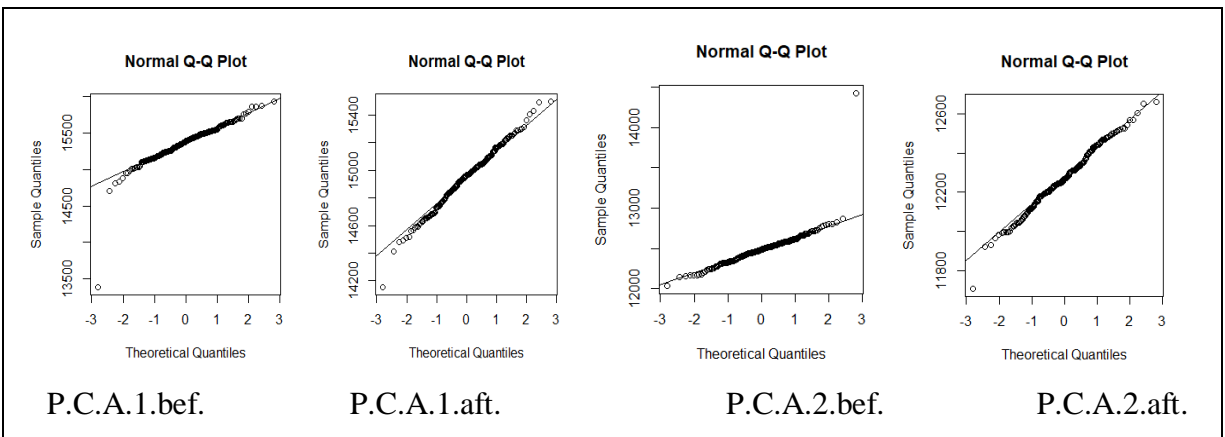
Figure (4-25) shows the Q-Q Norm test for  $^{137}\text{Cs}$  source spectrum for all the studied samples before and after subtracting B.G. to show that follow to normal distribution or not. This is done through the matching the straight line to the points of the studied samples where the greater the percentage of fit the more the sample is following to a normal distribution. Therefore, it is clear from figures that only samples P.N.A., E.R., and P/V ratio are only following to a normal distribution.



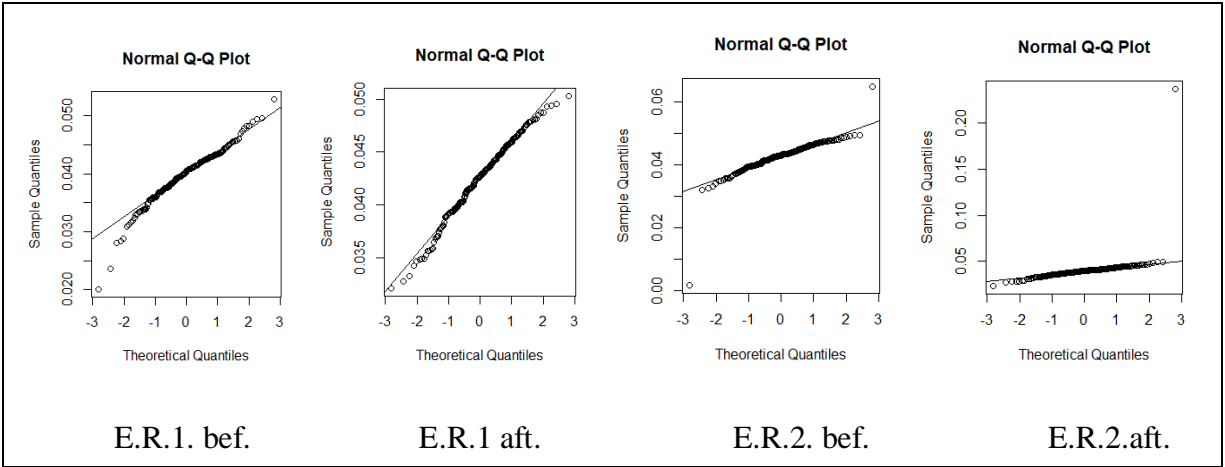
**a- T.A. (before and after subtracting B.G.)**



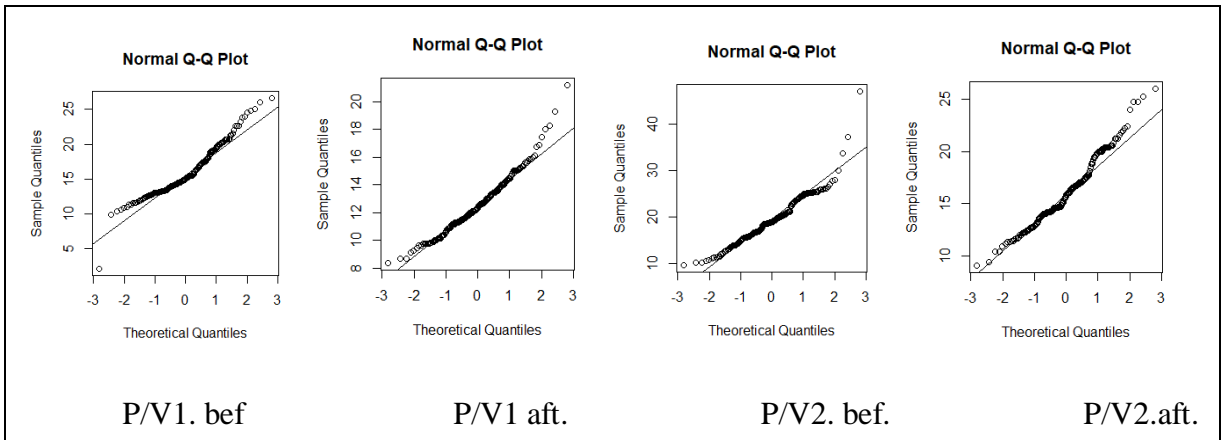
**b- P.N.A. (before and after subtracting B.G.)**



**c- P.C.A. (before and after subtracting B.G.)**



**d- E.R. (before and after subtracting B.G.)**

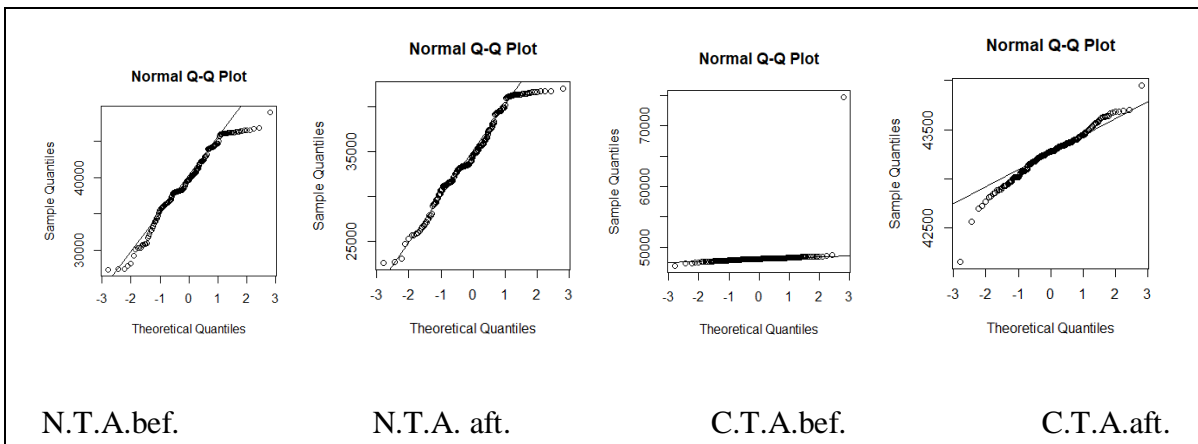


**e- P/V ratio (before and after subtracting B.G.)**

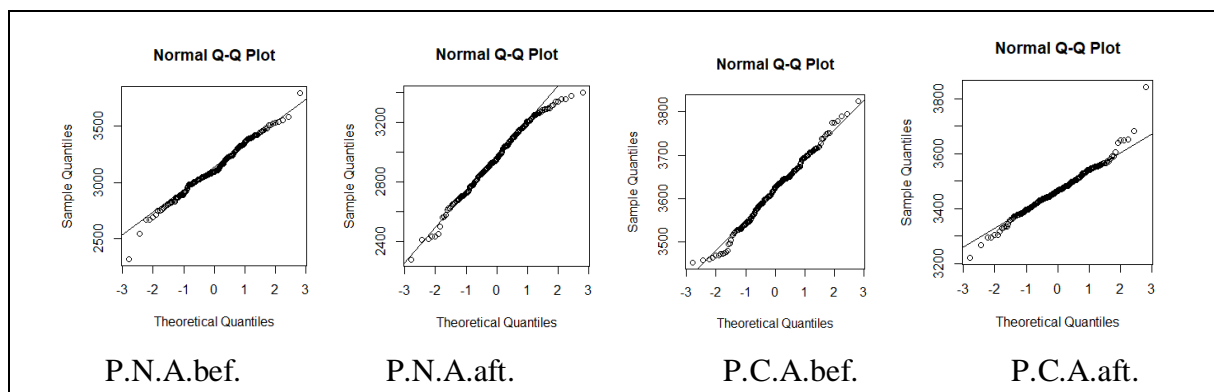
**Figure (4-26) Q-Q-Norm to spread of data for samples for  $^{60}\text{Co}$  source.**

**a- T.A.      b- P.N.A.      c- P.C.A.      d -E.R.      e- P/V ratio.**

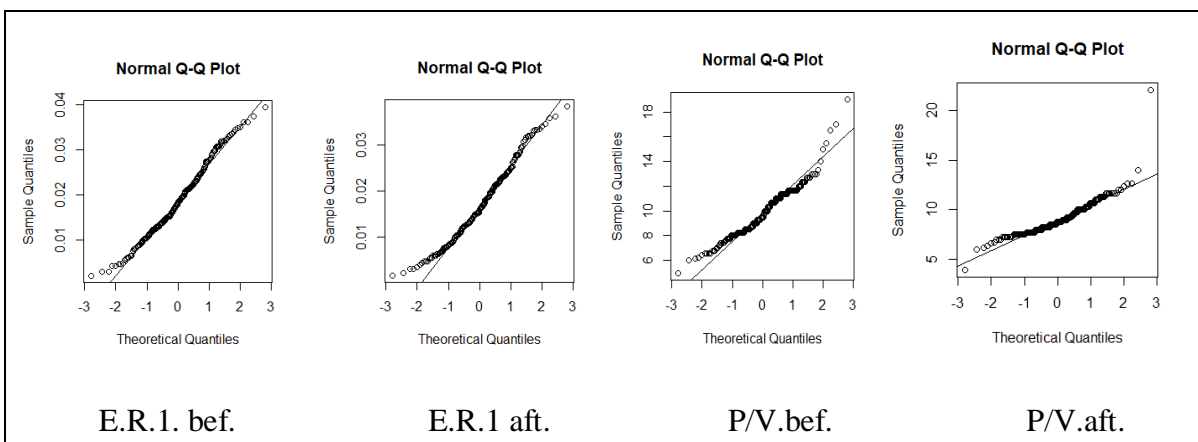
Figure (4-26) shows the Q-Q Norm test for  $^{60}\text{Co}$  source spectrum for all the studied samples before and after subtracting B.G., it notes that in all the studied samples there is no total match between the straight line and the points of the samples, which indicates that the samples are not follow to a normal distribution. The figure (4-27) illustrates the Q-Q Norm test for  $^{22}\text{Na}$  source for all samples.



**a- T.A. (before and after subtracting B.G.)**



**b- P.N.A. and P.C.A. (before and after subtracting B.G.)**



**c- E.R. and P/V ratio (before and after subtracting B.G.)**

**Figure (4-27) Q-Q-Norm to spread of data for samples for  $^{22}\text{Na}$  source.**

**a- T.A.      b- P.N.A.      c- P.C.A.      d -R.E.      e- P/V ratio.**

Figure (4-27) show that in all the studied samples there is no total match between the straight line and the points of the samples, which indicates that the samples are not following a normal distribution.

#### 4.4 Correlation and Regression

In this study, Pearson correlation coefficient was used to study the existence of a relation between the variables of the studied samples using the R program. The studied data were divided into groups before and after the subtracting B.G., as shown in tables (4-9) to (4-11).

**Table (4-9) Pearson Correlation for  $^{137}\text{Cs}$  Source.**

No.	Group	Data	P. value	Correlation	Type correlation
1	Total area	T.AN.bef. and T.A.N.aft	0.1169	0.1112169	Positive
2		T.A.C.bef. and T.A.NC.aft.	0.1341	0.1063096	Positive
3		T.AN. bef. and T.A.C.bef.	0.9364	0.005676041	Positive
4		T.A.N.aft and T.A.NC.aft.	0.9364	0.1801442	Positive
9	Photopeak	sample and P.P.N.bef	0.2001	-0.09097193	negative
10		sample and P.P.N.aft.	0.00763 3	-0.1881396	negative
11		sample and P.P.C.bef	0.4414	0.05473915	Positive
12		sample and P.P.C.afr.	0.2451	-0.08255838	negative
13		P.P.N.bef and P.P.N.aft.	0.04924	0.1392459	Positive
14		P.P.C.bef. and P.P.C.after	$2.2e^{-16}$	0.916583	Positive
15		P.P.C.bef. and P.P.N.bef	0.01206	0.1772236	Positive
16		P.P.C.aft. and P.P.N.aft.	$2.2e^{-16}$	0.6545183	Positive
17	Energy	E.R.bef. and E.R.aft.	$2.2e^{-16}$	0.5959189	Positive
18		sample and E.R.bef.	0.2713	-0.07815767	negative
19		sample E.R..aft.	0.2089	-0.08924087	negative
20	P/V	sample and P/V.bef	0.09134	-0.119707	negative
21		sample and P/V.aft.	0.029	-0.154437	negative
22		P/V.bef and P/V.aft.	0.06295	0.1317439	Positive

Table (4-9) shows the Pearson correlation coefficient for the  $^{137}\text{Cs}$  source spectrum, the samples were divided into four groups, each group comprising four subtests. The Pearson test depends on the p-value if it is less than 0.05 is take the value of the Pearson coefficient into consideration and interpret the results if they are positive or negative, and therefore it notes that p- value in the second group of (13-16) was less than 0.05 and the Pearson coefficient was positive and its value was close to zero. This means that the relation between N.T.A. and C.T.A. is an extreme moderate relation, meaning the greater the value of N.T.A. leads to increasing in C.T.A.

**Table (4-10) Pearson Correlation for  $^{60}\text{Co}$  Source.**

No.	Groups	Data	P.value	Correlation	Type correlation
1	Total area	sample and X\$T.A.N.Be	0.07886	-0.1245608	negative
2		sample and X\$T.A.N.Af	0.004432	-0.2004302	negative
3		sample and X\$T.A.C.Be	4.656e <sup>-08</sup>	-0.3745517	negative
4		sample and X\$T.A.C.Af	2.597e <sup>-08</sup>	-0.3810583	negative
5		T.A.N.Be and T.A.N.Af	2.2e <sup>-16</sup>	0.6683332	positive
6		T.A.C.Be and T.A.C.Af	2.2e <sup>-16</sup>	0.9449271	positive
7		T.A.N.Be and T.A.C.Be	0.08873	0.1206744	positive
8		T.A.N.Af and T.A.C.Af	0.02437	0.1591639	positive
9	P.N.A	sample, P.P1.N.be	0.006151	0.193103	positive
10		sample, P.P1.N.af.	0.9198	0.00716472	positive
11		sample, P.P2.N.be	0.6571	0.03157958	positive
12		sampleP.P2.N.af.	0.9222	-0.006953211	negative
13		P.P1.N.be, and P.P1.N.af.	0.007449	0.1887062	positive
14		P.P2.N.be and P.P2.N.af.	0.4866	0.04947323	positive
15		P.P1.N.be and P.P2.N.be	0.008446	0.1857721	positive
16		P.P1.N.af and P.P2.N.af.	0.005431	0.1959165	positive
17	P.C.A.	sample and X\$P.P1.C.be	0.8661	-0.01200013	negative
18		sample and X\$P.P.1C.af	0.3868	-0.06151824	negative
19		sample and X\$P.P.2C. be	0.7265	0.02488923	positive
20		sample and X\$P.P.2C.af	0.1074	-0.1141802	negative
21		P.P1.C.be and P.P.1C.af	3.953e <sup>-05</sup>	0.2863226	positive
22		P.P2.C.be and P.P.2C.af	2.2e <sup>-16</sup>	0.5954239	positive
23		P.P1.C.be and P.P2.C.be	0.3663	0.06421573	positive
24		P.P.1C.af and P.P.2C.af	0.9649	-0.003128296	negative

Contain Table (4-10)					
25	Energy	sample and E.R.1.bef.	0.8116	-0.01695725	negative
26		sample and E.R.1.af.	0.5479	-0.04273668	negative
27		sample and E.R.2.bef.	0.2792	-0.07688718	negative
28		sample and E.R.2.af.	0.7821	0.01967985	positive
29		E.R.1.bef. and E.R.2aft.	0.9014	-0.008812509	negative
30		E.R.2.bef. and E.R.2.af.	0.6031	-0.03698669	negative
31		E.R.1.bef. and E.R.2bef.	0.8601	0.01254324	positive
32		E.R.1.af. and E.R.2.af.	0.5607	-0.04137616	negative
33	p/v ratio	sample and p/v1.bef	0.5161	0.04618177	positive
34		sample and p/x1.af.	0.03757	-0.1471638	negative
35		sample and p/v2.bef	0.000246	-0.2565105	negative
36		sample and p/v2.af.	0.005738	-0.1946794	negative
37		p/v1.bef and p/v1.af.	0.6872	0.0286443	positive
38		p/v1.bef and p/v2.bef	0.01052	0.1805462	positive
39		p/v2.bef and p/v2.af.	0.3211	0.07051039	positive
40		p/v2.af. and p/v2.af.	0.1938	0.09225949	positive

Table (4-10) shows the Pearson correlation coefficient of the  $^{60}\text{Co}$  source spectrum, the samples were divided into five samples, each sample includes eight subtests. It was found in the first sample that there is a medium inverse relation between the number of repetitions of the spectrum with T.A., as it was observed in the same group that there is a strong extreme relation between N.T.A. before and after subtracting B.G. and the same case and C.T.A. before and after the subtracting B.G., which means that with an increase in N.T.A. and an increase in C.T.A. before the subtracting B.G. leads to an increase in the N.T.A and C.T.A. after subtracting B.G., There was also a weak extreme relation between the values of the P.P.N. of the first and the second peak before and after the subtracting B.G., meaning that this is a simple variable of P.P.A. The same relation was found in the third sample between the one P.C.A.1 before and after subtracting B.G., and this means it cannot be certain that there is a close relation linking the photopeak to each other.



As for the fourth model, it was noted that it was not affected by the Pearson test, and this indicates that the E.R. is not related to any other variable, while there was a weak extreme relation linking the (P/V)1 ratio to (P/V)2 ratio. Rather, it was found that the higher the number of frequencies the lower the peak ratio according to what it is in the fifth sample.

**Table (4-11) Pearson Correlation for <sup>22</sup>Na Source.**

No.	Group	Data	P.value	Correlation	Type correlation
1	Total area	sample T.NA.bef.	0.1832	-0.09449193	negative
2		sample T.N.A.aft.	0.2151	-0.08804251	negative
3		sample and T.C.A.bef.	0.0368	-0.1477574	negative
4		sample and T.CA.aft.	7.738e <sup>-06</sup>	-0.3103415	negative
5		T.N.A.bef. and T.N.A.aft.	2.2e <sup>-16</sup>	0.7682296	positive
6		T.N.A.bef. and T.C.A.bef.	0.7881	-0.01912386	negative
7		T.C.A.bef.and T.C.A.aft.	0.752	0.02248003	positive
8		T.N.A.aft. and T.C.A.aft.	0.6271	-0.03455408	negative
9	Photopeak Net	sample, P.N.A1.bef.	0.03703	-0.1475804	negative
10		sample, P.N.A.1.aft.	0.4472	0.05405186	positive
11		sample, P.N.A.2.bef.	0.8798	0.01075981	positive
12		sample, P.N.A.2.aft.	0.7186	0.02563359	positive
13		P.N.A.1.bef., andP.N.A.1.aft.	0.002414	0.2133875	positive
14		P.N.A.1.bef.and P.N.A.2.bef.	0.8423	-0.01415568	negative
15		P.N.A.2.bef. and P.N.A.2.aft.	0.01073	0.1800509	positive
16		P.N.A.1.aft.and P.N.A.2.aft.	0.4858	0.04956629	positive
17	Photopeak Cross	sample and P.C.A.1.bef.	3.704e <sup>-05</sup>	-0.2873217	negative
18		sample and P.C.A.1.aft.	0.1385	-0.10512	negative
19		sample and P.C.A.2.bef.	0.2569	-0.0805364	negative
20		sample and P.C.A.2.aft.	0.6534	0.03194813	positive
21		P.C.A.1.bef. and P.C.A.1aft.	2.2e <sup>-16</sup>	0.7754246	positive
22		P.C.A.1.bef. and P.C.A.2.bef.	0.8198	0.01620985	positive
23		P.C.A.2.bef. and P.C.A.2.aft.	2.2e <sup>-16</sup>	0.7437411	positive
24		P.C.A.1.aft. and P.C.A.2.aft.	0.7458	-0.02306239	negative
25	Energy Resolution	sample and E.R.bef.	0.5829	-0.03906133	negative
26		sample and E.R.1aft.	0.8422	-0.01416753	negative
27		sample and E.R.2bef.	0.4617	0.05233417	positive
28		sample and E.R.2aft.	0.2968	0.07413366	positive
29		E.R.bef.1 and E.R.1aft.	2.2e <sup>-16</sup>	0.8349304	positive
30		E.R.bef.1 and E.R.2bef.	0.2659	-0.07904522	negative
31		E.R.bef.2 and E.R.2aft.	2.2e <sup>-16</sup>	0.7514206	positive
32		E.R.aft.1 and E.R.2aft.	0.9322	0.006052353	positive

Contain Table (4-11)					
33	p/v ratio	sample and p/v.1bef1	0.1392	0.1049412	positive
34		sample and p/v.1aft1	3.335e <sup>-07</sup>	0.3514895	positive
35		sample and p./v2.bef	0.009737	0.1823972	positive
36		sample and p/v2.aft	0.0006407	0.2393725	positive
37		p./v.1bef. and p/v.1.aft.	0.001549	0.2224103	positive
38		p/v1.bef. and p/v2.bef.	0.007658	0.1880642	positive
39		p/v2.bef. and p.v2.aft.	1.954e <sup>-05</sup>	0.296962	positive
40		p/v1.aft. and p/v2.aft.	0.0002127	0.2590091	positive

Table (4-11) shows the Pearson correlation coefficient of the <sup>22</sup>Na source spectrum, the samples were divided into five groups, each group includes eight subtests. Where it was found that there is a weak inverse relation between the frequency and T.A., where the increase the frequency leads to discount of T.A. Also, it was found in the first group that there is an extreme relation between T.A. before and after the subtracting B.G. The greater the area before the subtracting B.G. the successively the total area after the subtracting B.G.

In the second group, it was found that there is a weak direct relation between the P.P.N1 and the P.P.N2. While the relation was strong and extreme between the peak crossover P.C.A. before and after the subtracting B.G. as well as the case in the fourth group, where the increase the value of the E.R. before the subtracting B.G., leads to increasing the E.R. after the subtracting B.G.

In the fifth group, there was a weak relation between (P/V)1 ratio with (P/V)2 ratio before and after the subtracting B.G.

Pearson's test gives confidence that the probability of 95 percent is that other samples will be taken for the same data and the result will be the same.

In this study, linear regression was used to find the relation between the two variables, it was noticing the effect of the first variable (x) in predicting the second variable (y). In other words, it has been found the relation (y) in terms of a linear relation linking it to (x), as shown in the table (4-12).

**Table (4-12) Linear Regression Test for <sup>137</sup>Cs Source.**

No.	Model	Data	P.value	Std. Error	Estimate	Min	Max	median	R-squared
1	Total area	sample ~ T.A.N.bef.	2.2e-16	7.072e-18	1.000e+00	-5.053e-14	1.081e-14	4.710e-16	1
2		sample ~ T.A.N.aAft	0.1169	4.209e-04	6.628e-04	-99.265	94.030	1.309	0.01237
3		sample ~ T.A.C.bef.	0.9364	2.658e-04	2.123e-05	-99.637	99.283	0.134	3.222e-05
4		sample ~T.A.NC.aft.	0.9269	3.980e-03	3.655e-04	-99.076	99.255	-0.595	4.26e-05
5		T.AN.bef. ~.A.C.bef.	0.9364	2.658e-04	2.123e-05	-99.637	99.283	0.134	3.222e-05
6		T.A.N.aft~ A.NC.aft.	0.0107	6.568e-01	1.693e+00	-64196	9669	2372	0.03245
7	Photopeak	sample ~ .P.N.bef	0.2001	0.001696	-0.002181	-99.100	99.164	-1.082	0.003267
8		sample ~ .P.N.aft.	0.00763	8.259e-03	-2.226e-02	-105.293	101.992	-2.512	0.03052
9		sample ~ P.C.bef.	0.441	1.261e-02	9.729e-03	-100.313	102.377	0.116	0.002996
10		sample P.C.aft.	0.00763	8.259e-03	-2.226e-02	-105.293	101.992	-2.512	0.03052
11		P.P.N.bef~ P.P.N.aft.	0.0492	3.474e-01	6.874e-01	-32719	1563	205	0.01444
12		P.P.C.bef~P.P.C.after	2e-16	3.016e-02	9.730e-01	-374.02	414.69	4.40	0.8393
13		P.P.C.bef~P.P.N.bef	2e-16	9.432e-03	2.390e-02	-1814.73	-11.25	1096.24	0.02652
14		P.P.N.aft~P.P.C.after	2e-16	8.568e-02	1.044e+00	-1272.51	746.50	1.48	0.4255
15	Energy	sample ~ E.R.bef.	0.2713	1665.5	0.5959189	-100.500	98.516	2.622	0.001089
16		sample ~ E.R.aft.	0.2089	2410.7	-3039.3	-103.127	99.336	2.606	0.002954
17		E.R.bef. ~ E.R.aft.	2e-16	0.082681	-0.089240	-0.024119	0.0071061	0.0000161	0.3519
18	p/v	sample~ p/v.bef	0.0913	0.1916	-0.3250	-109.473	106.070	-1.998	0.009352
19		Sample ~ p/v.aft.	0.029	0.09009	-0.19815	-104.507	113.333	0.205	0.01892
20		p/v.bef ~p/v.aft.	0.0629	0.03329	0.06226	-58.677	75.229	4.516	0.01239

Table (4-12) shows the simple linear regression of the studied samples for <sup>137</sup>Cs source, where the table contains p-value if it is less than (0.05) this indicates that this variable has importance and influence in the studied samples, and the table also contains the error rate (std. error) in calculating the predicted variable according Eq.(2-24), and the median whenever it is close to zero means there is a small difference between the variables, in addition to the min and max. value and the residuals that represent the difference between the actual values of the variable and the values predicted through the Eq.(2-24), where the more the value of the residuals is close to zero, the better the sample.

The samples have been divided into four groups representing the first group T.A. contains four relations between variables, the second is represents the P.P.A.

contains eight relations linking the studied variables and the third group is E.R. contains three relations for random variables, then the last group is the P/V ratio contains three relations between random variables. For the second group contained six linear relations, which indicates the close relation between number of samples with P.P.A. either net and cross after subtracting B.G., also the relation between the P.N.A. and P.C.A. before and after subtracting B.G.

For the first sample, it notices one linear relation between the number of samples and the net total area. While there was a linear relation between the E.R. before and after the subtracting B.G., which indicates that increasing the first energy leads to an increase in the value of the second. Also, the same case in fourth sample.

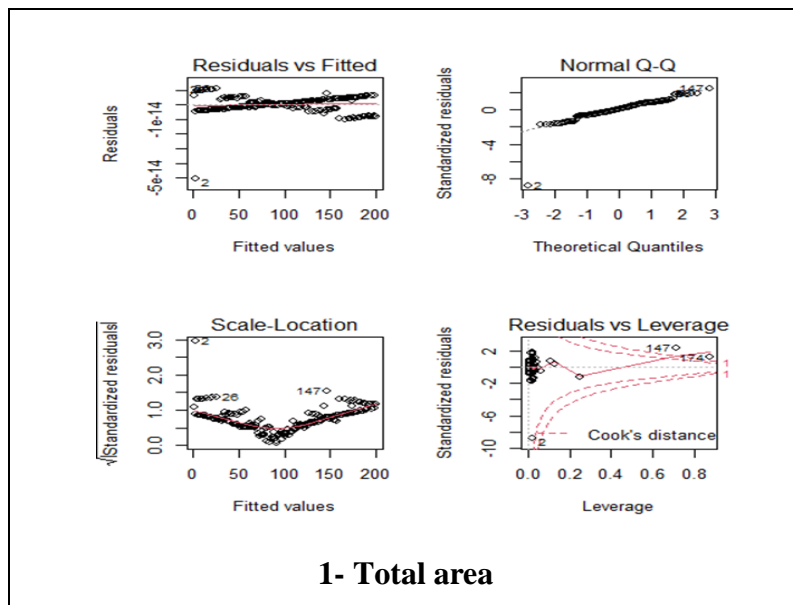
Accordingly, it was found that the second group has greater importance than the rest of the samples, and to find out the effective and supportive samples for the other sample, the multiple linear regression test was used, as in Table (4-13).

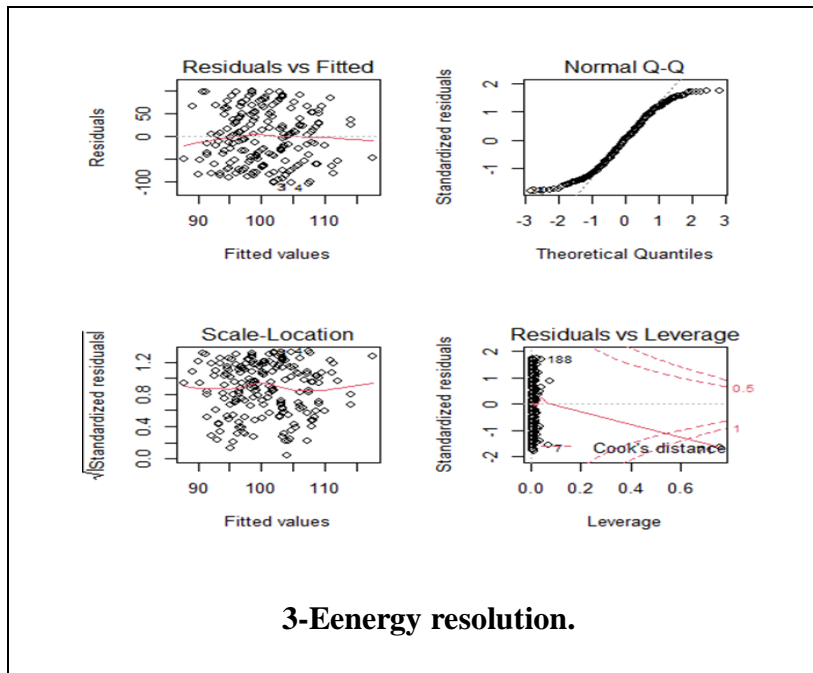
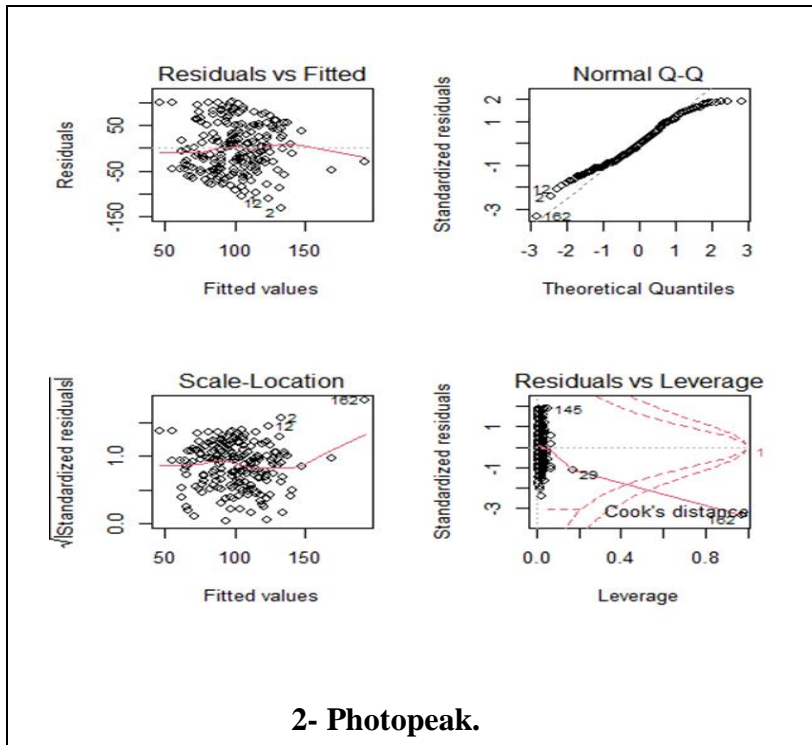
**Table (4-13) Multiple Linear Regression for <sup>137</sup>Cs Source.**

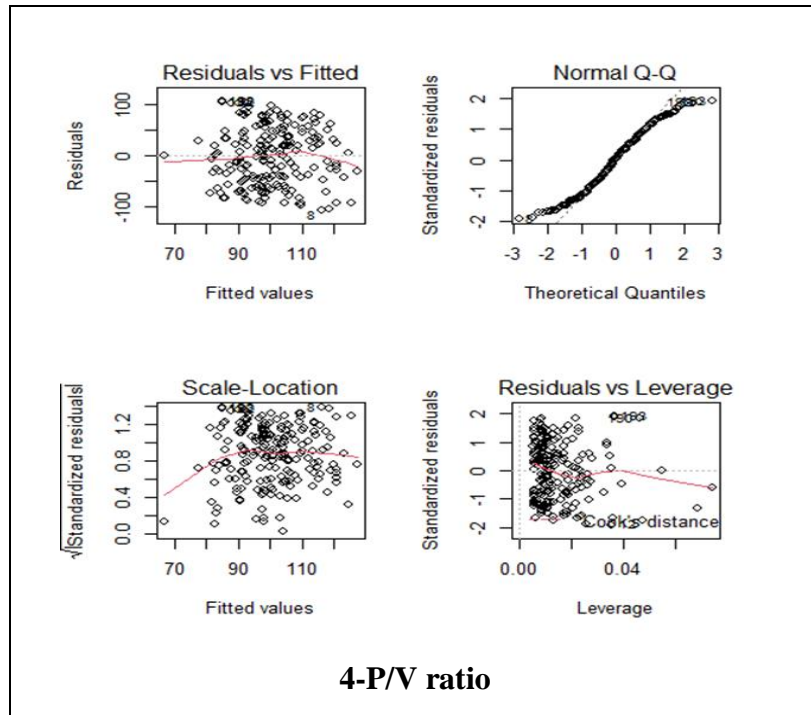
No.	Models	Data	P.value	Std. Error	Estimate	Residual standard error	Min	Max	R-squared	p-value (total)
1	T.A.	T.AN.bef.	<2e-16	7.158e-18	1.000e+00	5.799e-15	-5.042e-14	1.091e-14	1	2.2e-16
2		T.A.C.bef.	0.650	3.033e-20	-1.380e-20					
3		T.A.N.aft.	0.732	4.916e-20	-1.688e-20					
4		T.A.NC.aft.	0.347	4.045e-19	3.813e-19					
5	P.P.A.	P.P.N.bef.	0.062578	1.641e-03	-3.073e-03	54.3	-131.158	101.450	0.1198	7.827e-06
6		P.P.N.aft.	0.245557	1.089e-02	-1.268e-02					
7		P.P.C.bef.	6.78e-06	3.123e-02	1.445e-01					
8		P.P.C.after	0.000225	3.721e-02	-1.399e-01					
9	E.R.	E.R.bef.	0.6615	2076.3	-910.5	57.91	-103.395	99.364	0.008931	0.4133
10		E.R.aft.	0.4547	3008.1	-2253.2					
11	p/v	p/v.bef	0.1539	0.19180	-0.27453	57.18	-108.079	107.753	0.02409	0.03348
12		p/v.aft.	0.0471	0.09064	-0.18106					

Table (4-13) shows the multiple regression of the  $^{137}\text{Cs}$  source spectrum. The table contains four groups (T.A. ,P.P.A.,E.R. and P/V) in addition to the p-value 0.05 for total the sample, means that this variable is independent and has an importance in influencing the sample, also ,it contains estimate value or (expected value) to the error rate of the precipitate for all population study , in addition to the std error in the residuals and its lowest and highest value it .The table also contains the value of the total error of the sample, which shows the effect of the sample by changing the variable.

It was found from the table that in the sample T.A. The only important variable was N.T.A.bef. and the residual standard error was 5 %. that means N.T.A.bef. affects by 5% with the change in the number of samples. Whereas in the P.P.A. form. P.C.A.aft. was the most important and influential variable in the sample, with standard error 54%, it means that 54% of the change in the P.C.A.aft. can be determined depending on the number of samples according to Eq. (2-24), while the E.R. sample was not affected by the change in the number of samples, and for P/V ratio sample. The ratio after the subtracting B.G., is the important variable on the model at 57%, as shown in figure (4-28).







**Figure (4-28) Multiple linear regression for  $^{137}\text{Cs}$  source of all samples (1,2,3 and 4).**

From tests the conditions of linear regression as shown in figure (4-28) regarding the first drawing (Residuals vs Fitted) it studies the validity of the existence of a linear relation between residuals and the estimators. where it notes that the relation does not take a specific shape, which indicates the existence of a problem in the model to achieve this hypothesis.

The second drawing (Q-Q Normal) shows the normal distribution of residuals when data are collected around the straight line, it indicates commitment of residuals to normal distribution.

The third drawing (Scale Location) shows the homogeneity of residuals variation, that is, it shows the mechanism of data spreading, where the beginning and end of the drawing must be similar in shape, and when one end is different from the other, this indicates the heterogeneity of residuals variation.

The fourth drawing in figure (4-28) is (Residuals vs Leverage) show the presence of outliers, as the smaller the sample size will lead to an imbalance in some of the requirements of multiple linear regression.

For the <sup>60</sup>Co source, the results of the linear regression test are shown in the tables (4-14) and (415).

**Table (4-14) Linear Regression Test for <sup>60</sup>Co Source.**

No.	Models	Data	P.value	Std. Error	Estimate	Min	Max	R -Squared
1	T.A.	sample ~ T.A.N.bef.	0.078856	5.687e <sup>-04</sup>	-1.005e <sup>-03</sup>	-112.170	102.365	0.01552
2		sample ~ T.A.N.aft.	0.00443	5.778e <sup>-04</sup>	-1.663e <sup>-03</sup>	-120.341	111.608	0.04017
3		sample ~ T.A.C.bef.	4.66e <sup>-08</sup>	9.719e <sup>-03</sup>	-5.524e <sup>-02</sup>	-130.47	118.19	0.1403
4		sample ~ T.A.C.Af.	2.6e <sup>-08</sup>	9.965e <sup>-03</sup>	-5.779e <sup>-02</sup>	-130.45	118.41	0.1452
5		T.A.N.bef. ~ T.A.N.aft.	2e <sup>-16</sup>	5.440e <sup>-02</sup>	6.877e <sup>-01</sup>	-27101.7	18257.4	0.4467
6		T.A.C. bef. ~ T.A.C. aft.	2e <sup>-16</sup>	2.392e <sup>-02</sup>	9.717e <sup>-01</sup>	-983.75	1035.24	0.8929
7		T.A.C. bef. ~ T.A.N.bef.	0.0887	3.858e <sup>-03</sup>	6.599e <sup>-03</sup>	-1057.57	1242.03	0.01456
8		T.A.N. aft. ~ T.A.C. aft.	0.0244	1.282e <sup>+00</sup>	2.909e <sup>+00</sup>	-21134	13804	0.02533
9	P.N.A.	sample ~ P.P1.N.bef.	0.00615	0.01043	0.02888	-104.506	109.304	0.03729
10		sample ~ P.P1.N.aft.	0.920	0.01012	0.00102	-99.200	99.511	5.133e <sup>-05</sup>
11		sample ~ P.P2.N.bef.	0.657	0.009356	0.004160	-99.690	101.401	0.0009973
12		sample ~ P.P2.N.aft.	0.922	0.010210	-0.000999	-98.834	99.279	4.835e <sup>-05</sup>
13		P.P1.N.be ~ P.P1.N.aft.	0.00745	6.647e <sup>-02</sup>	1.797e <sup>-01</sup>	-833.27	1150.47	0.03561
14		P.P1.N.be ~ P.P2.N.bef.	0.00845	6.151e <sup>-02</sup>	1.636e <sup>-01</sup>	-863.71	1111.96	0.03451
15		P. P1.N.af. ~ P.P2.N.aft.	0.00543	0.0703	0.1976	-992.27	1032.23	0.03838
16		P.P2.N.be ~ P.P2.N.aft.	0.487	7.742e <sup>-02</sup>	5.396e <sup>-02</sup>	-3883.4	837.8	0.002448
17	P.C.A.	sample ~ P.P1.C.bef.	0.866	0.016397	-0.002769	-99.724	101.084	0.000144
18		sample ~ P.P1.C.aft.	0.387	0.01921	-0.01666	-101.829	108.597	0.003784
19		sample ~ P.P2.C.bef.	0.726	2.036e <sup>-02</sup>	7.131e <sup>-03</sup>	-100.193	98.564	0.0006195
20		sample ~ P.P2.C.aft.	0.1074	0.02644	-0.04275	-104.979	105.875	0.01304
21		P. P1.C.bef. ~ P.P1.C.aft.	3.95e <sup>-05</sup>	7.990e <sup>-02</sup>	3.360e <sup>-01</sup>	-2096.44	558.30	0.08198
22		P.P1.C.bef. ~ P.P2.C.bef.	0.366	8.806e <sup>-02</sup>	7.974e <sup>-02</sup>	-1949.05	561.75	0.004124
23		P.P1.C.aft. ~ P.P2.C.aft.	0.965	9.828e <sup>-02</sup>	-4.326e <sup>-03</sup>	-791.98	553.47	9.786e <sup>-06</sup>
24		P.P2.C.bef. ~ P.P2.C.aft.	2e <sup>-16</sup>	7.462e <sup>-02</sup>	7.782e <sup>-01</sup>	-229.51	1952.44	0.3545
25	E.R.	sample ~ E.R.1bef.	0.81163	931.84	-222.38	-99.90	100.33	0.0002875
26		sample ~ E.R.1.af.	0.54792	1136.10	-683.83	-99.679	100.810	0.001826
27		sample ~ E.R.2bef.	0.279192	848.04	-920.22	-99.981	101.097	0.005912
28		sample ~ E.R.2.aft.	0.782	280.84	77.79	-99.330	99.243	0.0003873
29		E.R.1bef. ~ E.R.1aft.	0.901	0.086709	-0.010753	-0.019757	0.012911	7.766e <sup>-05</sup>
30		E.R.1bef. ~ E.R.2bef.	0.86	0.064854	0.011448	-0.0197392	0.013059	0.0001573
31		E.R.2bef. ~ E.R.2aft.	0.603	0.023454	-0.012215	-0.040825	0.022170	0.001368
32		E.R.1af. ~ E.R.2aft.	0.561	0.017540	-0.010221	-0.0103448	0.007905	0.001712
33	PV ratio	sample ~ (p/v) 1.bef	0.516	1.1873	0.7724	-99.951	101.683	0.002133
34		sample ~ (p/v) 1.aft.	0.0376	2.012	-4.213	-108.661	102.906	0.02166
35		sample ~ (p/v) 2.bef	0.000246	0.8001	-2.9880	-115.590	104.927	0.0658
36		sample ~ (p/v) 2.aft.	0.00574	1.266	-3.535	-112.802	113.854	0.0379
37		(p/v) 1.bef ~ (p/v)2aft.	0.687	0.12160	0.04903	-13.5779	10.7531	0.0008205
38		(p/v)1bef ~ (p/v) 2.bef	0.0105	0.04868	0.12575	-13.6085	10.0504	0.0105
39		(p/v) 2.bef ~ (p/v)2aft.	0.321	0.1105	0.1099	-9.6961	27.5982	0.004972
40		(p/v)1aft. ~ (p/v)2aft.	0.194	0.04488	0.05851	-4.4446	8.5872	0.008512



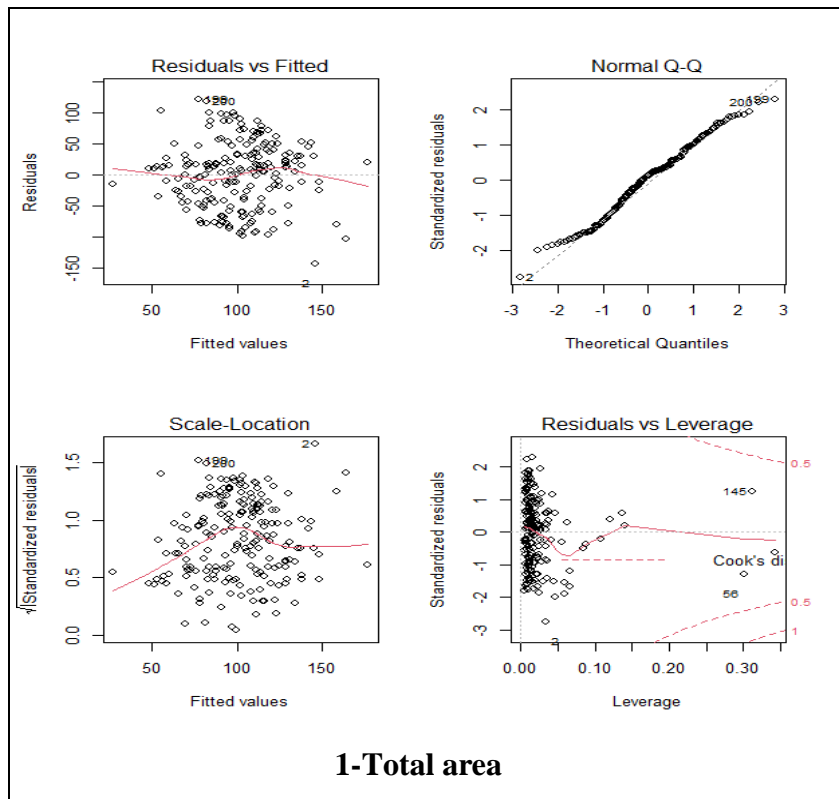
Table (4-14) shows the simple linear regression of the studied samples of the <sup>60</sup>Co source, where the samples were divided into five groups, and each group contains eight relations between variables, the first group represents T.A., the second group is P.N.A., the third group is P.C.A. the fourth group is the E.R. and then the last group is the P/V ratio. It was found in this study that the E.R. group was not affected and there is no linear relation between the random variables. While it had been found a linear relation between the number of samples and the variables in T.N.A., P.N.A., P.C.A. and P/V ratio, as well as a linear relation between the T.N.A., T.C.A., P.N.A., P.C.A., (after and before subtracting B.G.) in the first three samples.

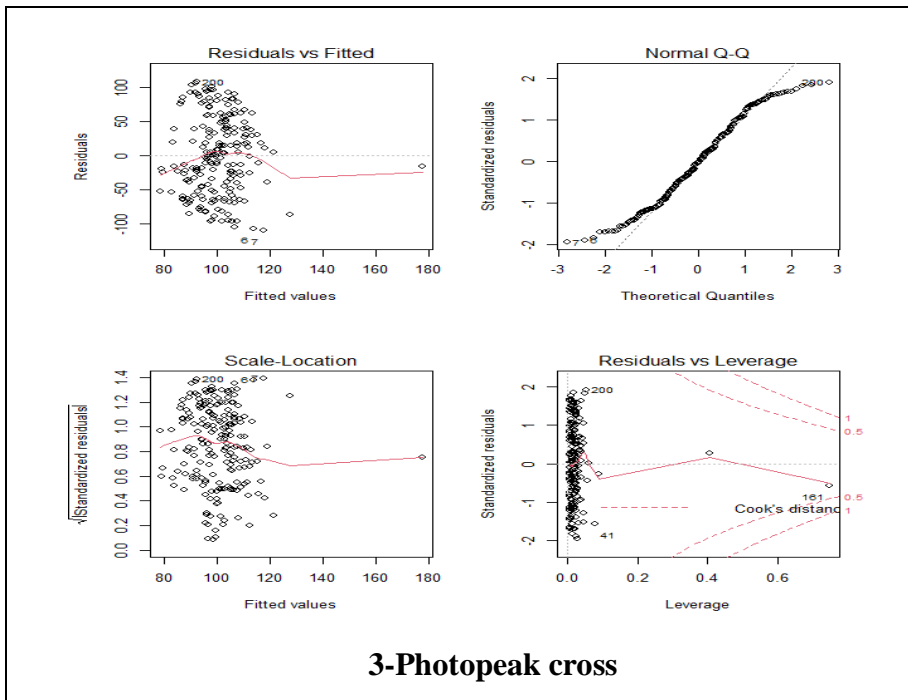
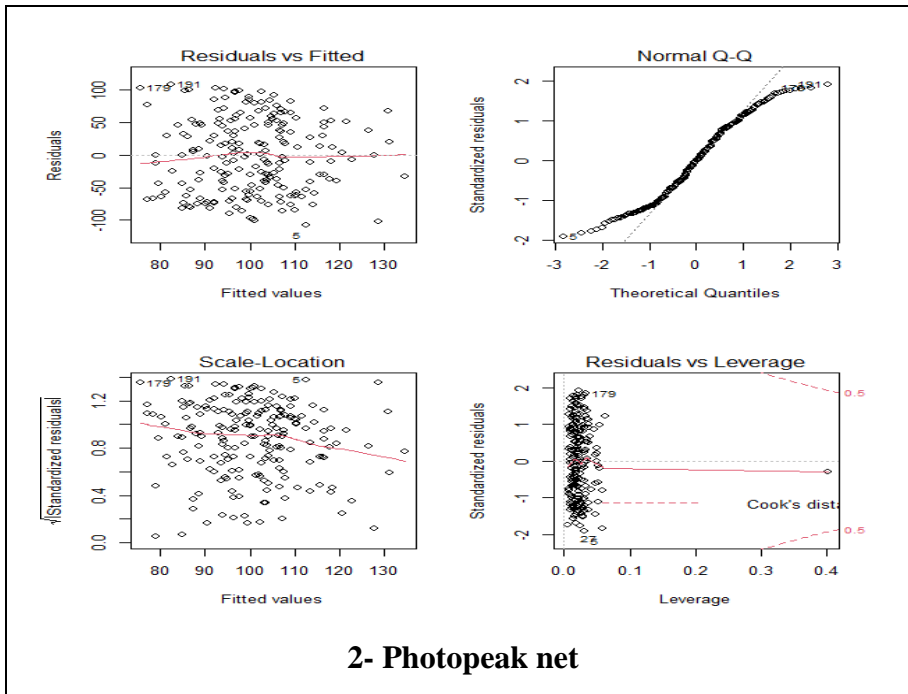
So, to find out the effective models the multiple linear regression test was used, as in Table (4-15).

**Table (4-15) Multiple Linear Regression for <sup>60</sup>Co Source.**

No.	Model	Data	P.value	Std. Error	Estimate	Residual standard error	Min	Max	R-squared	p.value (total)
1	T.A.	T.A.N.bef.	0.6947	7.088e-04	2.786e-04	53.32	-144.174	121.392	0.1515	2.665e-07
2		T.A.N.aft.	0.0573	7.334e-04	-1.402e-03					
3		T.A.C.bef.	0.4248	2.948e-02	-2.358e-02					
4		T.A.C.aft.	0.3020	3.042e-02	-3.148e-02					
5	P.N.A.	P.P1.N.bef.	0.00663	1.090e-02	2.992e-02	57.34	-107.694	108.644	0.03825	0.1055
6		P.P1.N.aft.	0.66263	1.043e-02	-4.556e-03					
7		P.P2.N.bef.	0.96612	9.442e-03	-4.016e-04					
8		P.P2.C.aft.	0.90548	1.034e-02	1.229e-03					
9	P.C.A.	P.P1.C.bef.	0.9727	1.705e-02	-5.849e-04	57.59	-110.399	107.438	0.02984	0.2039
10		P.P1.C.aft.	0.4333	1.996e-02	-1.567e-02					
11		P.P2.C.bef.	0.1087	2.525e-02	4.070e-02					
12		P.P2.C.aft.	0.0247	3.290e-02	-7.448e-02					
13	E.R.	E.R.1.bef.	0.7701	967.59	-283.21	58.28	-100.285	101.779	0.006642	0.8603
14		E.R.1.aft.	0.9677	1408.91	57.15					
15		E.R.2.bef.	0.3776	1053.92	-932.08					
16		E.R.2.aft.	0.7620	291.84	88.51					
17	(p/v)	(p/v) 1.bef.	0.133332	1.1384	1.7161	54.63	-117.527	107.471	0.1271	2.348e-05
18		(p/v) 1.aft.	0.032408	1.9268	-4.1517					
19		(p/v) 2.bef.	0.000114	0.7952	-3.1320					

Table (4-15) shows the multiple regression of the  $^{60}\text{Co}$  source spectrum, where this test was divided into five groups, each group contains relation between four variables to show any independent variable and any dependent variable. It was found from the table that the first group T.A. It has a 53% effect on other variables, while the P.N.A. group has a 57% effect, meaning that 57% of the P.N.A.bef. value can change the values of the other variables in the sample. The effect of the third group was P.C.A. 57%, and it was noted that the E.R. group is not finding any clear and influential change in the rest of the groups. In contrast to the P/V sample, there were three variables that confounded them with a close linear relation, and their effect on the sample was 54%, as shown in figure (4-29).





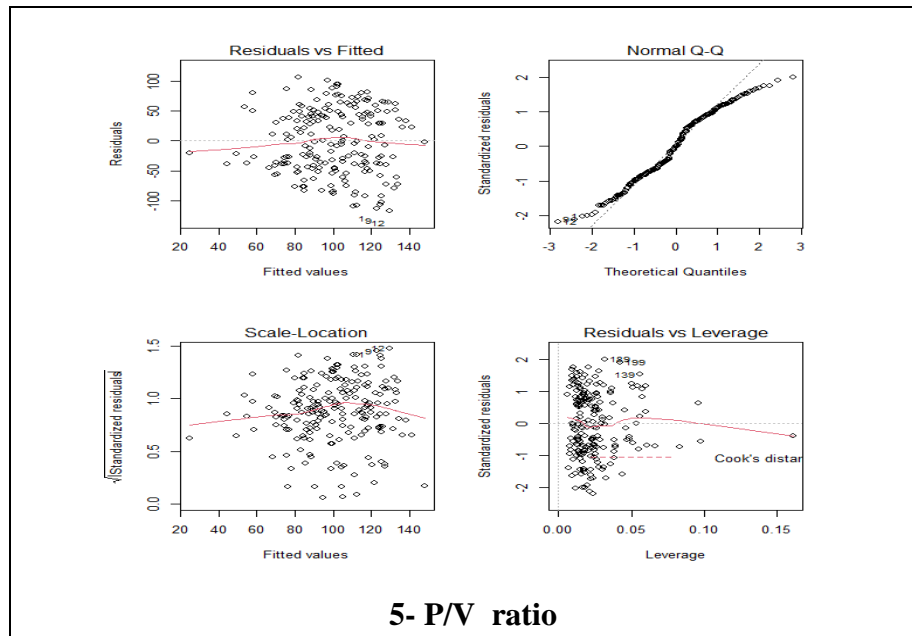
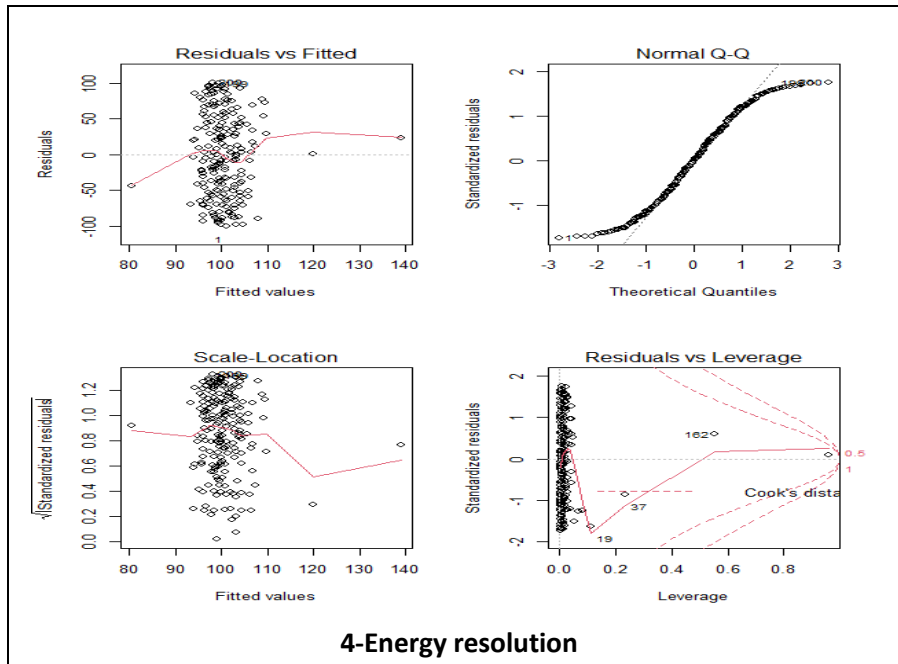


**Figure (4-29) Multiple Linear Regression for  $^{60}\text{Co}$  Source of all samples (1,2,3,4 and 5).**

The figure (4-29) is similar to the figure (4-28) where it notices that the residuals are not follow to the normal distribution in addition to the appearance of outliers values in all models except for the five groups P/V ratio that had p-value of less than (0.05) for three variables, meaning that these three variables have a linear correlation affecting this group.

For  $^{22}\text{Na}$  source the results of the linear regression test are shown in the tables (4-16) and (4-17).

**Table (4-16) Linear Regression Test for  $^{22}\text{Na}$  Source.**

No.	Model	Data	P.value	Std. Error	Estimate	Min	Max	R - squared
1	T.A.	sample ~ T.N.A.bef.	0.183	7.426e <sup>-04</sup>	-9.918e <sup>-04</sup>	-99.904	103.771	0.008929
2		sample ~ T.N.A.aft.	0.215	8.879e <sup>-04</sup>	-1.104e <sup>-03</sup>	-100.302	104.484	0.007751
3		sample ~ T.C.A.bef.	0.03680	0.002142	-0.004502	-100.126	96.789	0.02183
4		sample ~ T.C.A.aft.	7.74e <sup>-06</sup>	0.01712	-0.07863	-164.44	111.29	0.09631
5		T.N.A. bef. ~ T.N.A.aft.	2e <sup>-16</sup>	5.436e <sup>-02</sup>	9.180e <sup>-01</sup>	-31539.1	14737.8	0.5902
6		T.N.A. bef. ~ .C.A..bef.	0.788	2.063e <sup>-01</sup>	-5.551e <sup>-02</sup>	-39481	9472	0.0003657
7		T.C.A. bef. ~ .C.A..aft.	0.752	5.908e <sup>-01</sup>	1.869e <sup>-01</sup>	-993.8	26582.3	0.0005054
8		T.N.A. aft. ~ T.C.A. aft.	0.627	1.435	-0.698	-12396.6	7581.8	0.001194
9	P.N.A.	sample ~ P.N.A1.bef.	0.0370	0.02117	-0.04446	-118.12	977.91	0.02178
10		sample ~ P.N.A1.aft.	0.447	0.01553	0.01183	-130.88	956.91	0.002922
11		sample ~ P.N.A2.bef.	0.880	3.457e <sup>-02</sup>	5.235e <sup>-03</sup>	-107.77	966.15	0.0001158
12		sample ~ P.N.A2.aft.	0.719	0.024589	0.008872	-106.95	968.62	0.0006571
13		P.N.A.1bef. ~ .N.A1.aft.	0.00241	5.045e <sup>-02</sup>	1.551e <sup>-01</sup>	-972.81	889.70	0.04553
14		P.N.A.1.bef. ~.N.A.2.bef.	0.842	1.148e <sup>-01</sup>	-2.286e <sup>-02</sup>	-1057.98	989.42	0.0002004
15		P.N.A.2bef. ~ .N.A.2.aft.	0.0107	4.973e <sup>-02</sup>	1.281e <sup>-01</sup>	-786.97	675.58	0.03242
16		P.N.A.1.aft. ~ .N.A.2.aft.	0.486	1.122e <sup>-01</sup>	7.837e <sup>-02</sup>	-1125.5	4530.2	0.002457
17	P.C.A.	sample ~ P.C.A.1bef.	3.70e <sup>-05</sup>	0.0231	-0.0975	-115.941	108.368	0.08255
18		sample ~ P.C.A.1.aft.	0.1385	0.02589	-0.03851	-103.191	102.131	0.01105
19		sample ~ P.C.A.2.bef.	0.257	0.05554	-0.06314	-103.345	101.073	0.006486
20		sample ~ P.C.A.2.aft.	0.653	0.05226	0.02351	-98.040	100.054	0.001021
21		P.C.A.1bef. ~ .C.A.1.aft.	2e <sup>-16</sup>	4.844e <sup>-02</sup>	8.371e <sup>-01</sup>	-281.66	301.77	0.6013
22		P.C.A.1bef. ~ C.A.2.bef.	0.82	1.642e <sup>-01</sup>	3.745e <sup>-02</sup>	-447.27	487.00	0.0002628
23		P.C.A.2bef. ~ .C.A.2.aft.	2e <sup>-16</sup>	4.458e <sup>-02</sup>	6.980e <sup>-01</sup>	-175.138	143.043	0.5532
24		P.C.A.1.aft. ~ .C.A.2.aft.	0.746	1.427e <sup>-01</sup>	-4.632e <sup>-02</sup>	-464.68	588.62	0.0005319

Contain Table (4-16)								
25	E.R.	sample E.R.bef.1	0.5829	1151.18	-633.22	-99.995	103.041	0.001526
26		sample ~ E.R.aft.1	0.842	1127.61	-224.82	-99.603	100.235	0.0002007
27		sample ~ E.R.bef.2	0.462	504.49	372.02	-99.817	101.636	0.002739
28		sample ~ E.R.aft.2	0.297	502.47	525.60	-106.469	101.915	0.005496
29		E.R.bef.1' ~ XE.R.aft.1	2e <sup>-16</sup>	0.038286	0.817293	-0.0082506	0.0073637	0.6971
30		E.R.bef.1' ~ E.R.bef.2	0.266	0.0310658	-0.0346618	-0.0123688	0.0077915	0.006248
31		'E.R.bef.2' ~ E.R.aft.2	2e <sup>-16</sup>	0.0467682	0.7494426	-0.012141	0.018799	0.5646
32		'E.R.aft.1' ~ E.R.aft.2	0.932	0.0317514	0.0027041	-0.011749	0.008302	3.663e <sup>-05</sup>
33	(p/v) ratio	sample ~ p.v.bef1	0.139	1.623	2.410	-115.28	970.58	0.01101
34		sample ~ p.v.aft1	3.34e <sup>-07</sup>	1.513	7.994	-133.63	942.80	0.1235
35		sample ~ p.v.bef2	0.00974	3.537	9.234	-133.07	979.48	0.03327
36		sample ~ p.v.aft2	0.000641	4.191	14.538	-120.26	952.96	0.0573
37		p/v.bef1' ~ p.v.aft1	0.00155	0.06861	0.22023	-8.8946	14.3009	0.04947
38		p/v.bef1' ~ p.v.bef2	0.00766	0.1538	0.4145	-10.5537	14.9278	0.03537
39		p/v.bef2' ~ p.v.aft2	1.95e <sup>-05</sup>	0.08141	0.35625	-4.828	9.439	0.08819
40		p/v.aft1' ~ p.v.aft2	0.000213	0.1833	0.6916	-10.4666	14.9000	0.06709

Table (4-16) shows the simple linear regression of the studied samples from the <sup>22</sup>Na source, where the samples were divided into five groups, and each group contains eight relations between variables, and linear relation were found between the number of samples, T.N.A., T.C.A., P.N.A. and P.C.A. it is clear in the first and second group. also, it was found that the two peaks of <sup>22</sup>Na are related to each other by a linear relation. either net or cross before and after the subtracting B.G. , but it did not show any effect or correlation between the random variables in the E.R. sample, at on the contrary in the last sample P/V where the variables were linked to each other by a close linear relation .

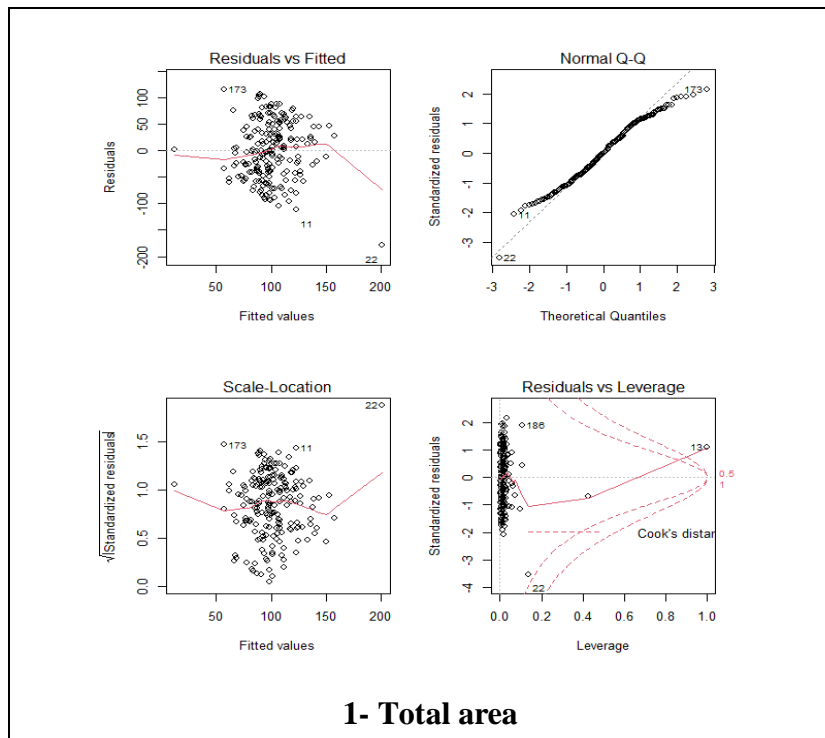
To find out the effective samples on the other sample, the multiple linear regression test was used, as in table (4-17).

**Table (4-17) Multiple Linear Regression <sup>22</sup>Na.**

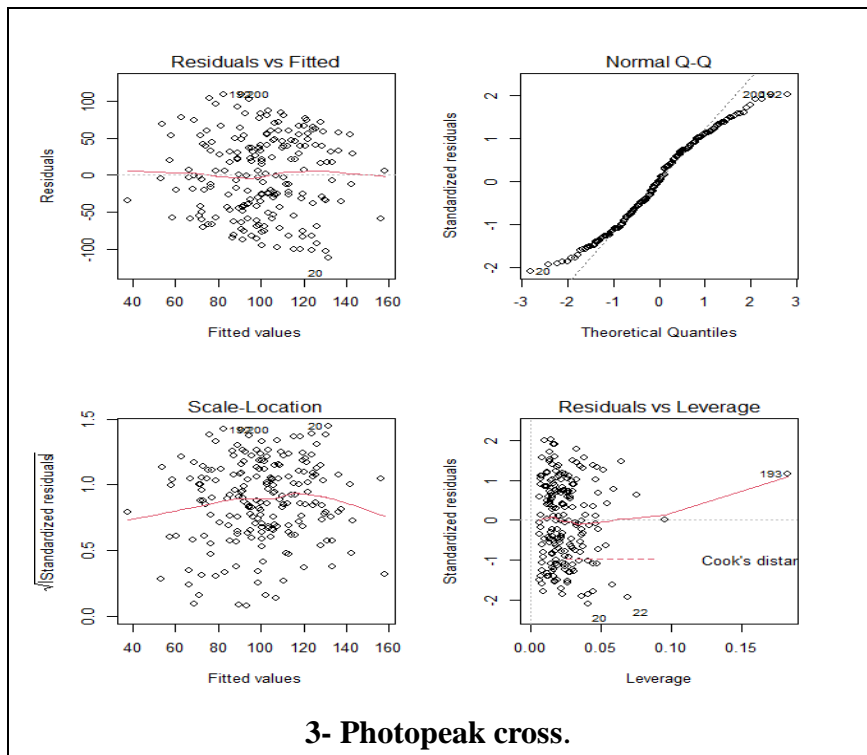
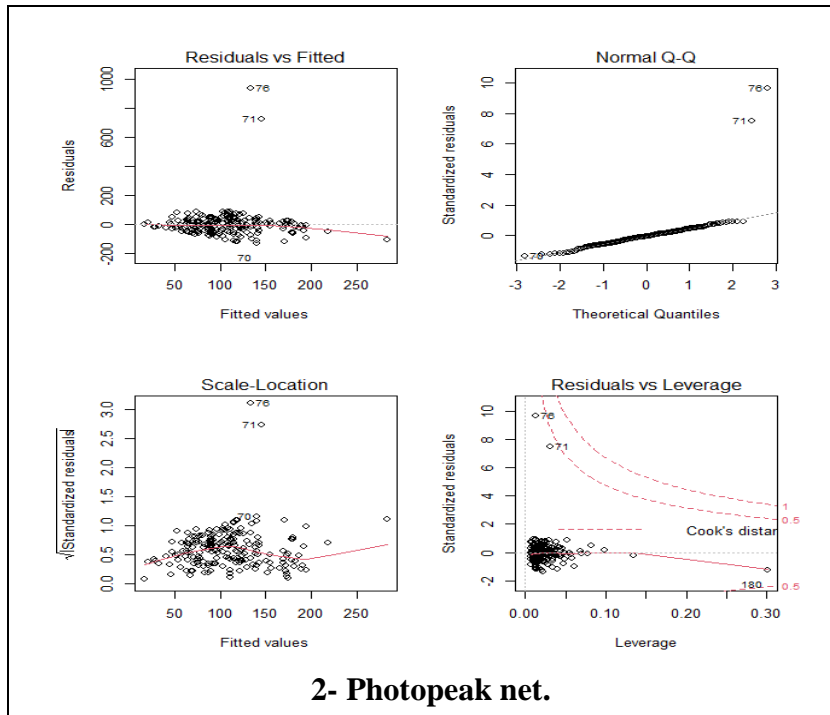
No.	Model	Data	P.value	Std. Error	Estimate	Residual Standard Error	Min	Max	R-Squared	P.value (total)
1	T. A.	T.N.A.bef.	0.6305	1.097e-03	-5.285e-04	54.61	-178.566	115.732	0.1277	2.208e-05
2		T.N.A..aft.	0.5419	1.312e-03	-8.016e-04					
3		T.C.A.bef.	0.0333	2.039e-03	-4.372e-03					
4		T.C.A.aft.	6.83e-06	1.697e-02	-7.847e-02					
5	P. N.A.	P.N.A.1.bef.	0.0226	0.021762	-0.050034	104.9	-154.91	963.09	0.02979	0.2047
6		P.N.A.1.aft.	0.2220	0.015829	0.019392					
7		P.N.A.2.bef.	0.9528	0.034888	0.002067					
8		P.N.A.2.aft.	0.8106	0.024858	0.005965					
9	P.C.A.	P.C.A.1.bef.	1.3e-05	0.03662	-0.16382	54.56	-111.448	109.340	0.02984	1.848e-05
10		P.C.A.1.aft.	0.0180	0.03971	0.09478					
11		P.C.A.2.bef.	0.1147	0.08034	-0.12730					
12		P.C.A.2.aft.	0.1388	0.07449	0.11072					
13	E.R.	E.R.1.bef.	0.485	2100.78	-1469.24	58.23	-108.59	104.82	0.008251	0.8045
14		E.R.1.aft.	0.645	2061.53	950.35					
15		E.R.2.bef.	0.912	776.69	-85.94					
16		E.R.2.aft.	0.444	771.39	592.15					
17	(p/v)	p.v.1.bef.	0.90955	1.5721	0.1788	98.16	-130.96	942.57	0.1507	1.908e-06
18		p.v.1.aft.	4.12e-05	1.6083	6.7490					
19		p.v.2.bef.	0.38346	3.5951	3.1404					
20		p.v.2.aft.	0.04413	4.2879	8.6870					

The Table (4-17) shows the multiple regression of the <sup>22</sup>Na source spectrum, the table contains five groups, each group contains relation between four variables to show which variables are affecting the rest of the variables. Where it was found in the first group T.A. was the variables T.C.A. (before and after subtracting B.G.) are important and influential, they have an impact rate of 54% on the rest of the variables in the model, while in the second group P.N.A., it was found that the only important variable was P.N.A. bef., and it had an effect of 104% on the rest of the values in the sample. For the third group P.C.A., it was found that there are two

variables P.C.A. (before and after subtracting B.G.) for the first peak with has energy (511 keV) that has the same effect on the rest of the changes in the sample, with a percentage of 54%. In the E.R. groups, there is no variable that has an effect on the rest of the variables, meaning that the energy resolution sample is considered independent by itself. In addition, it was found in the P/V ratio group that two variables P/V.aft. both two peaks (511 ,2472) keV, which have an important and significant influence on the rest of the variables in the sample, with an effect rate of 98% ,as shown in the figure (4-30).







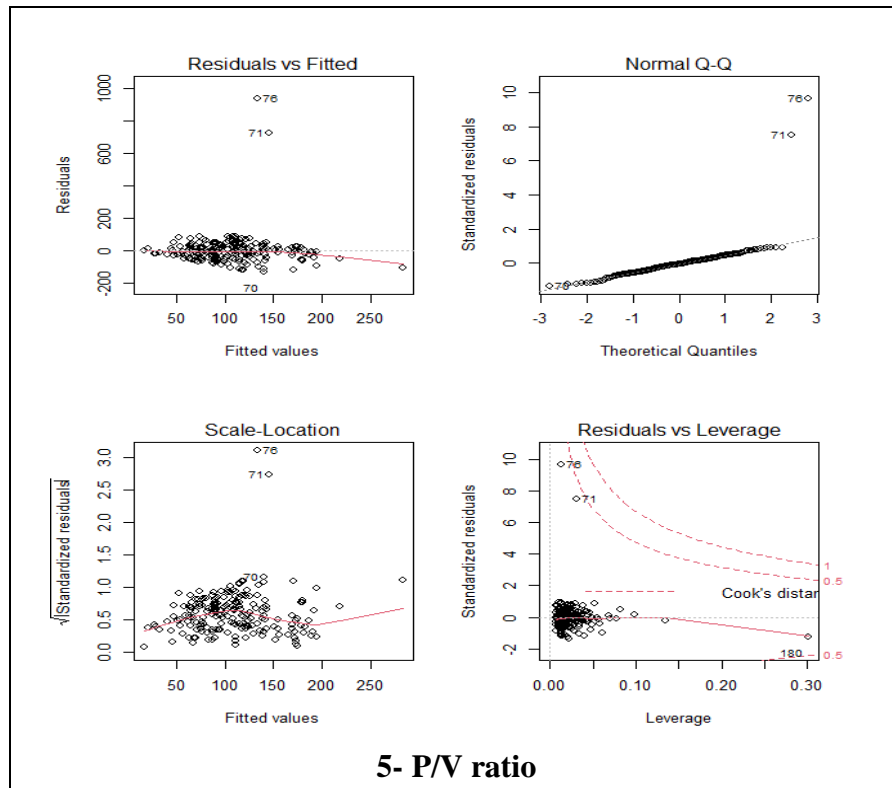
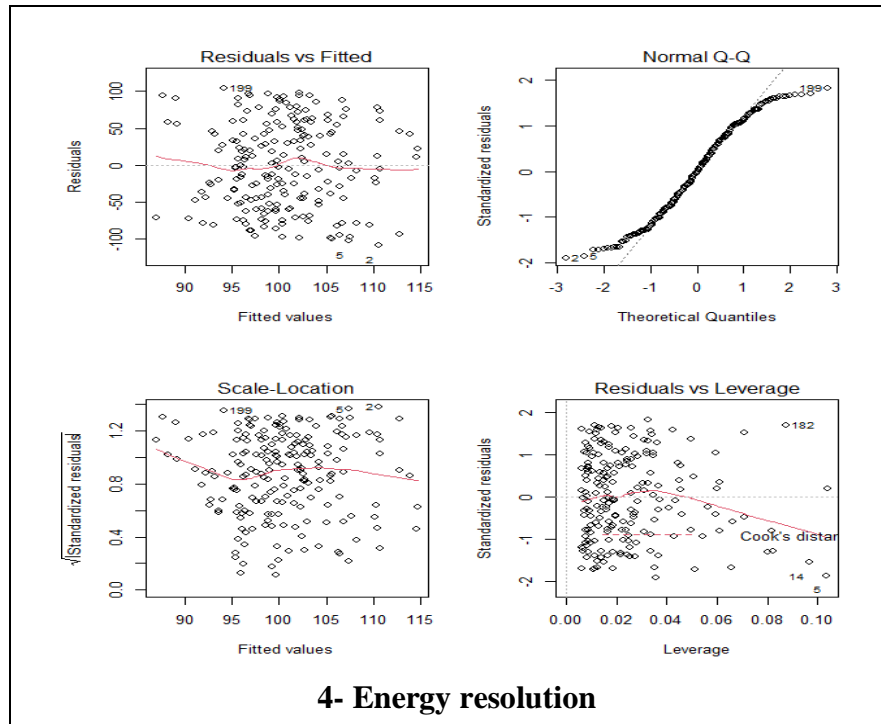


**Figure (4-30) Multiple linear regression for  $^{22}\text{Na}$  source of all samples (1,2,3,4 and 5).**

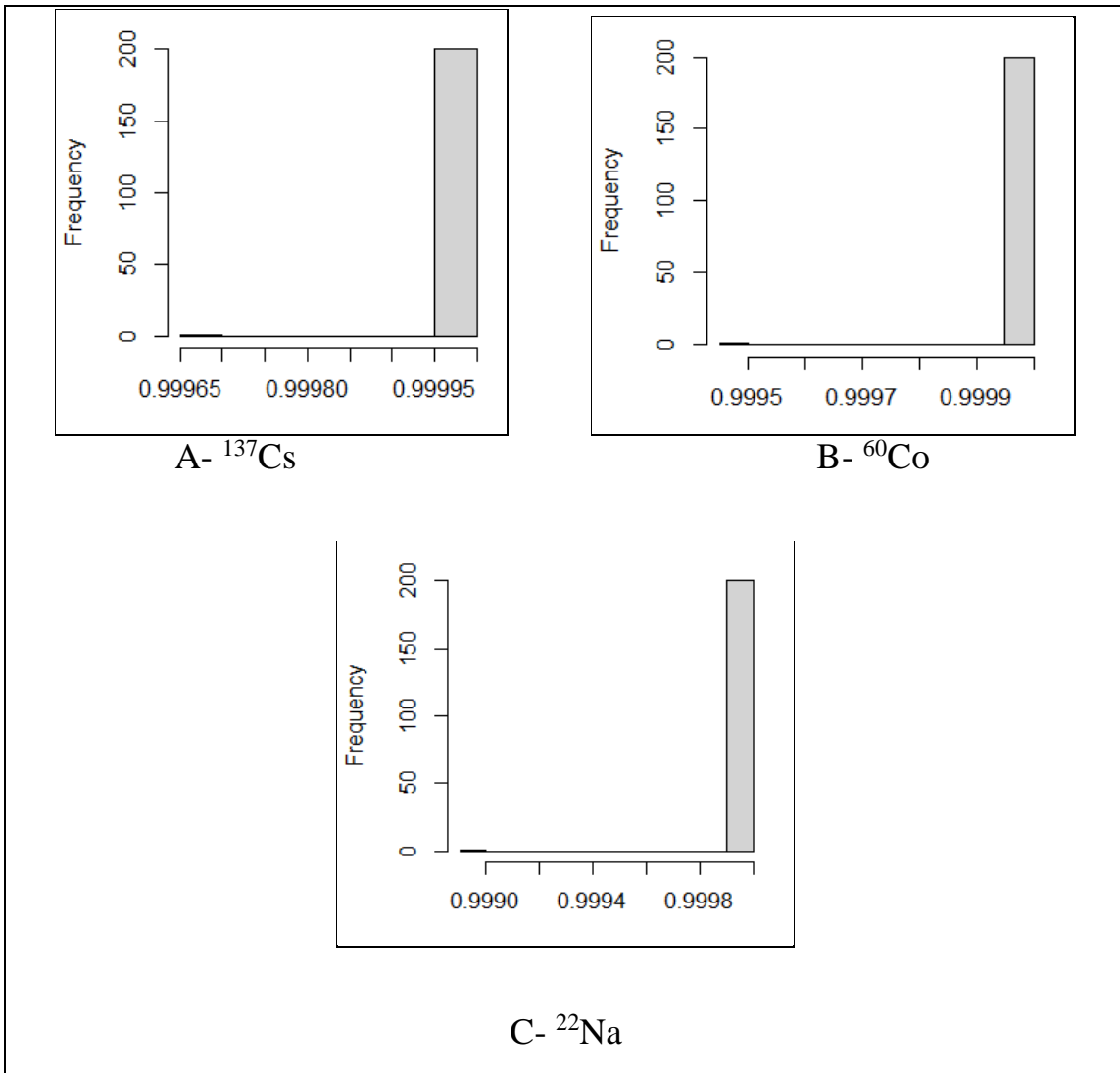
Figure (4-30) shows the conditions for the linear regression test for the  $^{22}\text{Na}$  source spectrum, where it is noted that the remaining values do not follow a normal distribution in addition to the appearance of outliers in all groups except for the five group P/V ratio whose total p value was less than 0.05, which means that these variables have a linear correlation that affects this sample.

#### 4.5 Statistical Distributions

Statistical applications by using the R program are the aspect that clearly shows the importance of this language in most statistical operations through the easy preparation of writing the code to get clear and detailed results. In this study, a number of statistical distributions of radioactive sources ( $^{137}\text{Cs}$ ,  $^{60}\text{Co}$  and  $^{22}\text{Na}$ ) were used, such as the binomial distribution, the poisson distribution, the exponential distribution, the uniform distribution, and the normal distribution as shown in appendices (6 to 20).

Appendix (6) shows the probability of the binomial distribution of the studied samples of  $^{137}\text{Cs}$  source spectrum. It was noted that the probability values of the samples were repeated for every hundred samples, as the probability started to increase from the value of  $(2.48e^{-60})$  to  $(1.03e^{-02})$  for the first hundred samples and then started decreasing inversely with the same probability exactly. This result was identical exactly what was found in the  $^{60}\text{Co}$  and  $^{22}\text{Na}$  sources, as appendix (7 and 8) respectively, because the binomial distribution code depends on the number of samples and in this study the number of samples was fixed (200 spectrum), therefore it is not possible to rely on the binomial distribution in explaining the behavior of the gamma-ray spectrum of radioactive sources.

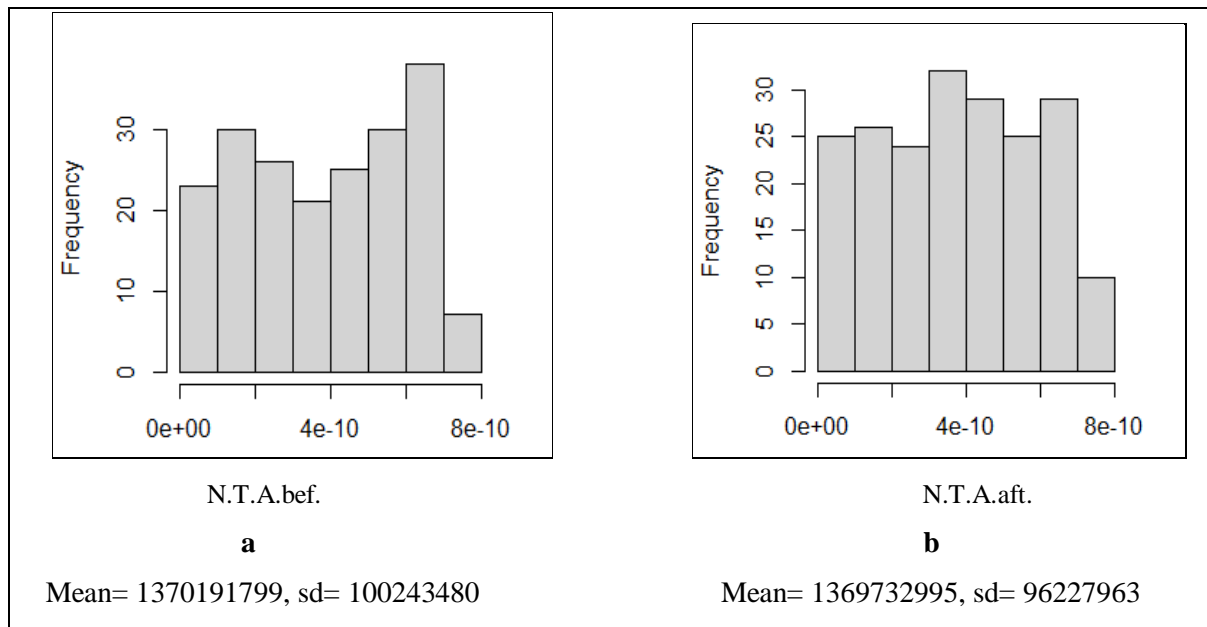
It is clear from appendix (9) that all samples for  $^{137}\text{Cs}$  source have the same probability value because the code depends on the half life of the radioactive element, and the same case was found when applying the Poisson distribution for the  $^{60}\text{Co}$  and  $^{22}\text{Na}$  sources as appendices (10-a) to (11-b), therefore it is not possible to rely on the poisson distribution in explaining the behavior of the gamma ray spectrum, as in the figure (4-31).



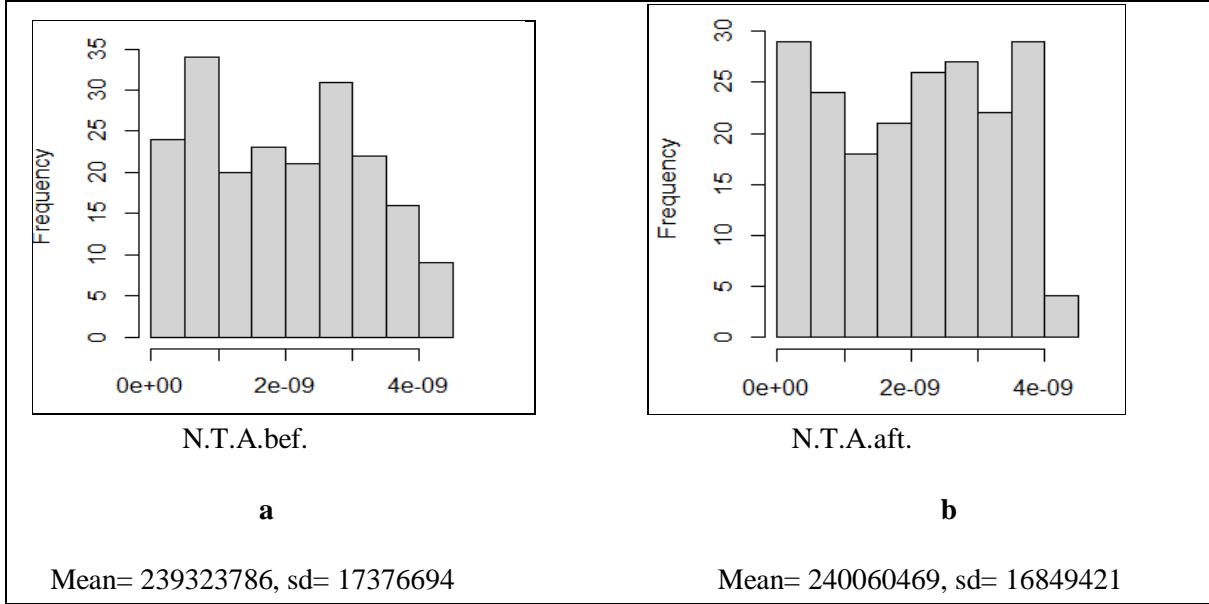
**Figure (4-31) Poisson distribution for radioactive sources.**

Figure (4-31) shows the behavior of the poisson distribution for the study samples of the radioactive sources, where the probability value of the Poisson distribution for the samples was equal.

The exponential distribution of  $^{137}\text{Cs}$  source samples was used using the R program as in appendix (12), where it was found that all samples have almost the same probability, the distribution gives a mean and standard deviation for the same sample and the same result was found for  $^{60}\text{Co}$  and  $^{22}\text{Na}$  sources as appendices (13-a) to (14-b) because the exponential distribution code depends on the decay constant of the radioactive source, and thus the distribution results were unified for the same measured model for the radioactive source, as shown in the figures (4-32) to (4-34) for this it is not possible to depend on the exponential distribution to explain the behavior of the gamma ray spectrum.



**Figure (4-32) Exponential distribution for total area of  $^{137}\text{Cs}$  source**  
**a -before subtracting B.G.      b-after subtracting B.G.**



**Figure (4-33) Exponential distribution for total area of  $^{60}\text{Co}$  source**  
**A -before subtracting B.G.      B-after subtracting B.G.**

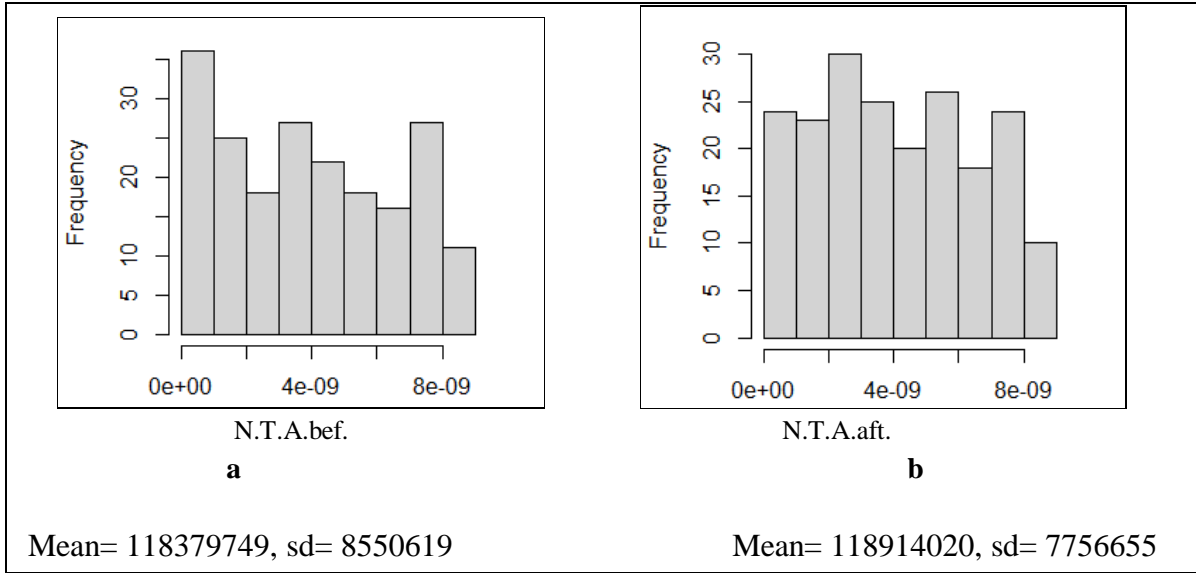


**Figure (4-34) Exponential distribution for total area of  $^{22}\text{Na}$  source**  
**A -before subtracting B.G.      B-after subtracting B.G.**

The Figures show the exponential distribution of the measured samples of the ( $^{137}\text{Cs}$ ,  $^{60}\text{Co}$  and  $^{22}\text{Na}$ ) sources, respectively before and after subtracting B.G., where it was found that the shapes are far from the exponential curve and thus it is considered that they are not clear behavior.

As for the uniform distribution, it was used in this study for all the samples studied for the  $^{137}\text{Cs}$  source, as in the appendix (15) and it was found that the same probability value for same sample, in addition to obtaining a special mean and statistical range for one sample and the similar result was obtained in the two sources for  $^{60}\text{Co}$  and  $^{22}\text{Na}$  source, as shown in the appendices (16-a) to (17-b), as in the figures (4-35) to (4-37). It cannot be considered that the results of the samples are follow to uniform distribution because the sum of the probabilities for the one sample is not equal to 1, and this is contrary to the condition of the uniform distribution.

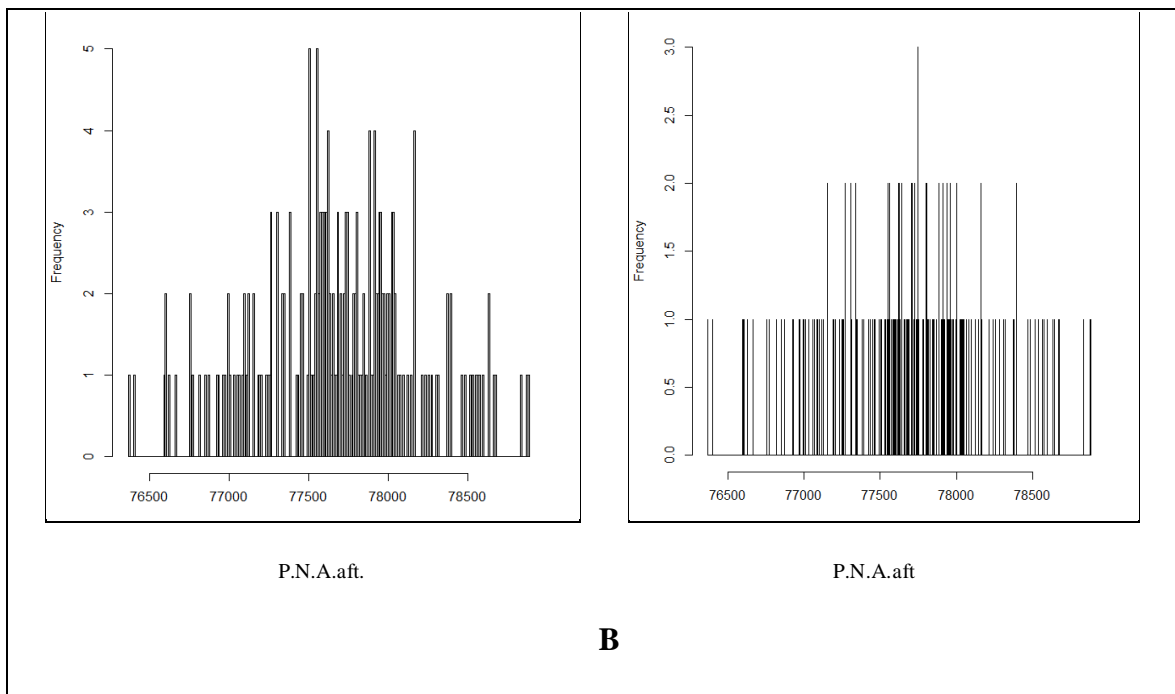
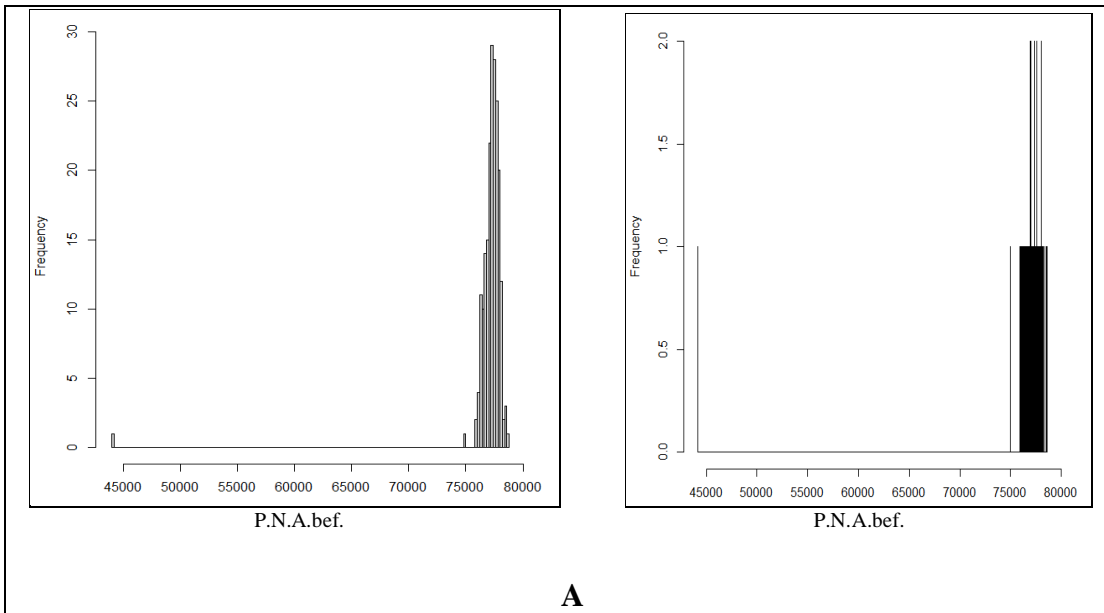


**Figure (4-35) Uniform distribution for  $^{137}\text{Cs}$  source A -before subtracting B.G.  
B-after subtracting B.G.**



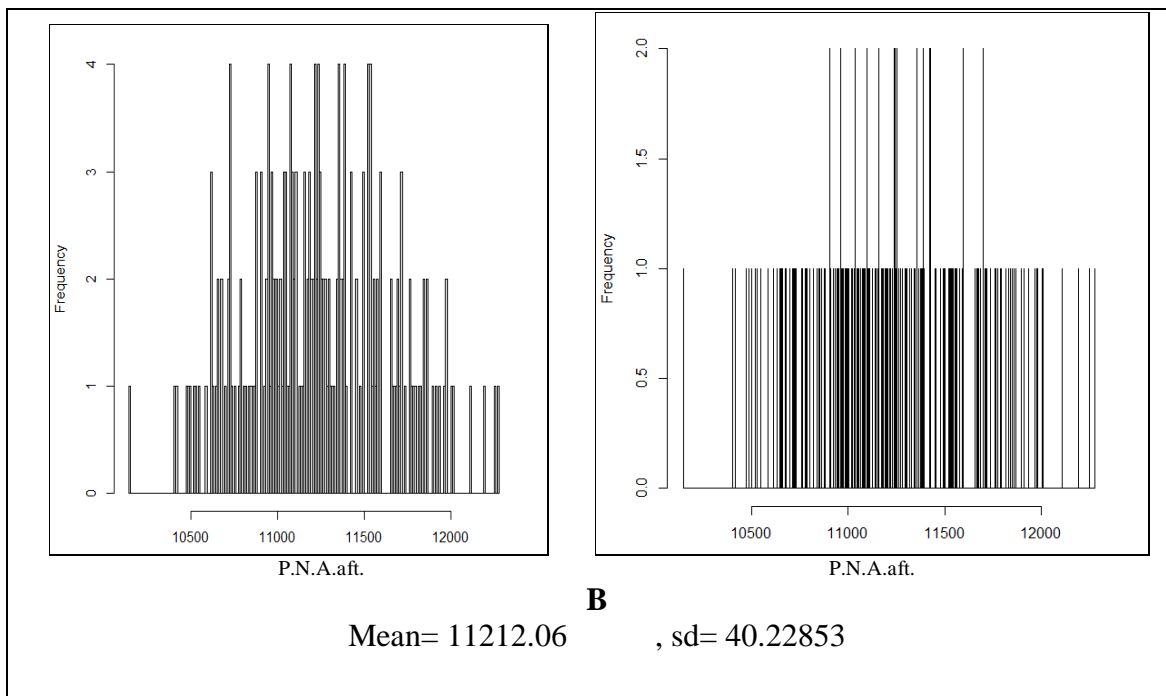
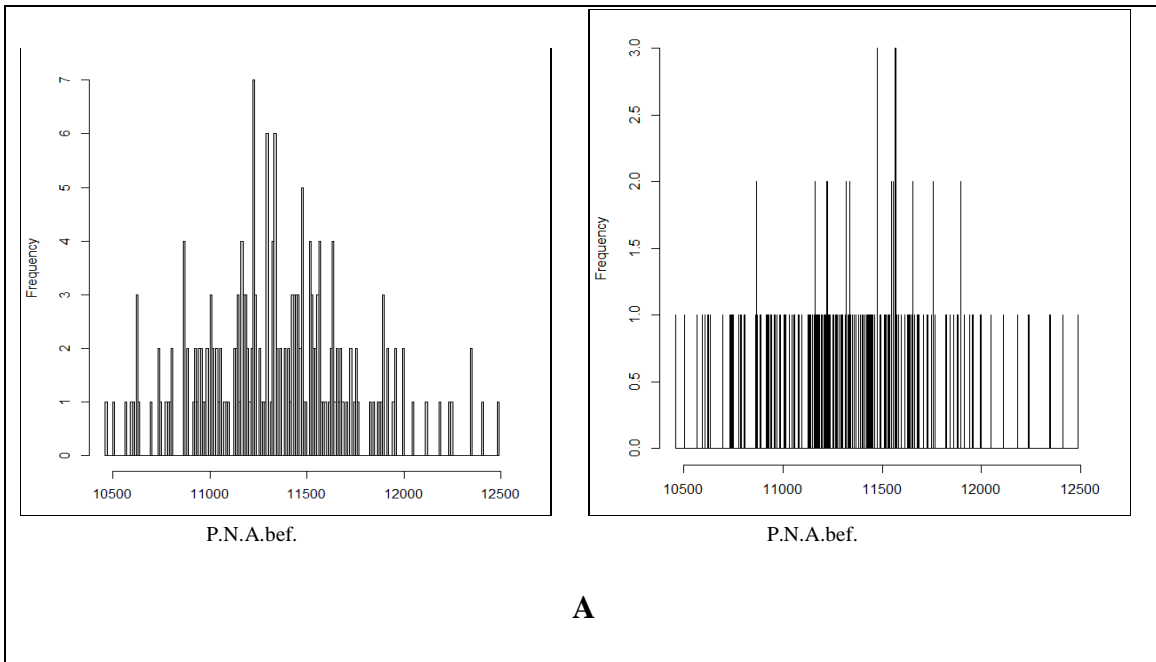


**Figure (4-36) Uniform distribution for  $^{60}\text{Co}$  source A -before subtracting B.G.  
B-after subtracting B.G.**

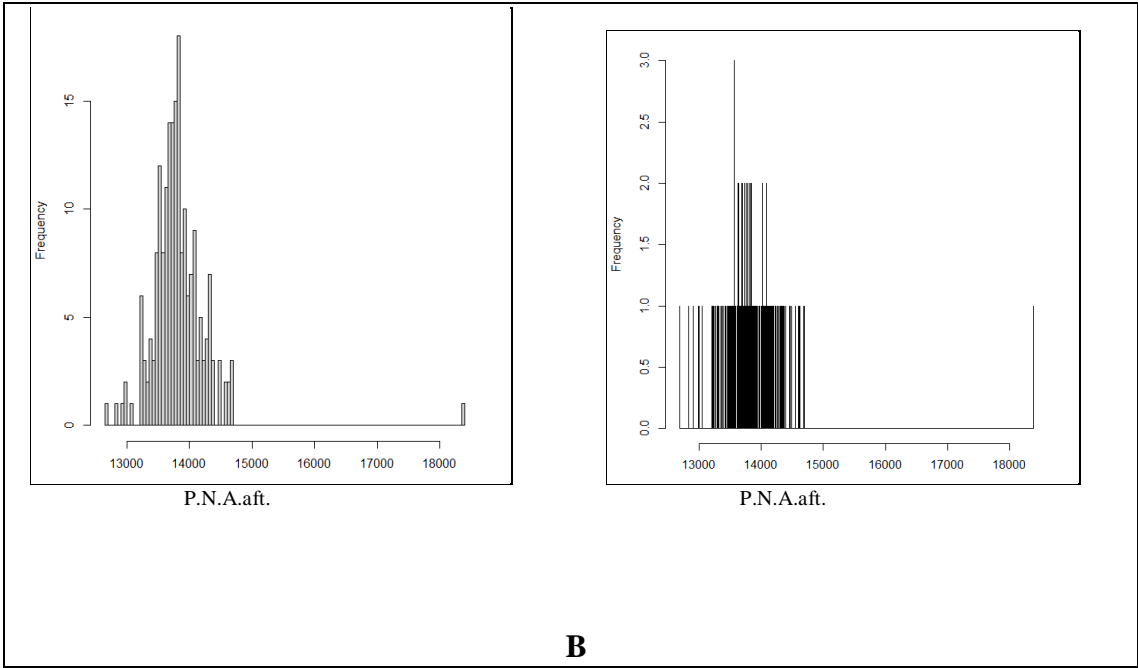
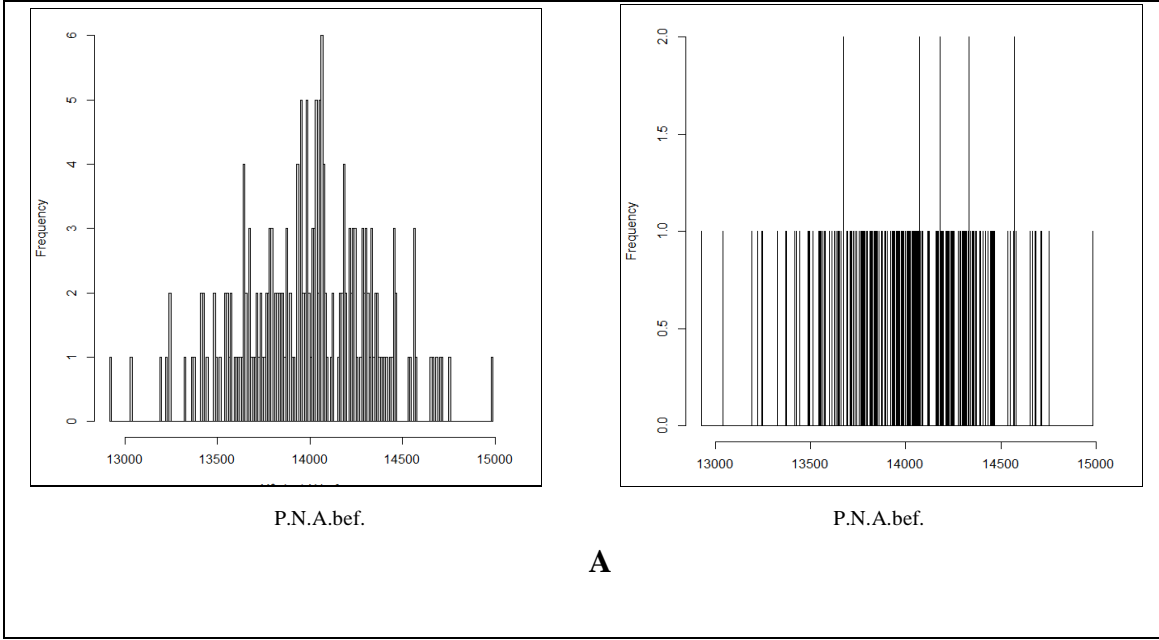


**Figure (4-37) Uniform distribution for  $^{22}\text{Na}$  source A -before subtracting B.G.B-after subtracting B.G.**

Figure (4-37) shows the uniform distribution of the samples in this study of ( $^{137}\text{Cs}$ ,  $^{60}\text{Co}$  and  $^{22}\text{Na}$ ) sources, respectively before and after subtracting B.G., where it was noted that the shape is almost uniform for all samples, where the probability was completely equal for the single sample, and this is indicated by the presence of parallel lines in the figure, but because of the integration of samples in one form the general behavior is similar to the shape of a bell.

The normal distribution was used to study the gamma ray spectrum of ( $^{137}\text{Cs}$ ,  $^{60}\text{Co}$  and  $^{22}\text{Na}$ ) sources, the distribution was measured for each sample. It was found that each sample had its own mean and statistical deviation as in appendix (18). By studying the behavior of the general sample, it was found that it does not follow completely the normal distribution, but rather approaches it, and this is a clear by difference in the values of the mean value from median value. If mean is equal to median, then the data is distributed uniformly and the shape of the curve is symmetrical, but if there is a difference between the mean and median, then the data is scattered and the shape of the curve is asymmetric and the behavior is close to the normal distribution and this is clear in figure (4-38).

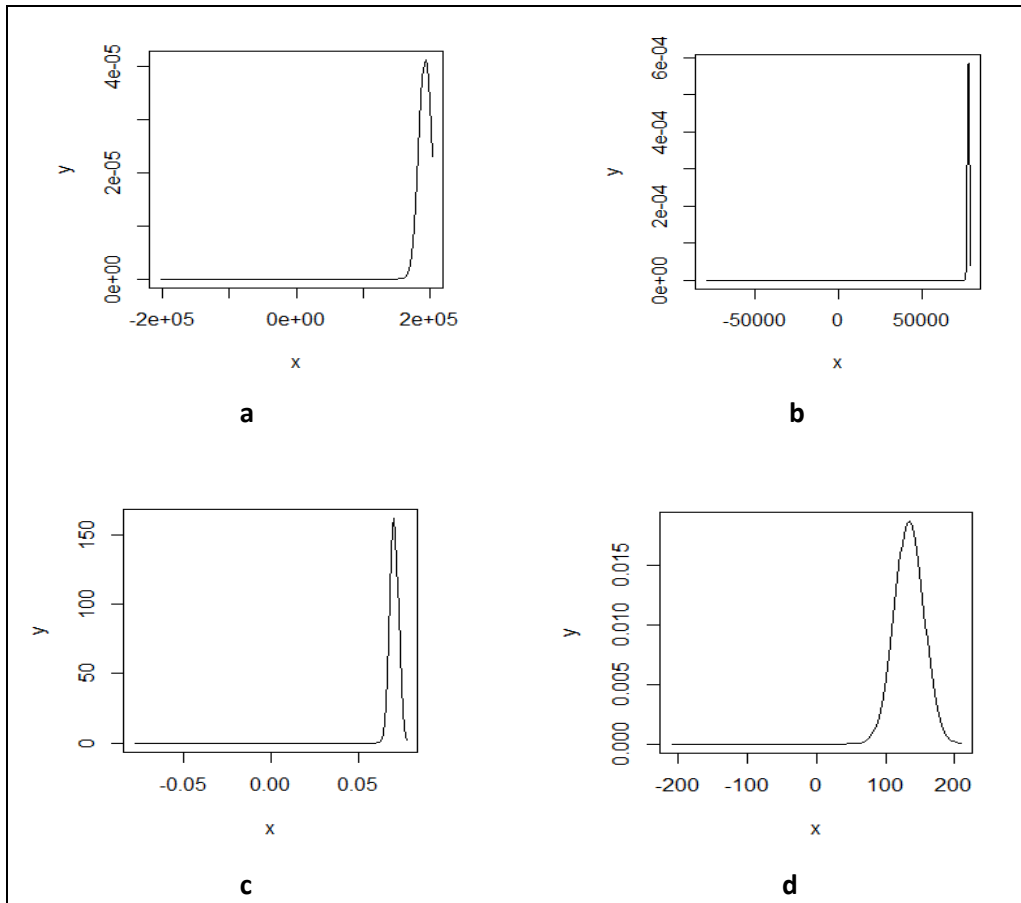


**Figure (4-38) Normal distribution for  $^{137}\text{Cs}$  source**  
**a-Total area   b- Photopeak area   c-Energy resolution   d- P/V ratio.**

The same result was obtained when study the spectra of  $^{60}\text{Co}$  and  $^{22}\text{Na}$  sources as in the appendices (19-a) to (20-b) as shown in the figures (4-39) and (4-40).

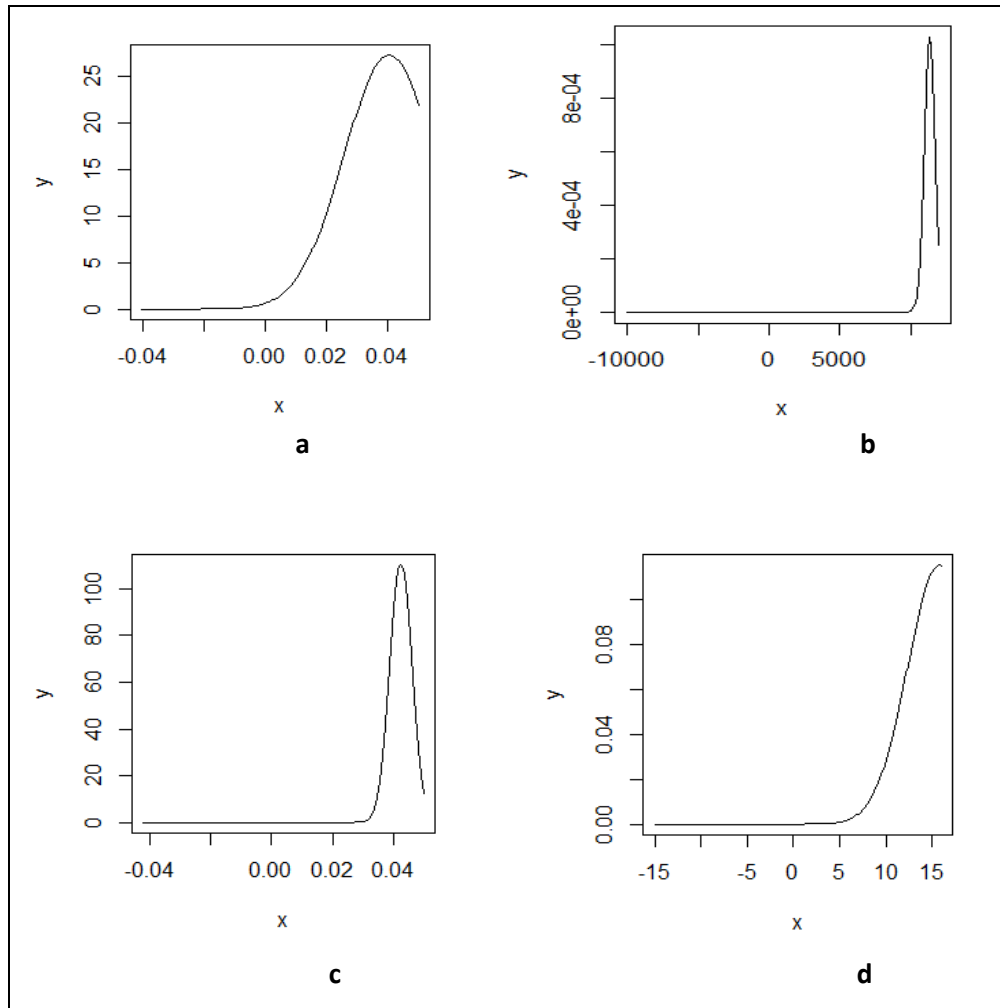


**Figure (4-39) Normal distribution for  $^{60}\text{Co}$  source**

**a-Total area    b- Photopeak area    c-Energy resolution    d- p/v ratio.**

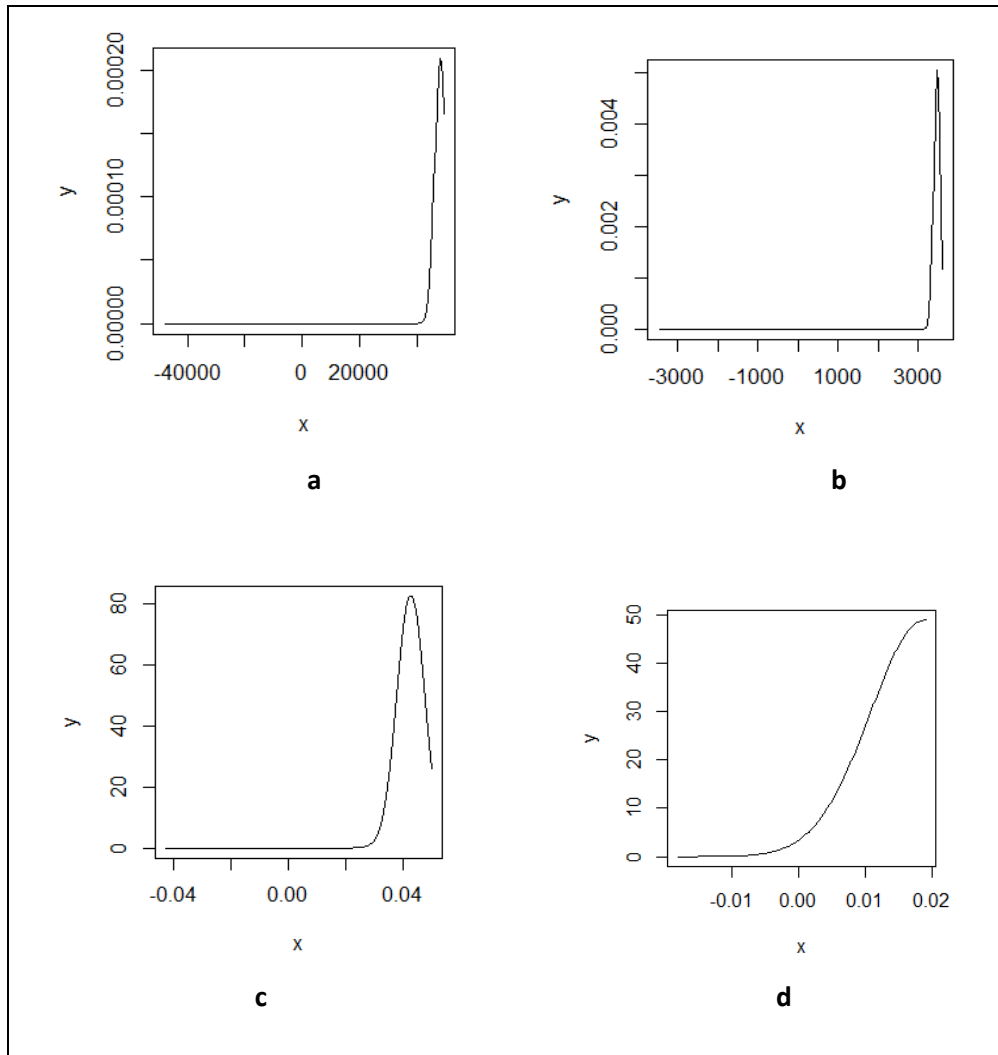


**Figure (4-40) Normal distribution for  $^{22}\text{Na}$  source**

**a-Total area    b- Photopeak area    c-Energy resolution    d- P/V ratio.**

This Figures show the calculation of the normal distribution of the gamma-ray spectrum for ( $^{137}\text{Cs}$ ,  $^{60}\text{Co}$  and  $^{22}\text{Na}$ ) sources, where the spectrum was divided into samples (T.A., P.P.A, E.R. and P/V ratio). From the results of the normal distribution, a difference was found in the probability values for each sample depending on the mean and its standard deviation. It was noted from the drawings that the samples approached from the shape of the normal distribution, but not completely follow to it.

# Chapter Five

## Conclusions and Recommendations

This chapter includes the conclusions which are extracted from the present study and recommendations for future studies.

### 5.1 Conclusions

In this study, statistical distribution and statistical testing software were used to study the behavior of gamma ray spectrum of radioactive sources, and we found the following:

1. Regarding the normality test for all studied models, it was found that most of the models were not follow to a normal distribution.
2. Using homogeneity tests, it was found that all the studied models were homogeneous and regular data.
3. In Pearson's corelation test it was found that there is a direct relation between the number of samples and the total area whether before or after the subtract the background radiation, therefor increase in N.T.A. leads to increasing in C.T.A. in all the studied samples in  $^{137}\text{Cs}$  source. As for the rest of the samples it was found that there is no close linking relation between them for the  $^{60}\text{Co}$  and  $^{22}\text{Na}$  sources.
4. Through the linear regression test, the fact was confirmed that a linear relation between the total area and the number of samples for all samples of radioactive source. Also, it was found that the energy resolution sample is an independent variable.

5. It had been found that the binomial distribution that it has no effect on the studied samples for all the radioactive sources.
6. In the Poisson distribution, the probability values were constant for all samples for one radioactive source because it depends on the half-life of the radioactive element, and the same behavior was taken for all the radioactive sources used in the study.
7. The exponential distribution probability was constant for all samples because it depends on the constant decay for the radioactive source.
8. For the uniform distribution, it had been found that each sample has one probability value of its own that differs from the probability value in the second sample for the same source, depending on the highest and lowest value in the same studied sample, which means that it does not affect the probability values of the studied samples.
9. As for the normal distribution, it was found that each value has its own probability. If the probability values of the sample values are collected by drawing one, it will be similar to the gaussian figure, except that it is asymmetrical, but rather skewed towards the right or left from the mean.
10. Accordingly, these distributions did not succeed in giving a clear explanation for the behaviour of radioactive decay, which requires reconsidering the prevailing concept about the random nature of decay, which means that more studies and research should be done in this field.



## **5.2 Future Work**

- 1.** Study of anomalies in the radioactive half live using the statistical program of the time series R.
- 2.** Using distributions and other statistical programs such as gamma distribution, beta distribution, binary geometric distribution and others to study the decay of gamma rays and compare the results with the results of this study.
- 3.** Statistical study using Manti Carlo simulation within the R statistical program and comparing the results obtained with the results of this study.

## Reference

- [1] G. E Knoll," Radiation detection and measurement", third edition, John Wiley and Sons, Ltd., (2000).
- [2] H.J. Arnikra, " Essentials of nuclear chemistry", fourth edition, New Age International (p), Ltd., (2005).
- [3] G. R. Gilmore, "Practical gamma-ray spectrometry", second edition, John Wiley and Sons, Ltd, (2008).
- [4] J.-L. Basdevant, J. Rich and M. Spiro," Fundamentals in nuclear physics", Springer Science-Business Media, Inc., (2005).
- [5] IAEA, "Analytical Techniques in Uranium exploration and ore processing", Technical report, International Atomic Energy Agency, 341,81-99, IAEA, Vienna, (1992).
- [6] R. Development Core Team, " R: a language and environment for statistical computing. R Foundation for Statistical Computing, Vienna.", Austria, URL <http://www.R-project.org>, ISBN 3-900051-07, (2018).
- [7] K.M.Wainio and G.F.Knoll , "Calculated gamma-ray response characteristics of semiconductor detectors", Nuclear Instruments and Methods, 44(2), 213-223, (1966).
- [8] F. W. Lima and L. T. Atalla, " A simple program in basic language for analysis of gamma-spectra using an on-line minicomputer", Journal of Radioanalytical Chemistry, 20(1), 769–777 (1974).

- [9] A. Gavron, " Statistical model calculations in heavy ion reactions ", Phys. Rev. C, 21 (1),230-236, (1980).
- [10] P. A. Aarnio, J. J. Ala-Heikkilä, T. T. Hakulinen and J. T. Routti, "Expert system for nuclide identification in gamma spectrum analysis " , Journal of Radioanalytical and Nuclear Chemistry, 193(2), 219–227 (1995).
- [11] J.Hovgaard and R.Grasty , "Reducing statistical noise in airborne gamma-ray data through spectral component analysis", Radiometric Methods and Remote Sensing , Fourth Decennial Internal Conference on Mineral Exploration , 753-764, (1997).
- [12] I.Gontchar ,L. Litnevsky and P.Fröbrich, "AC-code for combining a langevin fission dynamics of hot nuclei with a statistical model including evaporation of light particles and giant dipole  $\gamma$ -quanta" , Computer Physics Communications , 107 (1),223-245, (1997).
- [13] C .Theisen , N.Kintz , O.Stézowski and J. Vivien , "Improvement of high-fold  $\gamma$ -ray data processing: the spherical gate method", Nuclear Inst. and Methods in Physics Research, A, 432(2), 249-264,(1999).
- [14] P. A. Aarnio, M. T. Nikkinen and J. T. Routti , "UNISAMPO, comprehensive software for gamma-spectrum processing" , Journal of Radioanalytical and Nuclear Chemistry , 248(2), 371–375 (2001).
- [15] A. Simonits, J. Östör, S. Kálvin and B. Fazekas , "Hyper lab: A new concept in gamma-ray spectrum analysis", Journal of Radioanalytical and Nuclear Chemistry , 257(3), 589–595 (2003).

- [16] Z. Jiamei, S. Quanlin, B. Tao, Q. Shaojun, and C. Yongfu , "Effect of reducing statistical fluctuation of gamma spectra by method of wavelet analysis" , Atomic Energy Science and Technology, 39(4), 349-353, (2005).
- [17] N.S.Pattabirama ,S.S.Ghugra, S.K.Basu, U.Garg , S.Ray, A.K.Sinha and S.Zhu , "Subtraction of random coincidences in gamma -ray spectroscopy: a new approach", Nuclear Inst. and Methods in Physics Research, A, 562(1), 222-229,(2006).
- [18] V. Neti and R.W. Howell , "Lognormal distribution of cellular uptake of radioactivity: statistical analysis of  $\alpha$ -particle track autoradiography", Journal of Nuclear Medicine, 49(6),1009–1016,(2008).
- [19] J. M. Kirkpatrick and B. M. Young, "Poisson statistical methods for the analysis of low-count gamma spectra," in IEEE Transactions on Nuclear Science,56(3),1278-1282, (2009).
- [20] H. Mathkour, A. M. Al.Muatiri and A. S. Ahmad, "Computations of radioactive decay and electron trapped in an infinite potential well using lab view. ", IJCSNS International Journal of Computer Science and Network Security ,10(2),131-138, (2010).
- [21] M. Wasim, M. Arif and J. H. Zaidi, "Statistical data analysis of gamma-ray background spectra for quality assurance purposes", The Nucleus, 47(1), 1-6,(2010).
- [22] A.V. Shumakov, V.P. Kasatkin, "Comparison of statistical methods of radiation monitoring", Atomic Energy, 107, 209–217, (2010).

- [23] H. T. Dam, S. Seifert and D. R. Schaart , " The statistical distribution of the number of counted scintillation photons in digital silicon photomultipliers: model and validation", *Physics in Medicine & Biology*, 57(15), 4885-4871, (2012).
- [24] T. Kawanon , P. Talou and M.B. Chadwick , "Monte Carlo simulation for statistical decay of compound nucleus", *The European Physical Journal Conferences* 21(04001),1-10,(2012).
- [25]A. M. Adam, M. A. Eltaye, "Multivariate statistical analysis of radioactive variables in two phosphate ores from sudan", *Journal of Environmental Radioactivity*, 107(2),23-43,(2012).
- [26] S. Hauf, M. Kuster, M. Batič, Z. W. Bell, D.H. Hoffmann, P.M. Lang , S. Neff, M. G. Pia, G. Weidenspointner and A. Zoglauer , "Validation of Geant4-based radioactive decay simulation", *IEEE Transactions on Nuclear Science* 60(4),1-14,(2013).
- [27] Z. Jinzhao, T. Xianguo, "High-resolution gamma spectroscopy shift-invariant wavelet de-noising", *Chinese Physics C*, 14(34),2-8, (2013).
- [28] S. M. Ahmed, R. Yahaya and S. Radiman, "Clusterization probability in alpha-decay  $^{212}\text{Po}$  nucleus within cluster-formation model a new approach ", *Romanian Reports in Physics* 65(4),1281-1300, (2013).
- [29] R.Ravisankar, K.Vanasundari, M.Suganya ,Y.Raghu ,A.Rajalakshmi , A.Chandrasekaran ,S.Sivakumar ,J.Chandramohan ,P.Vijayagopal and B.Venkatraman, "Multivariate statistical analysis of radiological data of building materials used in Tiruvannamalai, Tamilnadu , India" , *Applied Radiation and Isotopes*, 85(2),114-127,(2014).

- [30] D. K. Yoon, J.Y. Jung, S. M.Han and T S. Suh, "Statistical analysis for discrimination of prompt gamma ray peak induced by high energy neutron: Monte Carlo simulation study" , Journal of Radioanalytical and Nuclear Chemistry volume 303 (1), 859–866 (2015).
- [31] M.Batmunkh , O. V. Belov, O. Lhagva, L. Bayarchimeg, M.Minjmaa and Purev . Battogtokh, "Simulations of radioactive decays: an application of low-energy electromagnetic packages for the nuclear medicine" , Mongolian Journal of Biological Sciences ,13(1), 55-64, (2015).
- [32] A. Sitek and A.M.Celler, "Limitations of Poisson statistics in describing radioactive decay", Physica Medica, 31(8), 1105-1107 (2015).
- [33] C.A. Kalfas, M. Axiotis and C. Tsabaris , "SPECTRW: A software package for nuclear and atomic spectroscopy" , Nuclear Inst. and Methods in Physics Research, A, 830(4 ) , 265-274,(2016).
- [34] G. Lorusso, S. M. Collins, K. Jagan, G. W. Hitt, A. M. Sadek, P. M. Aitken-Smith, D. Bridi and J. D. Keightley, "Measuring radioactive half-lives via statistical sampling in practice", EPL (Europhysics Letters), 120 (2), 1-7, (2017).
- [35] L. Schlattauer, L. Parali, J. Pechousek, I. Sabikoglu, C.Celiktas, G.Tektas, P. Novak, A. Jancar and V. Prochazka , "Calibration of gamma-ray detectors using Gaussian photopeak fitting in the multichannel spectra with a LabVIEW based digital system" , European Journal of Physics, 38(5) , 801-806 ,(2017).
- [36] K.J. Dayman and C.F. Weber, "Flexible classification with spatial quantile comparison and novel statistical features applied to spent nuclear

- fuel analysis", *Journal of Radioanalytical and Nuclear Chemistry* , 318(2), 605–618, (2018).
- [37] M.Å. Lindell; P. Andersson, S. Grape, C. Hellesen, A. Håkansson, and M.Thulin, "Discrimination of irradiated MOX fuel from UOX fuel by multivariate statistical analysis of simulated activities of gamma-emitting isotopes " , *Nuclear Inst. and Methods in Physics Research, A*, 885(9), 67-78,(2018).
- [38] K. Lam and W. Zhang, "Gamma peak search and peak fitting algorithm for a low-resolution detector with applications in gamma spectroscopy", *Journal of Radioanalytical and Nuclear Chemistry*, 322(3), 255-261 (2019).
- [39] L. Fei , G. Zhixing , G. Liangquan, L. Hui ,T. Xinyu ,L. Xinle and B.Hu, "Review of recent gamma spectrum unfolding algorithms and their application" , *Results in Physics*, 13 (3),461 ,(2019).
- [40] V. Kejzlar, L. Neufcourt, W. Nazarewicz and P. G. Reinhard, "Statistical aspects of nuclear mass models", *Journal of Physics G Nuclear and Particle Physics*, 47(9) ,1-32, (2020).
- [41] S. Longo, J.M. Roney, C. Cecchi, S. Cunliffe, T. Ferber, H. Hayashii, C. Hearty, A. Hershenhorn, A. Kuzmin, E. Manoni, F. Meier, K. Miyabayashi, I. Nakamura, M. Remnev, A. Sibidanov, Y. Unno, Y. Usov and V. Zhulanov , "CsI(Tl) pulse shape discrimination with the belle II electromagnetic calorimeter as a novel method to improve particle identification at electron-positron colliders", *Nuclear Inst. and Methods in Physics Research, A*, 982 (30),1-34 ,(2020).

- [42] P. Fanto, Y. Alhassid and H. A. Weidenmuller, "Statistical-model description of  $\gamma$  decay from compound-nucleus resonances", *Physical Review C*, 101(1), 1-10, (2020).
- [43] P. A. Amado, V.A. Amado and J. C. Aguiar, "Full-energy peak determination from total efficiency and peak-to-total ratio calculations", *Nuclear Inst. and Methods in Physics Research*, A,990(12),1-15, (2021).
- [44] M. G.-Fernandez, W. K. Wong, A. Tokuhiro, K. Welter, A. M. Alhawsawi, H. Yang and K. Higley, "Isotope identification using deep learning: An explanation", *Nuclear Inst. and Methods in Physics Research*, A, 988(2), 1-7, (2021).
- [45] T. Belgya and L.Szentmiklósi, "Monte-Carlo calculated detector response functions to unfold radiative neutron capture spectra" , *Nuclear Inst. and Methods in Physics Research*, A, 991(3), 1-7, (2021).
- [46] A.Vraničar, J.Nikolov ,N.Todorović ,I.Maksimović ,M. Mladenović, D.Mrđa and M.Travar, "Testing of EFFTRAN and angle software in comparison to GEANT 4 simulations in gamma spectrometry of cylindrical and noncylindrical sample geometries", *Nuclear Inst. and Methods in Physics Research*, A, 986(1) ,1-9,(2021).
- [47] A. Bukartas ,J. Wallin, R. Finck, and C.r Rääf, "Bayesian algorithm to estimate position and activity of an orphan gamma source utilizing multiple detectors in a mobile gamma spectrometry system" , 16(1) ,1-22, (2021).
- [48] R. André, C. Bobin , J.Bobin , J. Xu and A. de Vismes , "Metrological approach of  $\gamma$ -emitting radionuclides identification at low statistics:



application of sparse spectral unmixing to scintillation detectors", *Metrologia* , 58( 1), 155-161, (2021).

- [49] M. P. Allen and D. J. Tildesley, "Computer Simulation of Liquids ", Oxford: Oxford University Press, second edition, (1987).
- [50] M. Lavine, "Introduction to Statistical Thought", *Journal of the American Statistical Association*, 101(12),1719-1719, (2006).
- [51] M. M. El Sayed El Tokhy, "Development of Quantum Devices and Algorithms for Radiation Detection and Radiation Signal Processing", Ph.D. in Electrical Engineering, college of Engineering- Al-Azhar University, (2012).
- [52] M.L. Rizzo, " Statistical Computing with R", *Computer Science and Data Analysis Series*, Chapman & Hall/CRC, (2007).
- [53] R. D. Peng, "R Programming for Data Science", Lean Publishing, (2015).
- [54] M. R. Abonazel, "Statistical Analysis Using R" *Annual Conference on Statistics, Computer Sciences and Operations Research*, 1 (49), (2014).
- [55] B. Yakir, "Introduction to Statistical Thinking (With R, Without Calculus) ", The Hebrew University, (2011).
- [56] M.B. Zeina, "Statistical programming language R."1<sup>st</sup> Edition, Dar Al-Andalus for printing and publishing, (2017).
- [57] N. B. Jarrah, " Statistical programming language R. ", University of Basrah, (2018).

- [58] A. H. Hassan" Statistical programming language R. ", Dar Al-Andalus for printing and publishing, ISBN:978-9922-20-228-0, (2019).
- [59] A .Hands , "Practical Time Series Forecasting with R ", second edition, axelrod schnell publishers,(2016).
- [60] Spectrum techniques UCS-30-Manua "The universal computer spectrometer", USA, (2017).
- [61] A.M. Hamad and H. M. Qadr, " Gamma-Rays Spectroscopy by Using a Thallium Activated Sodium Iodide NaI(Tl) ", Eurasian Journal of Science and Engineering, 4(1),99-111,(2018).
- [62] ORTEC, Gamma-ray spectroscopy using NaI (Tl), Experiments in Nuclear Science Laboratory Manual Fourth Edition, (2014).
- [63] Z. A. Fattah, "Gamma–ray spectroscopy using NAI(TL) detector ", International Journal of Engineering Science and Research Technology, 5(7), (2016).
- [64] C.A. Kalfas, M. Axiotis and C. Tsabaris, "SPECTRW: A software package for nuclear and atomic spectroscopy", Nuclear Inst. and Methods in Physics Research, A, 830(26), 265-274, (2016).
- [65] T. Veronica, Y. Isozumi and T.AOK, "Determination of photopeak efficiencies of voluminal samples for the measurement of environmental radioactivities", Bull. Inst. Chem. Res., Kyoto Univ., 7(4),399-407, (1992).

# **Chapter Two**

## **Theoretical Part**

# **Chapter Three**

## **Experimental Part**

# **Chapter Four**

## **Results and Discussion**

**Chapter Five**  
**Conclusions and**  
**Future Work**

# References

# Appendices



## الخلاصة

هناك بعض الظواهر في الفيزياء النووية ليس لها تفسير واضح ومباشر مثل ظاهرة الانحلال الإشعاعي والانشطار النووي فهي مبنية على الإحصاء والاحتمالات. لذلك تم في هذه الدراسة استخدام قوانين الإحصاء والبرمجة الإحصائية ممثلة بلغة البرمجة R لدراسة انحلال وتفاعل أشعة كاما في مصادر السيزيوم والكوبالت والصدويوم من خلال جمع 200 طيف لكل مصدر ودراسة المناطق الطيفية من المصادر المشعة من حيث المساحة الكلية للطيف، مساحة القمة الضوئية، قابلية تحليل الطاقة ونسبة القمة التي تعتبر معيار لجودة الطيف قبل وبعد طرح الخلفية الإشعاعية

لغة البرمجة R هي نظام مفتوح المصدر يستخدم على نطاق واسع للتحليل الإحصائي وتم استخدام البرمجة الإحصائية في حساب التطبيقات الإحصائية الممثلة بالمتوسط والوسيط والتباين والانحراف المعياري حيث لوحظ أن قيم المتوسط الحسابي قبل طرح الخلفية الإشعاعية كانت أكبر مما هو عليه بعد طرح الخلفية الإشعاعية لجميع النماذج المدروسة للمصادر المشعة المستخدمة.

وجد في عينات مصدر  $^{137}\text{Cs}$  أن قيمة المتوسط الحسابي كانت أكبر من قيمة الوسيط مما يعني أن البيانات غير متماثلة، على عكس عينات مصدري  $^{60}\text{Co}$  و  $^{22}\text{Na}$  حيث كانت قيم الوسيط أكبر من قيم المتوسط الحسابي.

تم حساب اختبارات الحالة الطبيعية واختبارات تجانس التباينات بواسطة لغة البرمجة R ووجد أن جميع العينات المدروسة كانت متجانسة. وبالنسبة لمعامل بيرسون وجد أن هناك علاقة طردية بين عدد العينات والمساحة الكلية سواء قبل أو بعد طرح خلفية الإشعاع. كما وجد باستخدام اختبار الانحدار الخطي ان هناك علاقة خطية بين المساحة الكلية وعدد العينات.

كذلك تم حساب التوزيعات الإحصائية مثل التوزيع ذي الحدين وتوزيع بواسون والتوزيع الأسي والتوزيع المنتظم والتوزيع الطبيعي على العينات المدروسة ، فقد وجد من خلال هذه الدراسة أن هذه التوزيعات لم تنجح في إعطاء تفسير واضح لسلوك الانحلال الإشعاعي ، الأمر الذي يتطلب إعادة النظر في المفهوم السائد حول الطبيعة العشوائية للانحلال ، مما يعني ضرورة إجراء المزيد من الدراسات والبحوث في هذا المجال بحيث يتم استخدام توزيعات وطرق مختلفة لمحاولة الحصول على تفسير أفضل لهذه الظاهرة.



جمهورية العراق  
وزارة التعليم العالي والبحث العلمي  
جامعة بابل - كلية العلوم  
قسم الفيزياء

التوزيع الاحصائي لطيف الطاقة لنوى ( $^{137}\text{Cs}$ ,  $^{60}\text{Co}$ ,  $^{22}\text{Na}$ ) باستخدام  
كاشف NaI(Tl)

أطروحة مقدمة إلى  
مجلس كلية العلوم - جامعة بابل  
وهي جزء من متطلبات نيل درجة الدكتوراه في فلسفة العلوم/ الفيزياء

من قبل

**انعام هاني كاظم هادي**

بكالوريوس تربية فيزياء 2005

ماجستير علوم فيزياء 2012

بإشراف

**أ.د. خالد حسين هاتف العطية**

2021 م

1443 هـ